

A photograph of the International Space Station (ISS) in space. Two astronauts in white suits are visible, working on the exterior. Large spherical instruments, likely part of the COMPTEL experiment, are mounted on the station's structure. The Earth is visible in the background. The text 'The MeV Legacy of COMPTEL' is overlaid in yellow at the top right.

The MeV Legacy of COMPTEL

Mark McConnell
*Univ of New Hampshire
Southwest Research Institute*

The Legacy of COMPTEL

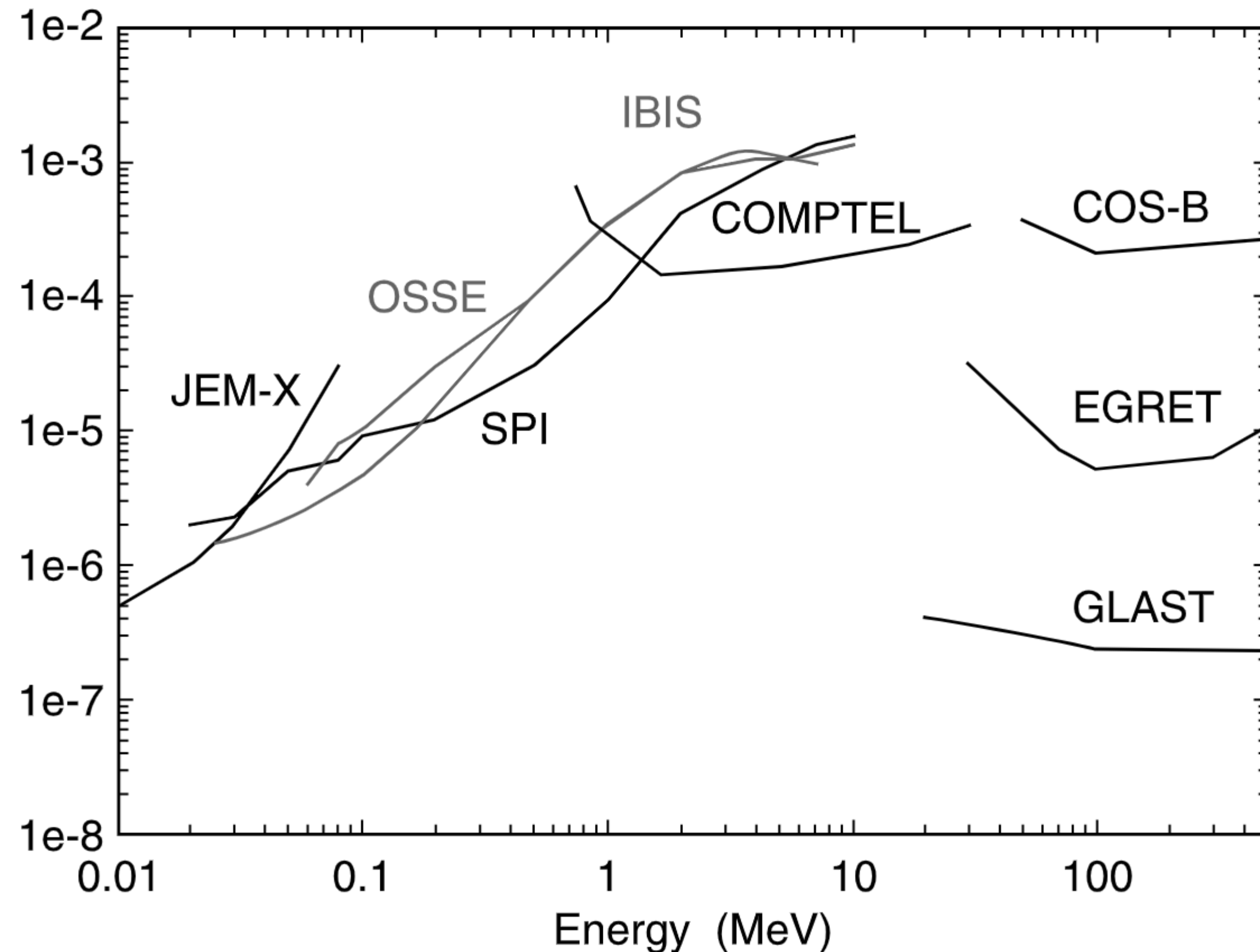
The MeV Gap

As the first on-orbit Compton telescope, COMPTEL has given us only a small taste of what we can learn from from the MeV spectrum.

It has left behind a clear gap in our exploration of the high energy sky, a gap that many of us would like to fill.

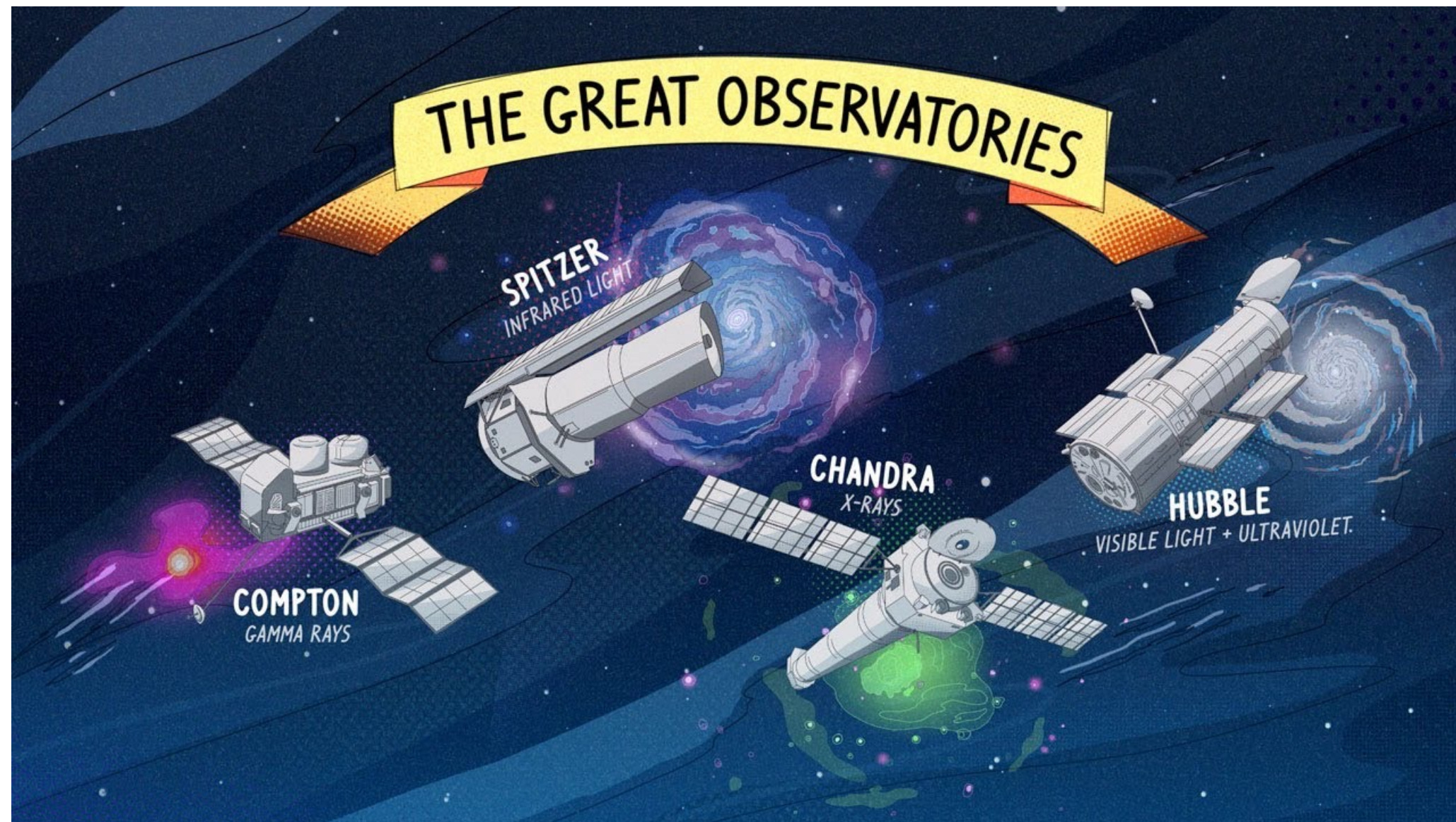
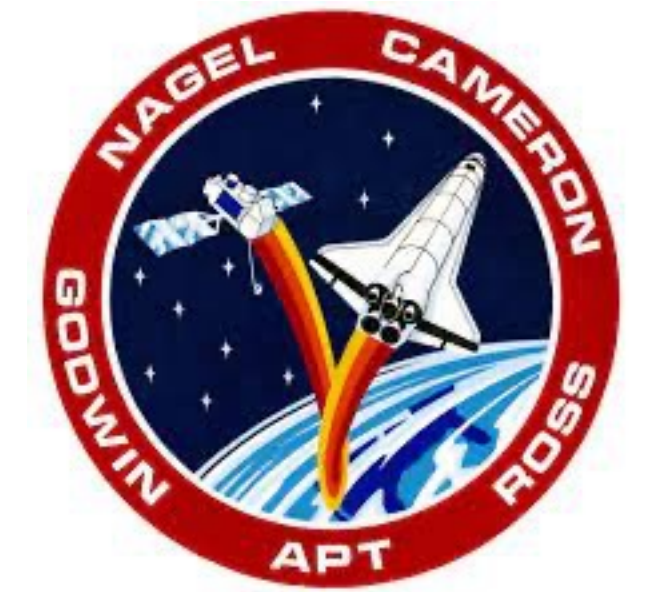
- Instrument Description
- Response Characterization
- Background Characteristics
- Observations
- Lessons Learned

Continuum Sensitivity * E^2
[MeV cm⁻² s⁻¹] $T_{\text{obs}} = 10^6$ s, $\Delta E = E$



Compton Gamma Ray Observatory

Launched on STS-37 – April 5, 1991



- CGRO provided the first all-sky coverage of there gamma-ray over a broad range of gamma-ray energies.
- Announcement of Opportunity issued in 1977.
- Proposals submitted in 1978.
- Four instruments selected in 1981.
- Originally scheduled for launch in 1985

COMPTEL

COMPon imaging TElescope

The double-scatter design grew out of work done on balloons at both MPE (Schönfelder et al.) and UNH (Lockwood et al.).

COMPTEL PI: Volker Schönfelder (MPE)

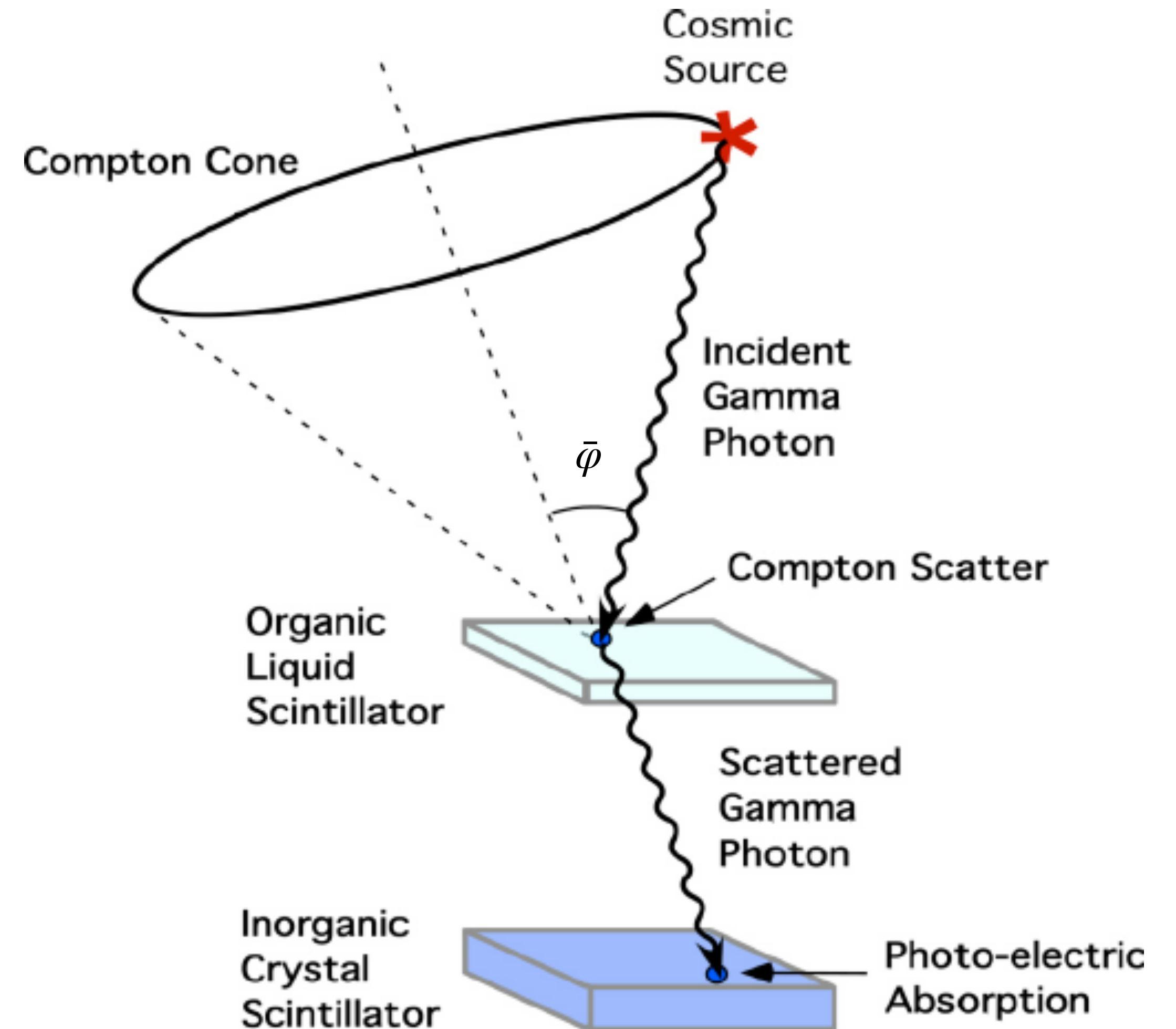
MPE - Max Planck Institute (Garching)

UNH - Univ of New Hampshire (Durham)

SSD - ESTEC (Noordwijk)

ROL - Univ of Leiden (Leiden)

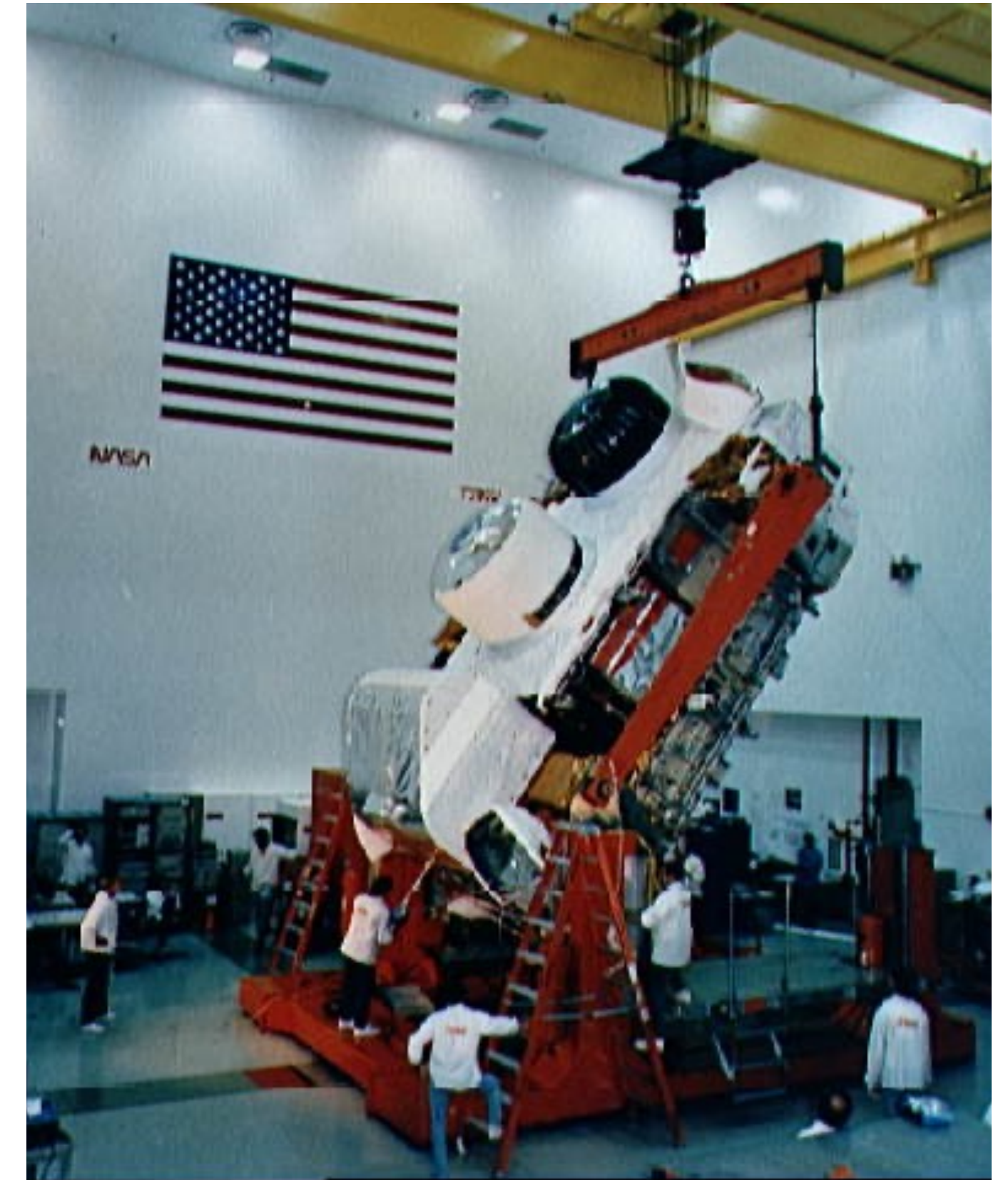
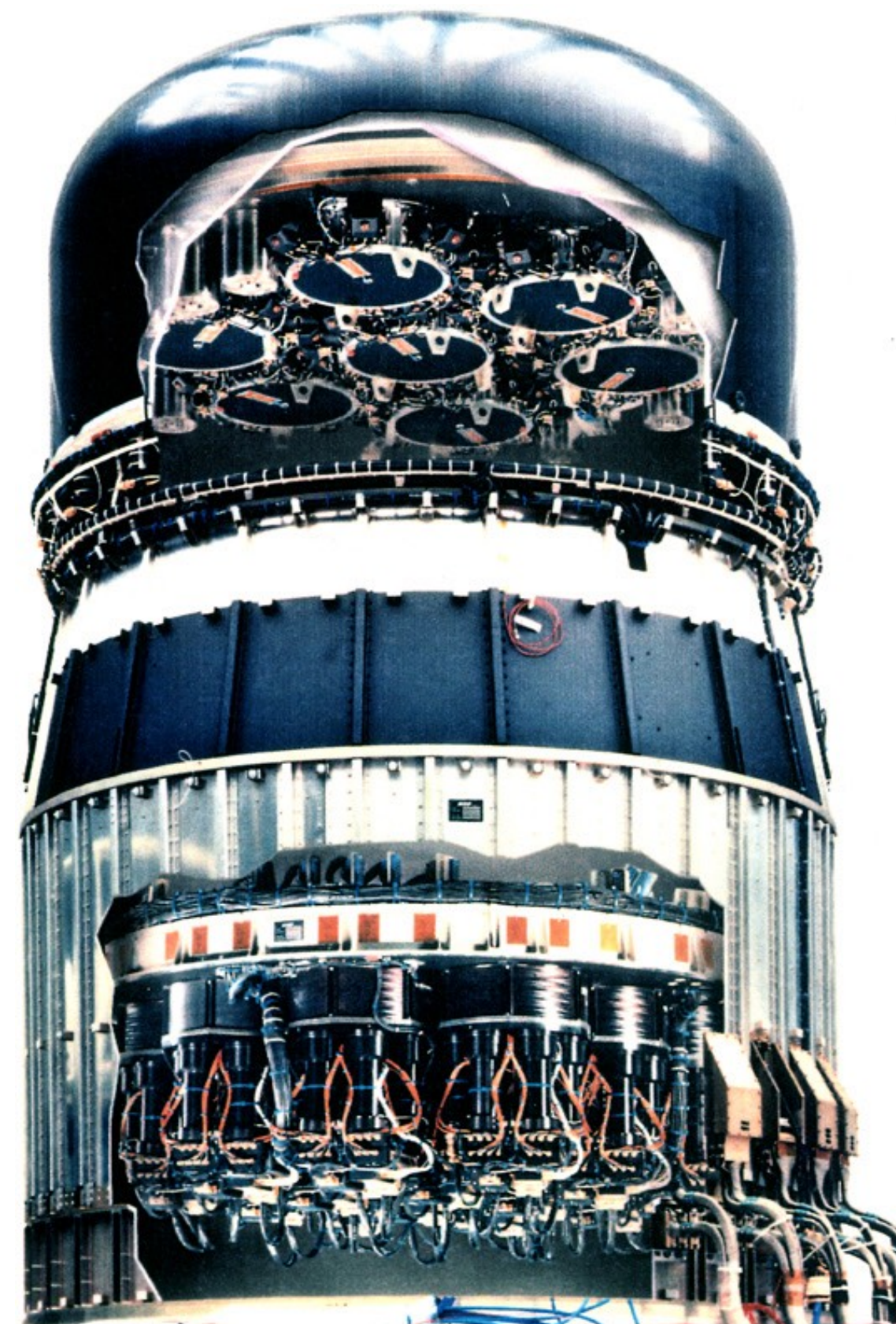
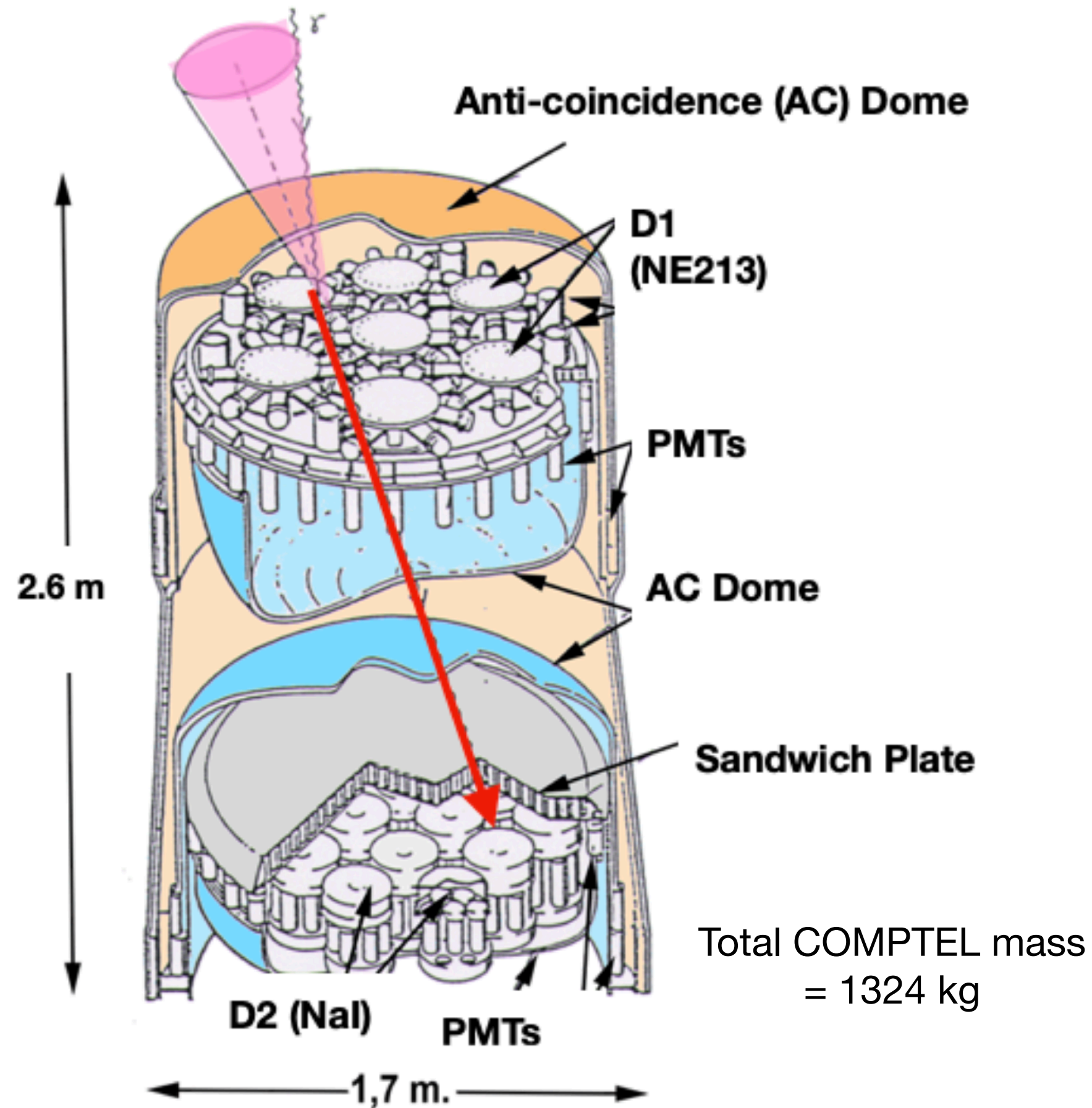
Schönfelder et al. (1993), Ap. J. Supp., 86, 657.



$$\cos \bar{\varphi} = 1 - \frac{m_0 c^2}{E_2} + \frac{m_0 c^2}{E_1 + E_2}$$

COMPTEL Instrument Description

One of 4 Experiments on CGRO



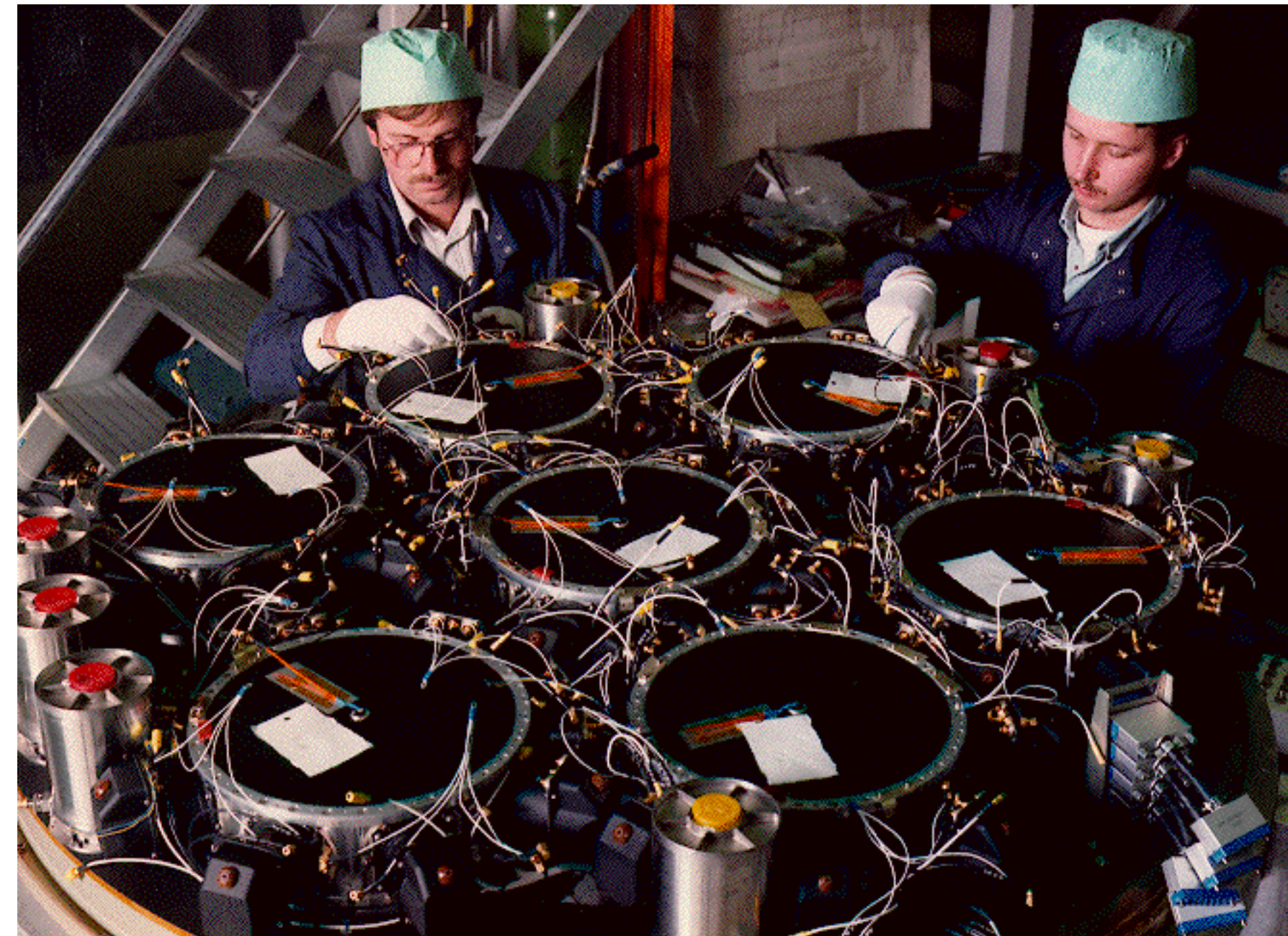
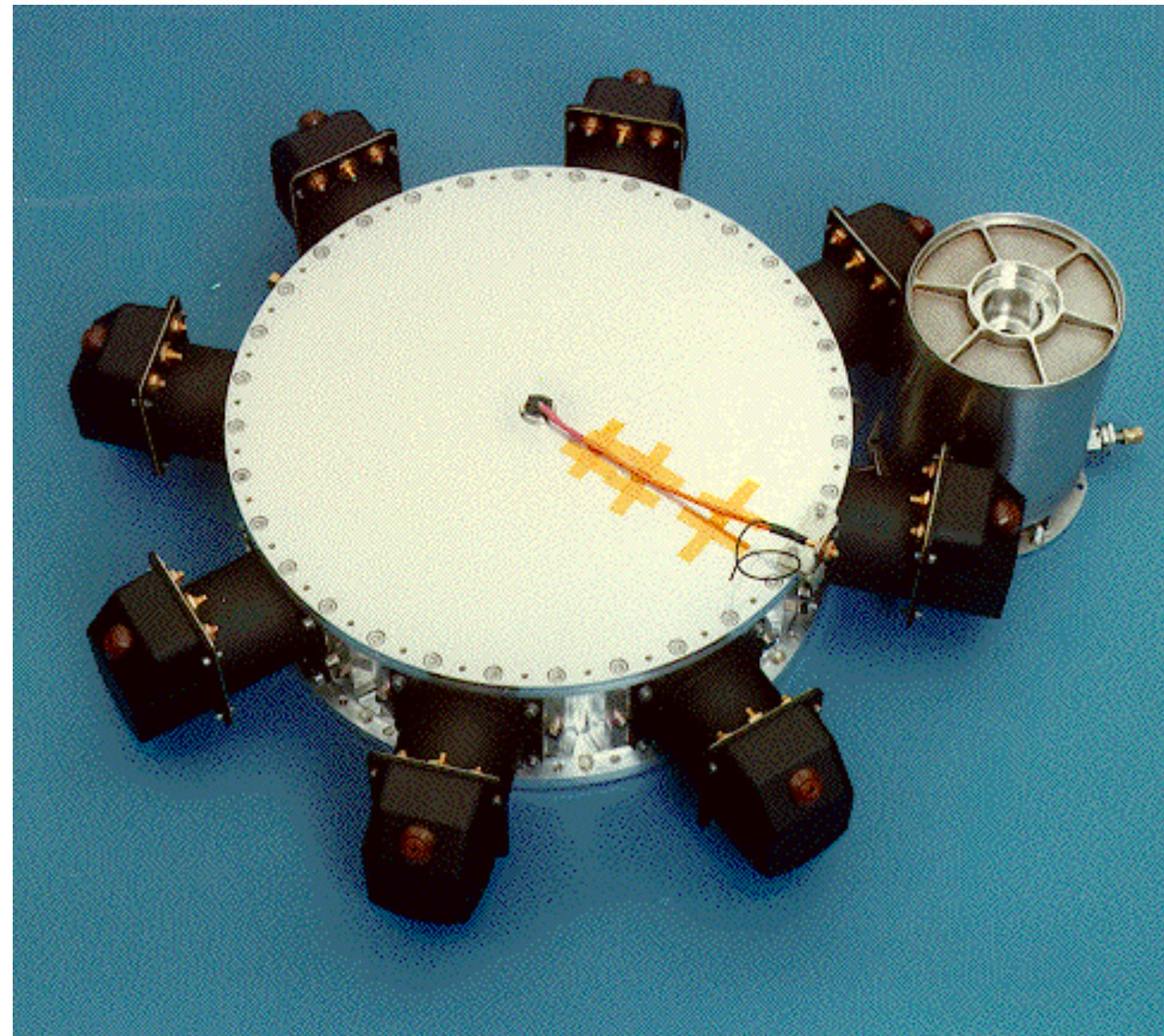
CGRO spacecraft provided by TRW (now part of Northrup-Grumman).

Total CGRO mass = 17,000 kg

COMPTEL was built by MBB (now part of the Airbus Group) in Munich.

COMPTEL D1 Subsystem

Upper Detector Layer



Each NE-213 liquid scintillator D1 module is 28 cm in diameter by 7 cm thick and read out by an array of 8 PMTs. Also seen here is the bellows used to accommodate expansion of the liquid scintillator.

The full D1 subsystem consisted of an array of 7 D1 modules. Note that PMTs were arranged around the perimeter of each cell to minimize mass along the path of scattered photons.

These detectors employed PSD to distinguish between photon (Compton) scatter events and neutron scatter events.

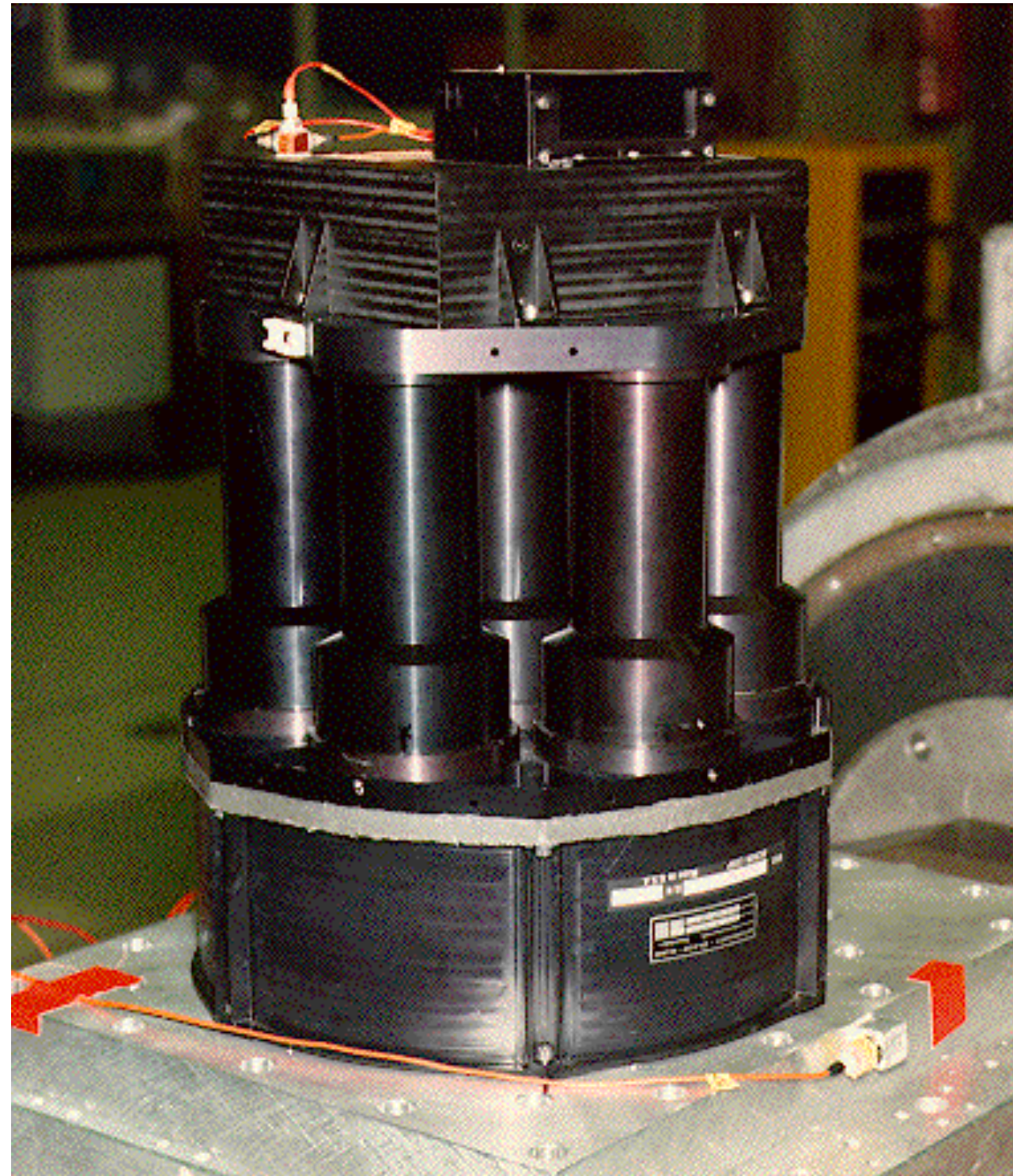
This allowed for both photon and neutron imaging.

Average localization ≈ 2.3 cm

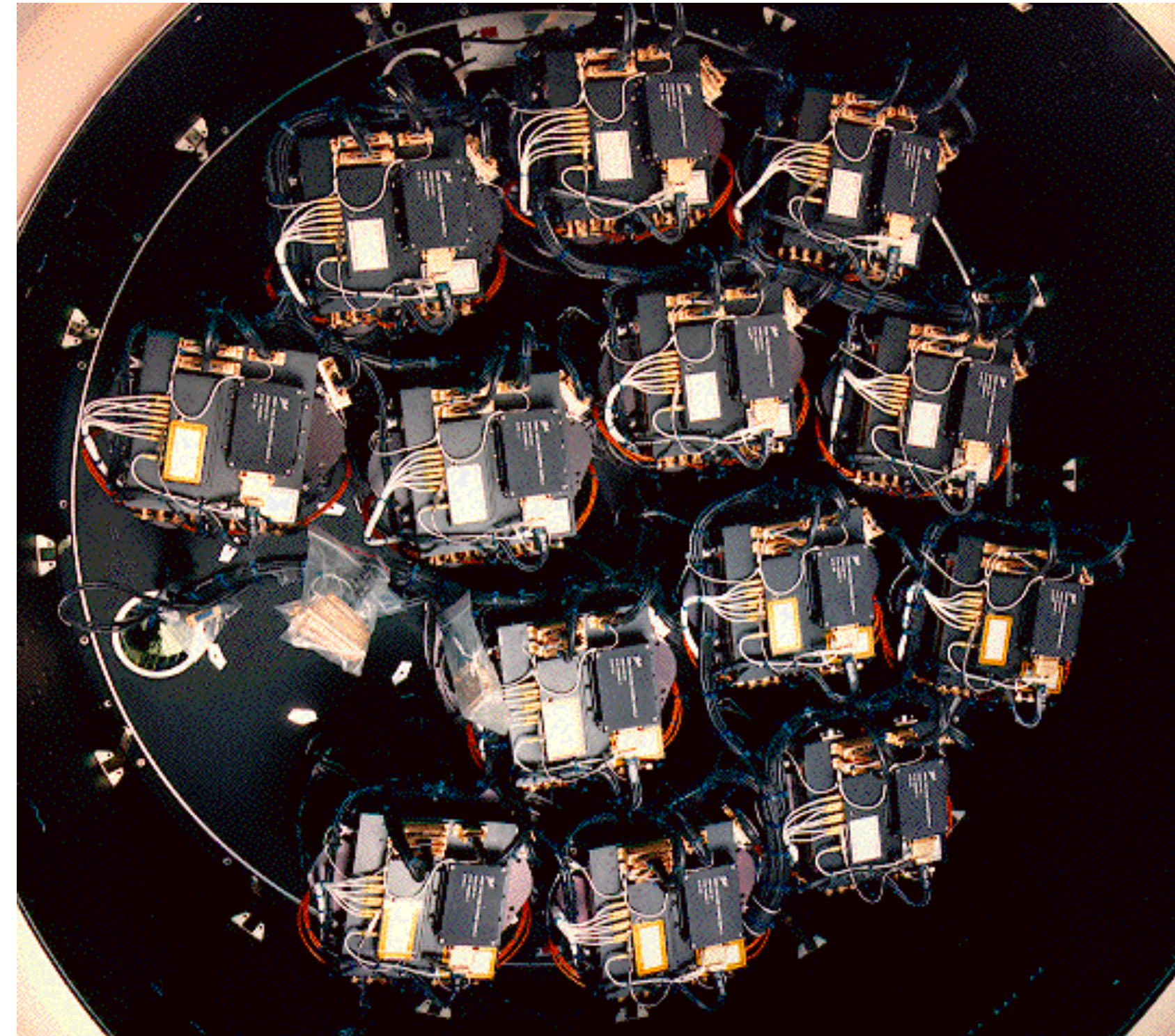
On occasion, COMPTEL was operated with only a single D1 detector to collect albedo neutron data.

COMPTEL D2 Subsystem

Lower Detector Layer



Each NaI(Tl) D2 module is 28 cm in diameter by 7 cm thick and read out by an array of 7 PMTs



The full D2 subsystem consisted of an array of 14 D2 modules.

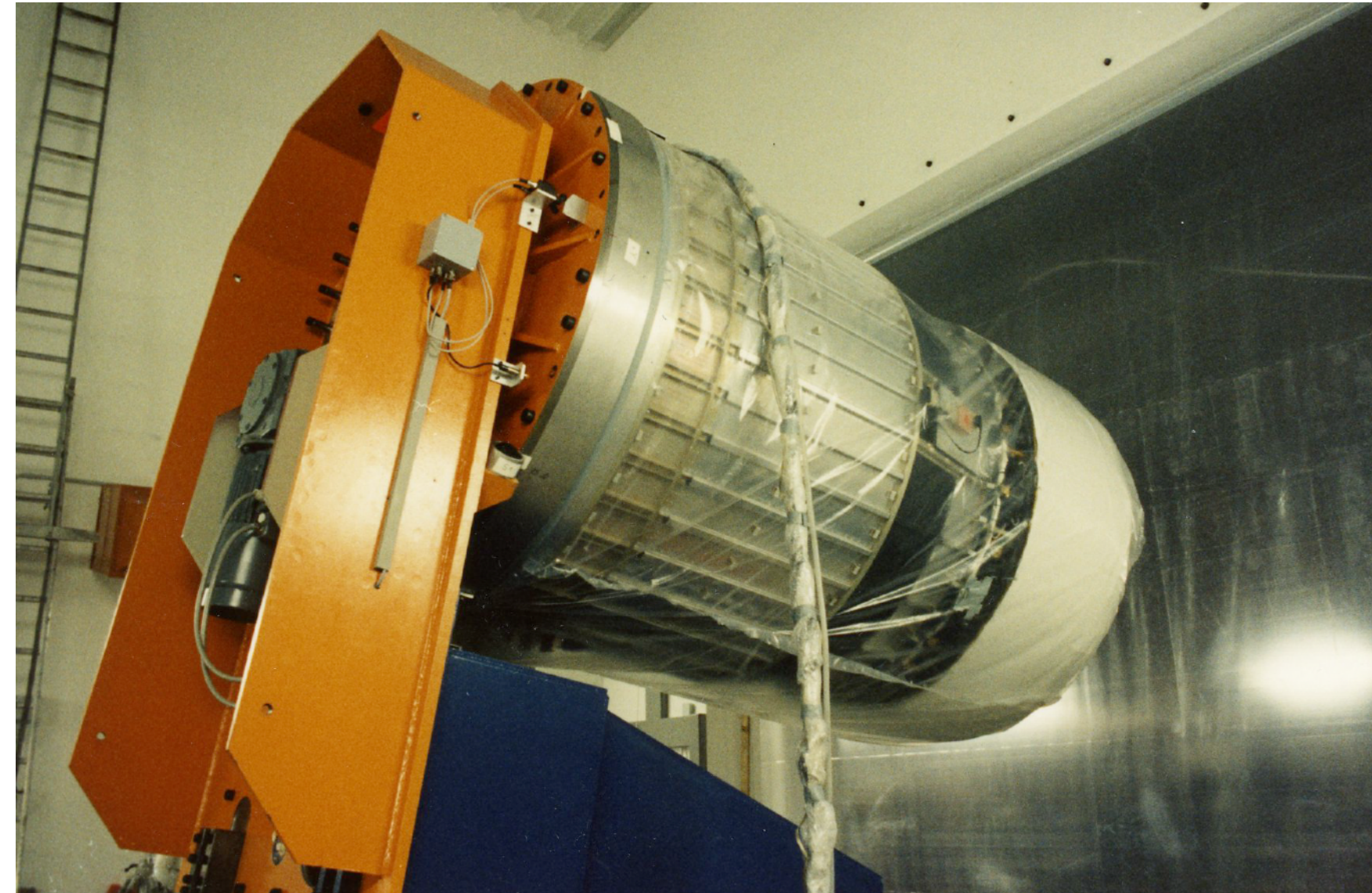
These high-Z detectors were designed to more completely absorb the full energy of the scattered photons.

Average localization ≈ 1.5 cm

Two of these detectors were used as independent burst detectors.

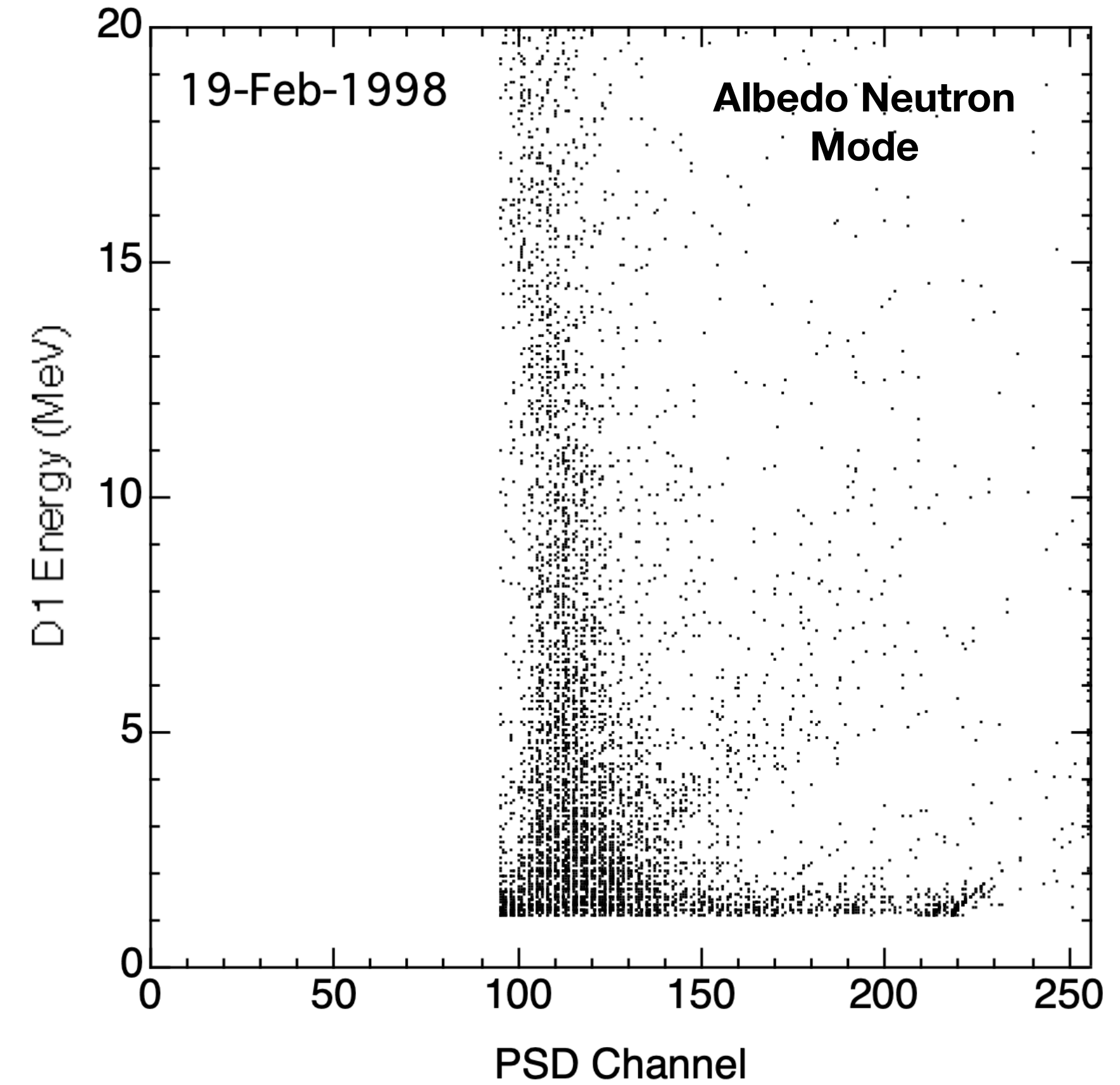
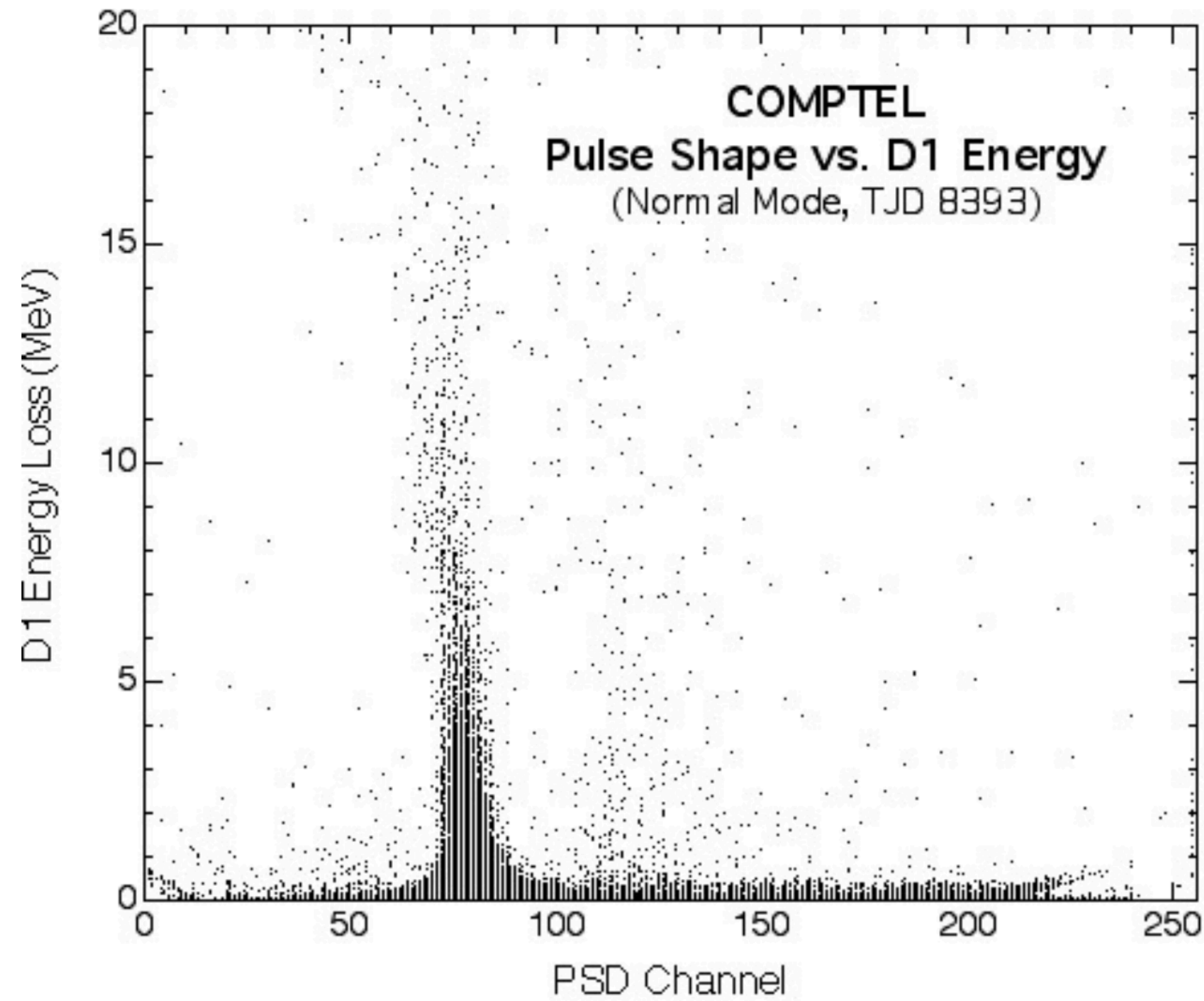
Pre-Flight Calibration Activities

1987 - Neuherberg, Germany



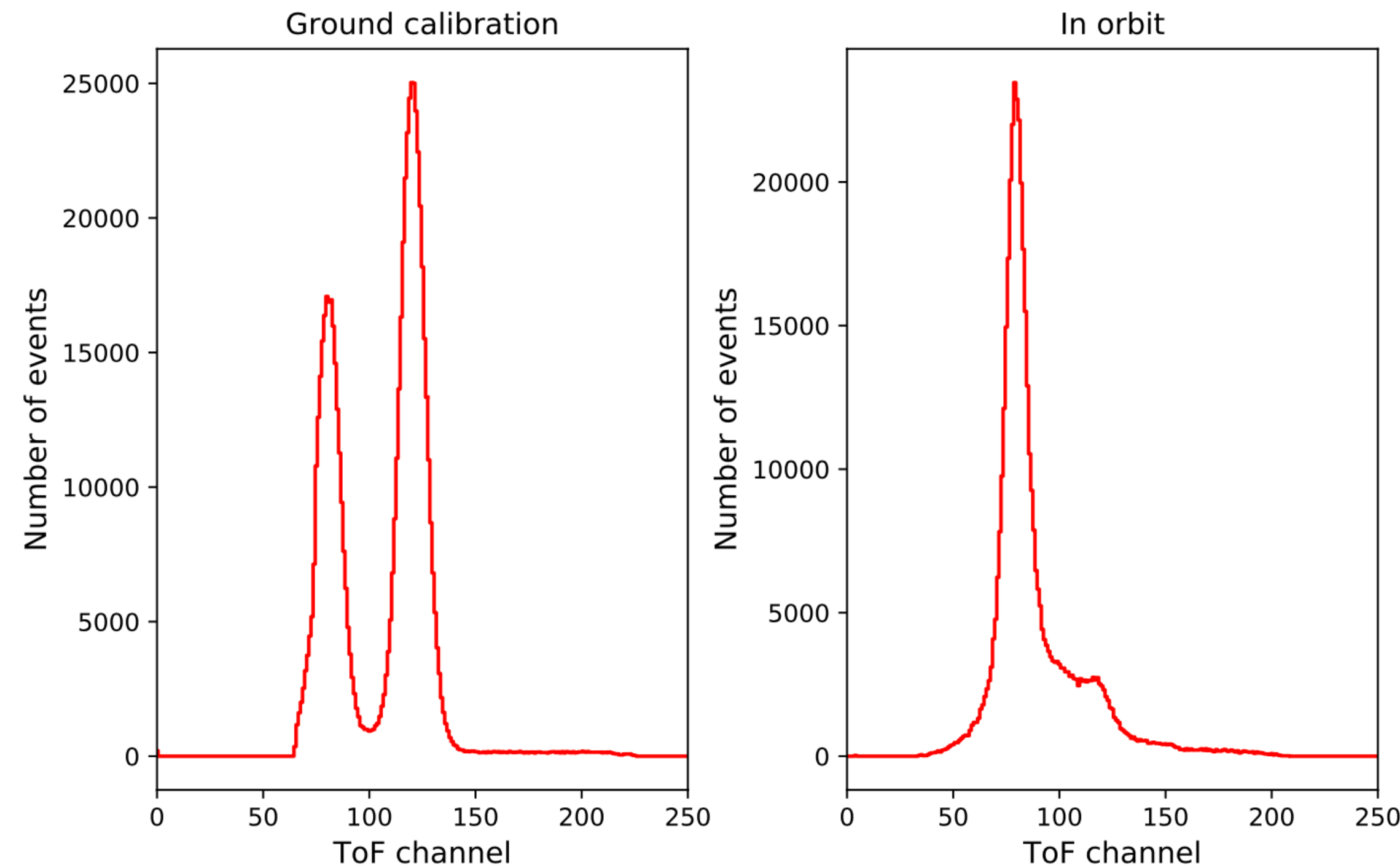
Pulse Shape Discrimination (PSD)

Used to Distinguish Gamma Rays from Neutrons

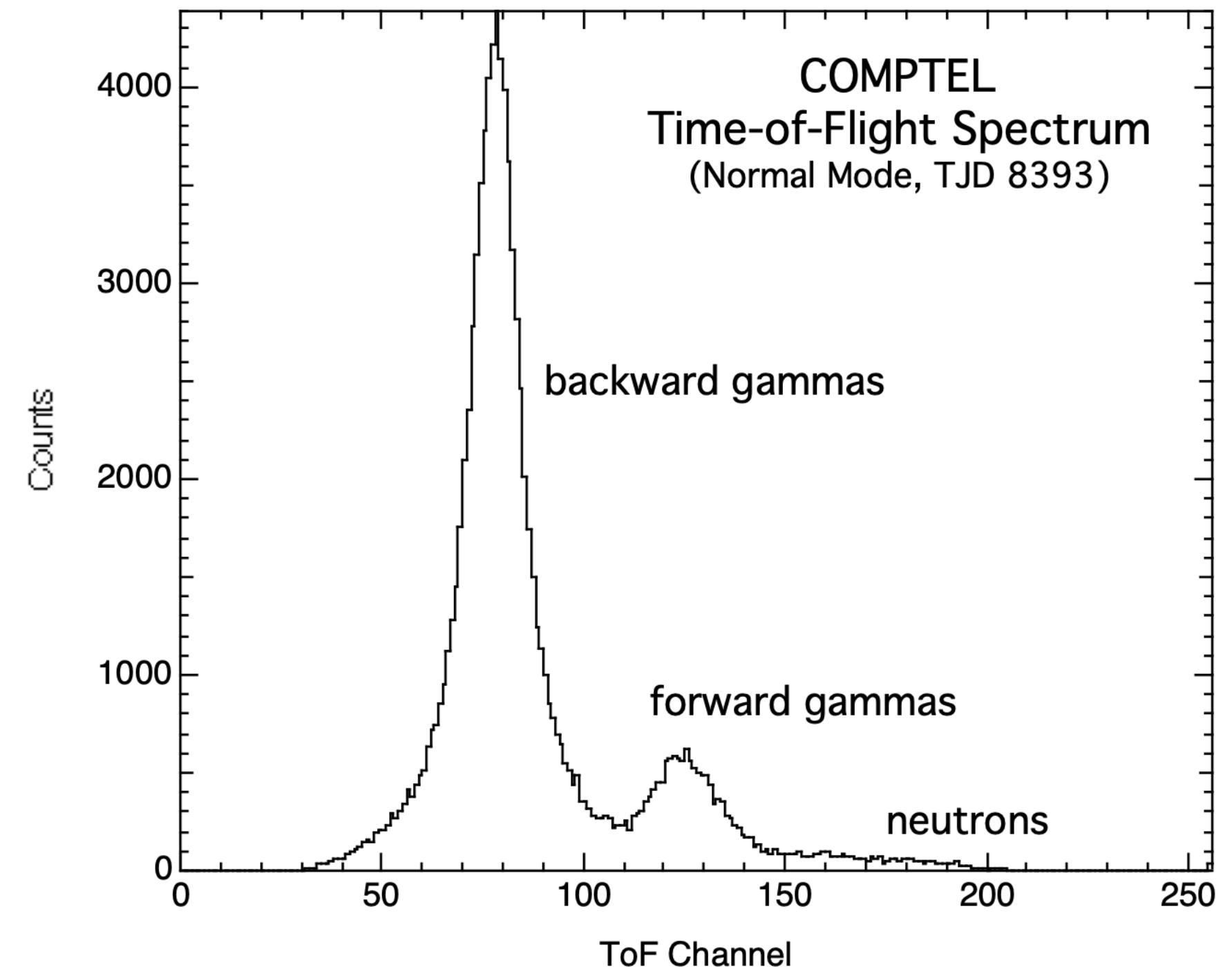


Time-of-Flight (TOF)

Used to Distinguish Downward and Upward Events



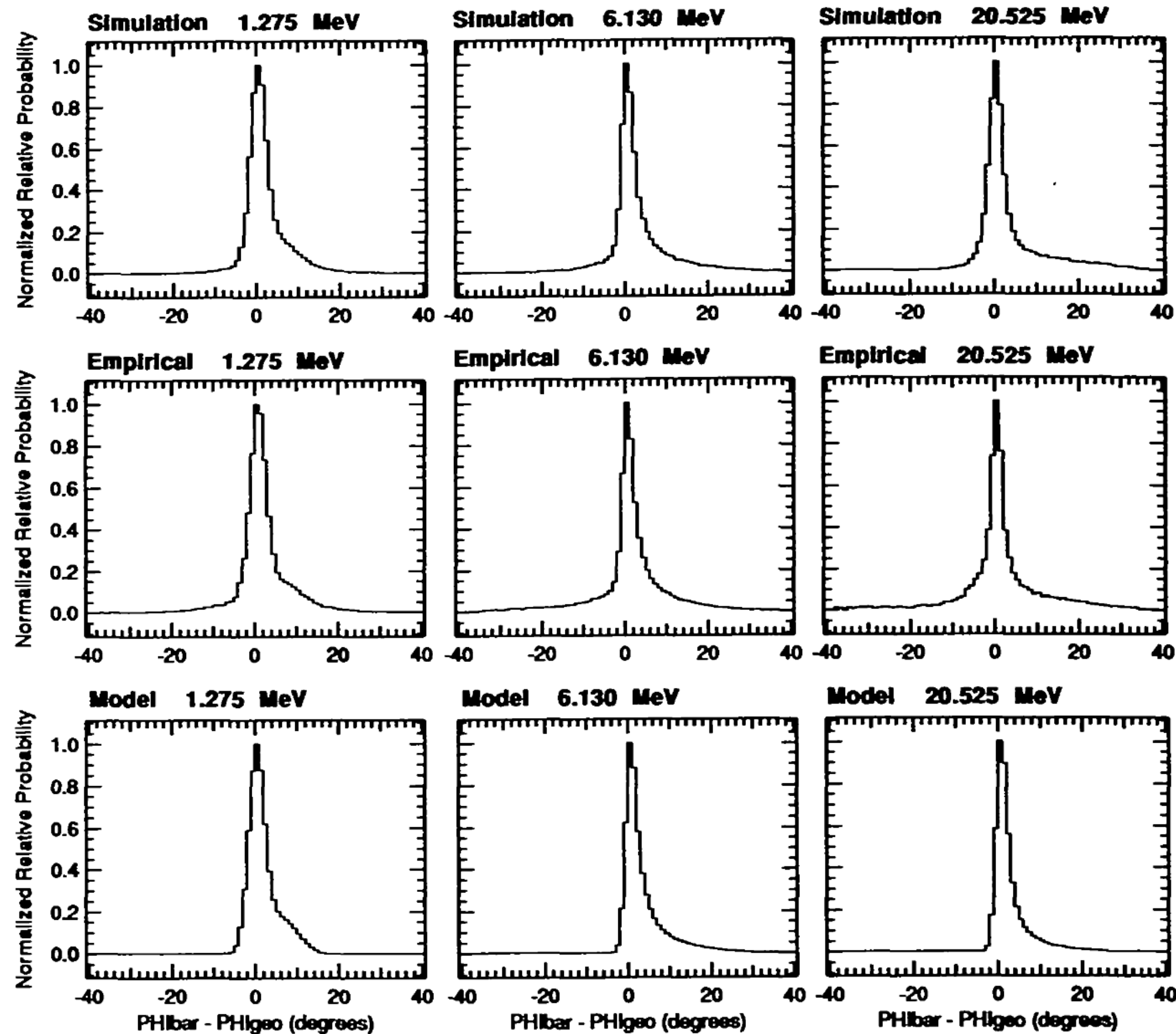
Knödlseher et al. (2022), Astr. Ap., in press.



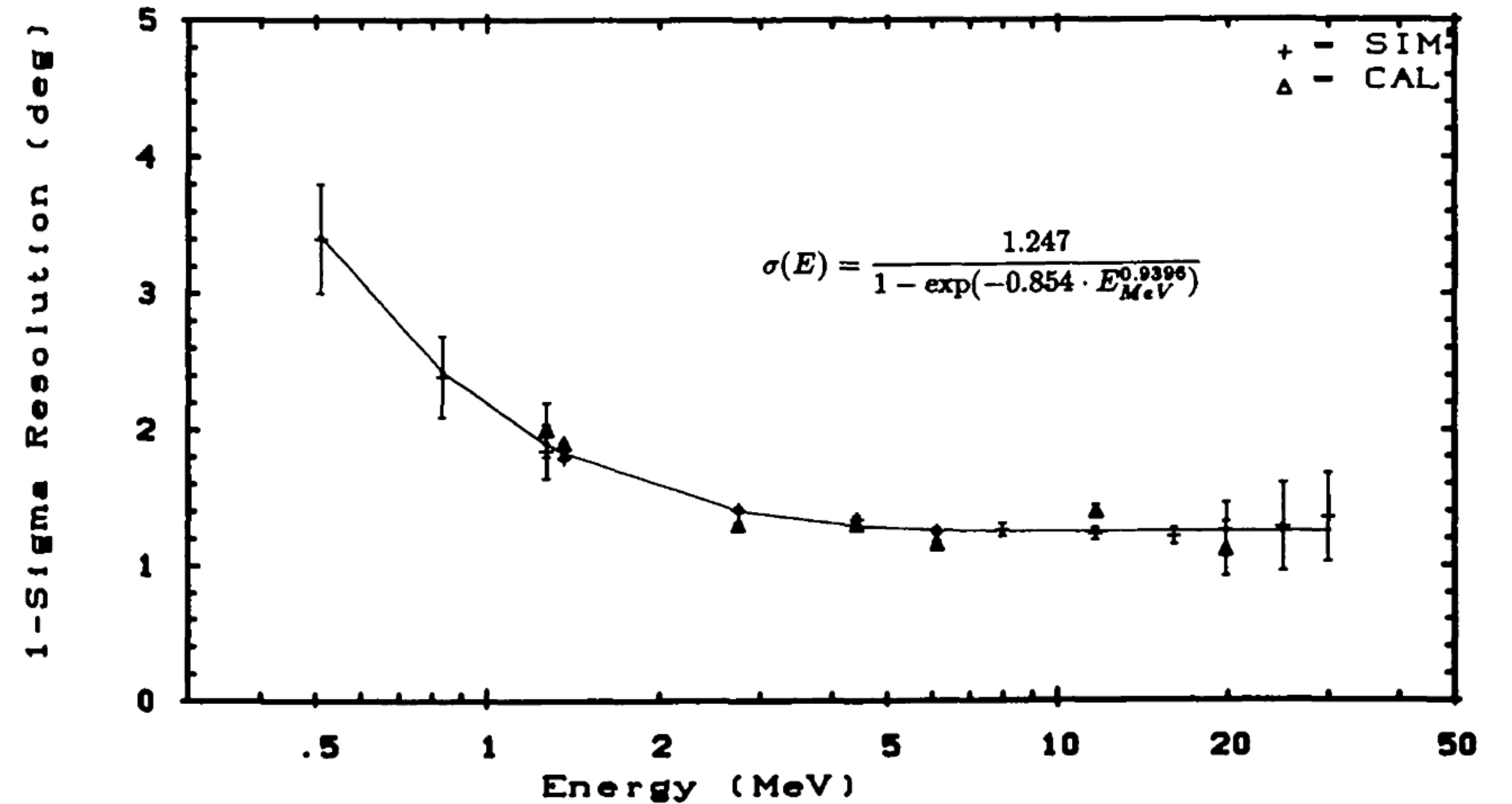
One ToF channel corresponds to 0.25 ns. Downward moving photons interacting first in D1 and then in D2 lead to a peak around channel 120 (≈ 5 ns), while upward moving photons interacting first in D2 and then in D1 produce a peak around channel 80.

COMPTEL Response

Angular Resolution Measure



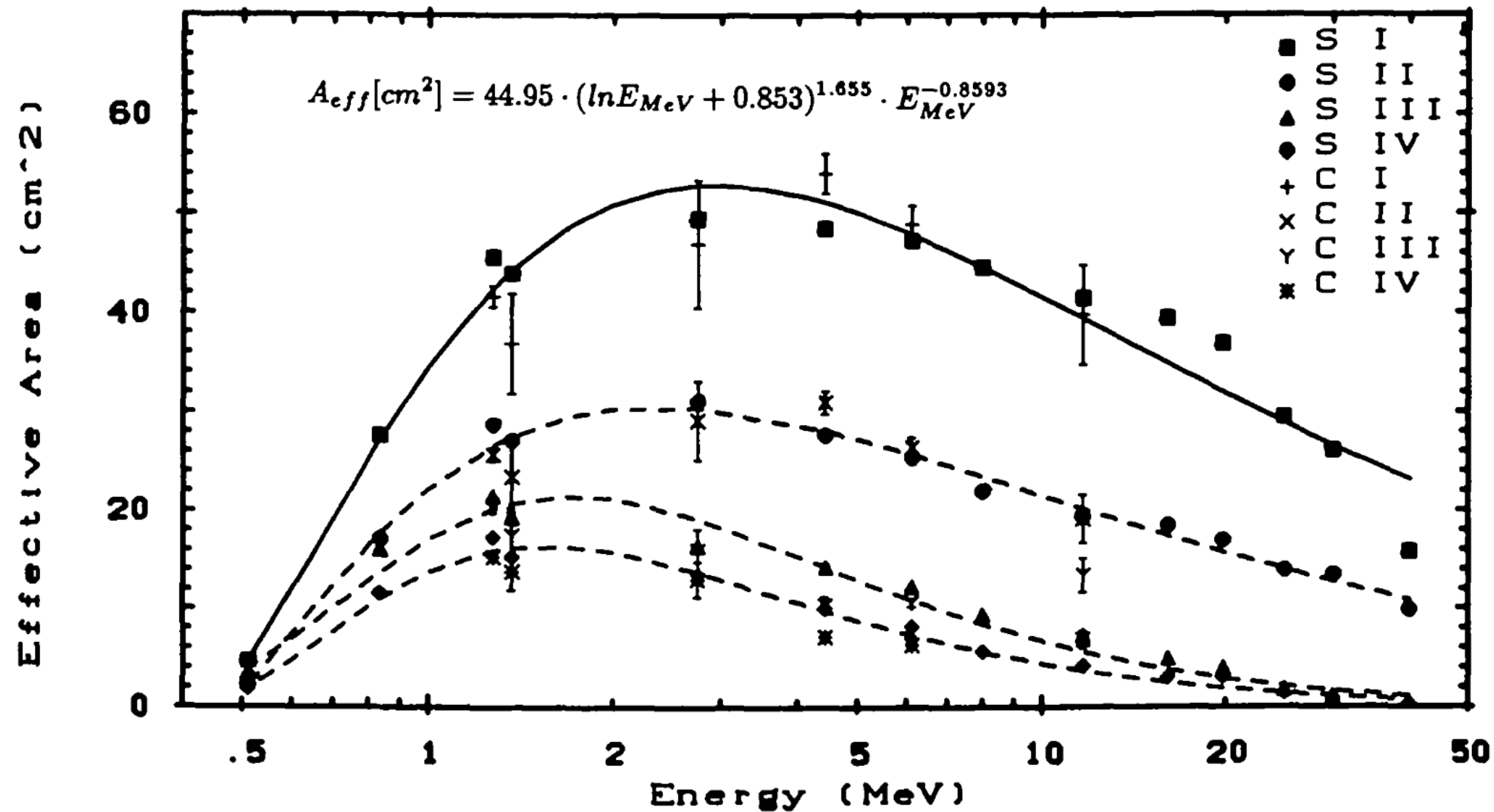
$$ARM = \bar{\varphi} - \varphi_{geo}$$



Schönfelder et al. (1993), *Ap. J. Supp.*, 86, 657.

COMPTEL Response

Effective Area



With typical event selections, the effective area peaks near 20 cm².

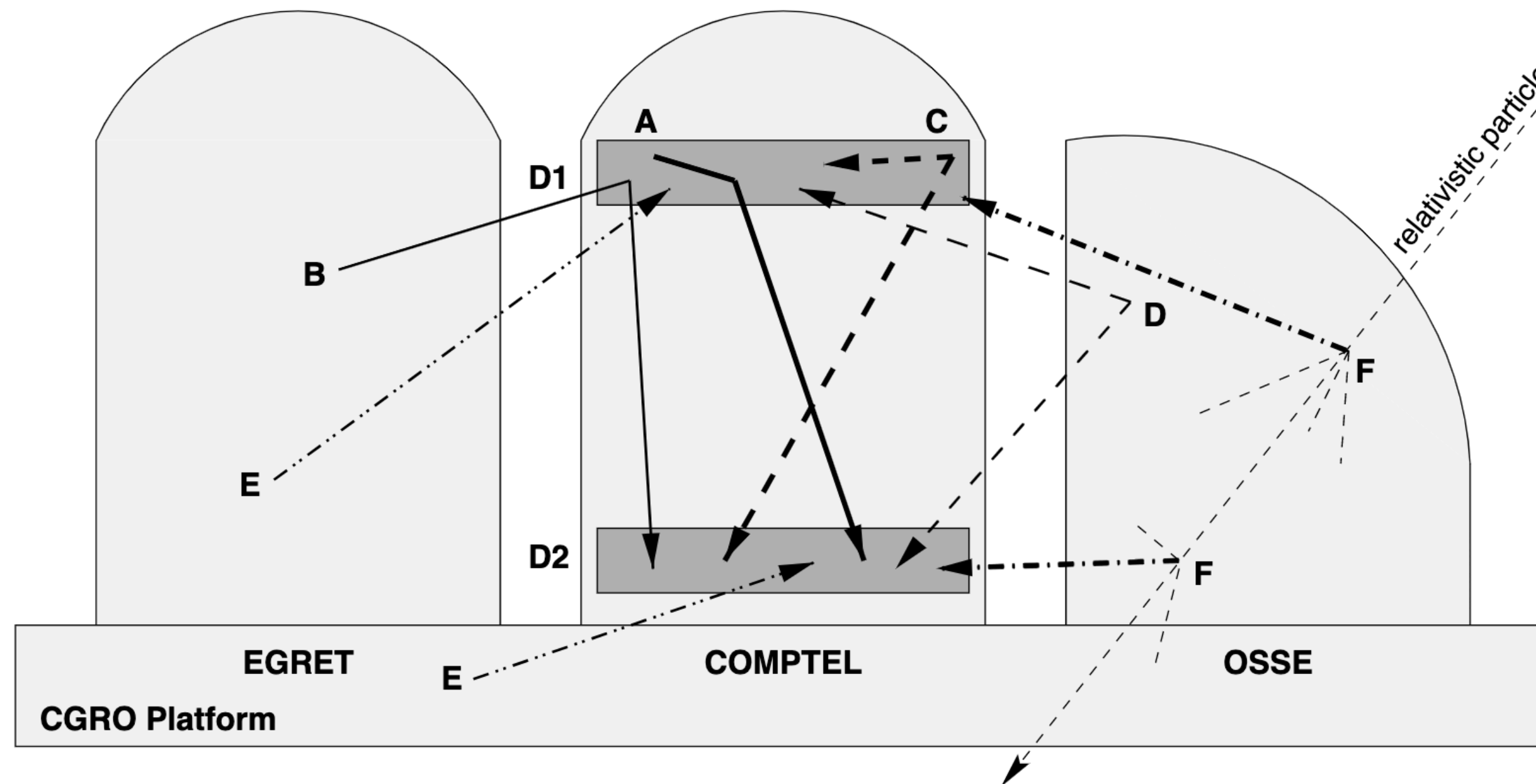
This may seem rather small, but COMPTEL was also a very low-background instrument.

FIG. 31.—Effective detection area determined from calibration and simulation at normal incidence and at a number of different energies. The symbols in the figure have the following meanings: S: data points from simulation; C: data points from calibration; I: no event selections applied; II: event selection according to “extreme” $\bar{\varphi}$ distribution, defined in § 2; III: event selection on 3 σ -wide full-energy peak; IV: event selection on 3 σ -wide ARM window around $\varphi_{geo} - \bar{\varphi} = 0$. An analytical fit to the top curve (no event selection applied) is given in the figure.

Schönfelder et al. (1993), *Ap. J. Supp.*, 86, 657.

COMPTEL Background

Background Event Types

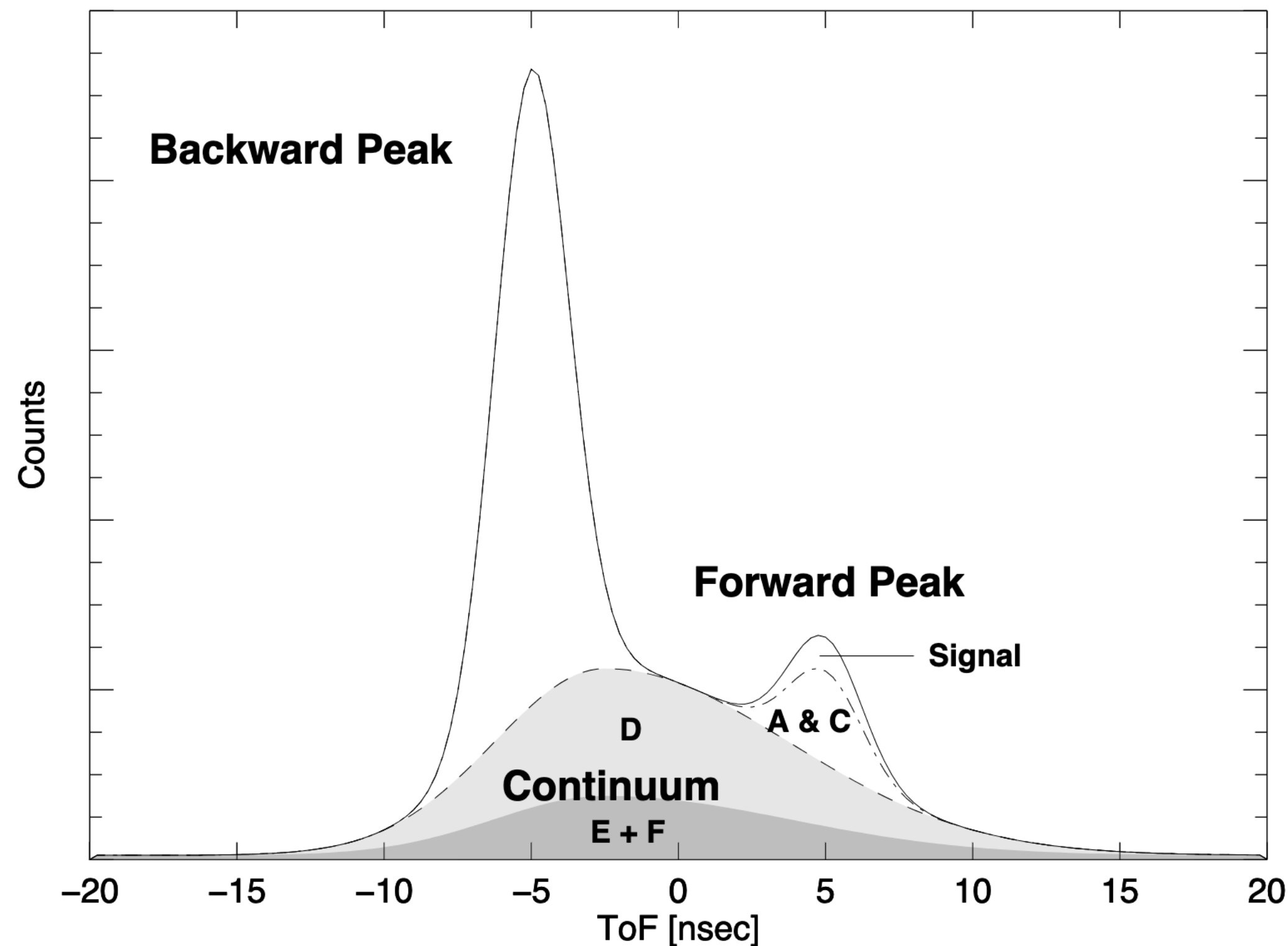


- Type A - Double scatter of a single photon generated near D1 (not rejected). Ex: 1.46, 2.22 MeV
- Type B - Double scatter of a single photon in regions outside of D1 (rejected by $\bar{\varphi}$ cut).
- Type C - Two or more photons that are both spatially and temporally correlated (“cascade” events) generated in region near D1 (not rejected). Ex: ^{24}Na decays from Aluminum activation.
- Type D - Two or more photons that are both spatially and temporally correlated (“cascade” events) generated in region between D1 and D2 (not rejected).
- Type E - Two photons that are both spatially and temporally uncorrelated (random coincidences).
- Type F - Two photons that are temporally correlated but spatially uncorrelated (cosmic rays generating photons along its path).

Weidenspointner et al. (2001), *Astr. Ap.*, 368, 347.

COMPTEL Background

Background Event Types in TOF Space

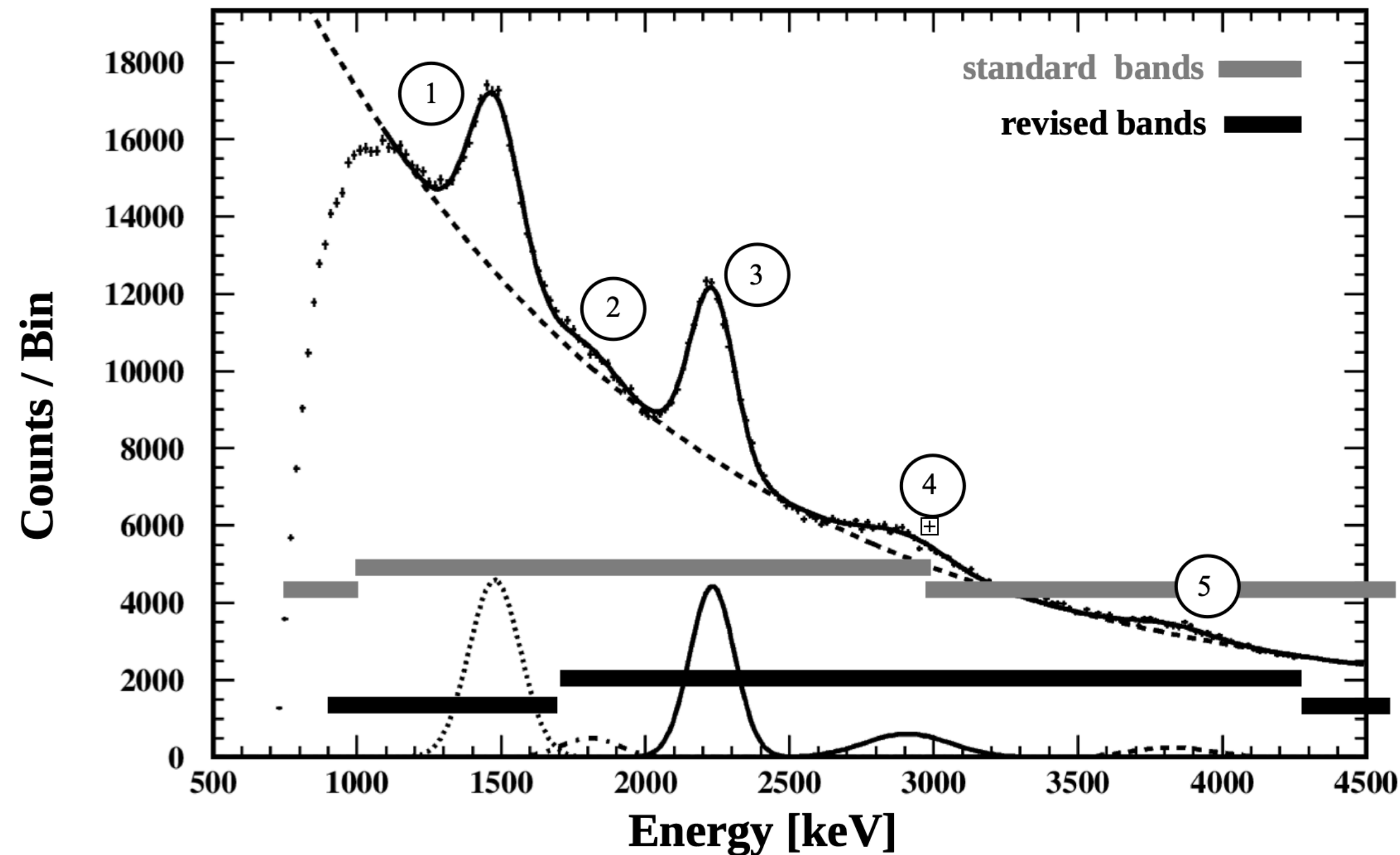


- Type A - Double scatter of a single photon generated near D1 (not rejected). Ex: 1.46, 2.22 MeV
- Type B - Double scatter of a single photon in regions outside of D1 (rejected by $\bar{\varphi}$ cut).
- Type C - Two or more photons that are both spatially and temporally correlated (“cascade” events) generated in region near D1 (not rejected). Ex: ^{24}Na decays from Aluminum activation.
- Type D - Two or more photons that are both spatially and temporally correlated (“cascade” events) generated in region between D1 and D2 (not rejected).
- Type E - Two photons that are both spatially and temporally uncorrelated (random coincidences).
- Type F - Two photons that are temporally correlated but spatially uncorrelated (cosmic rays generating photons along its path).

Weidenspointner et al. (2001), Astr. Ap., 368, 347.

COMPTEL Background

Total Energy Spectrum



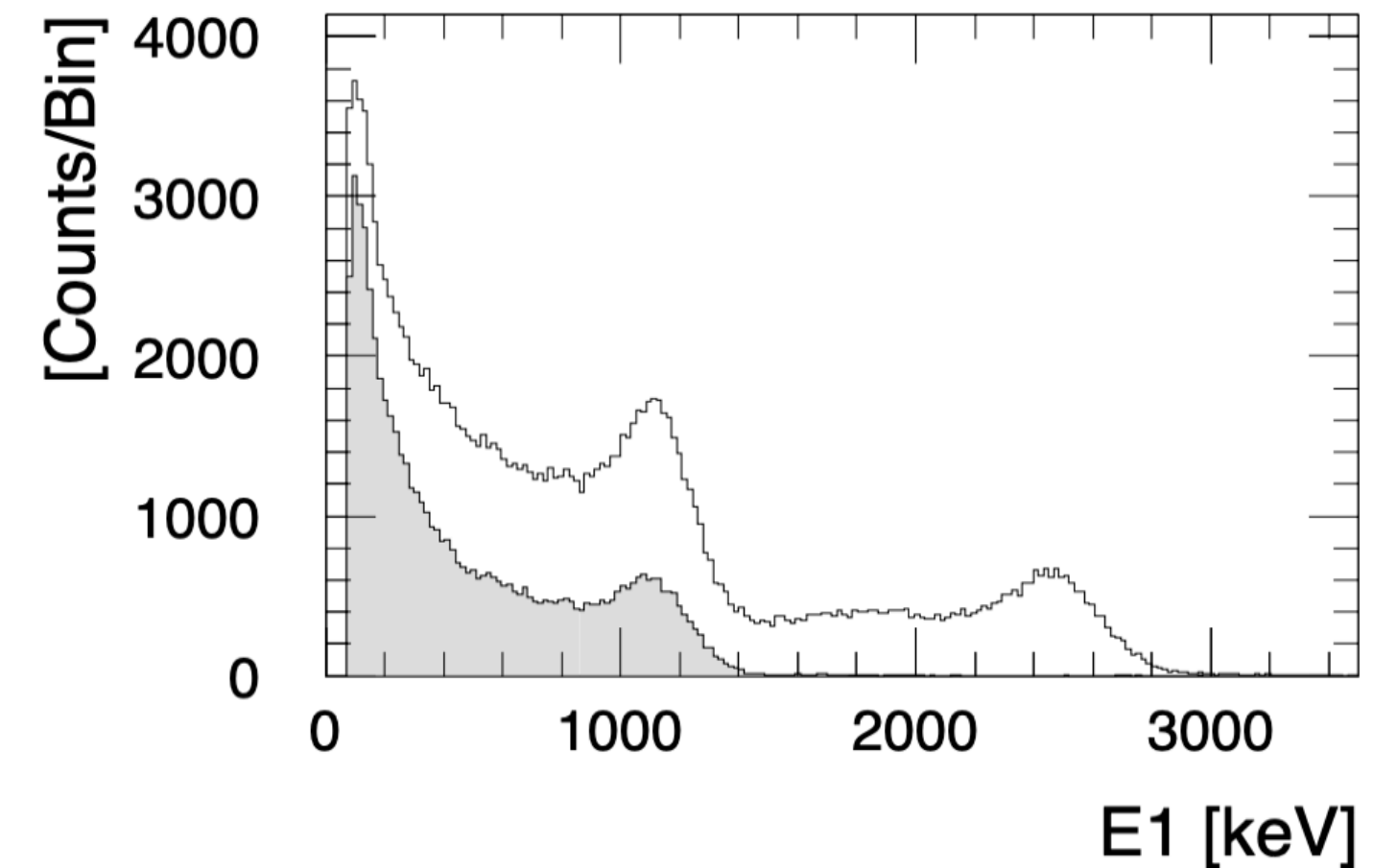
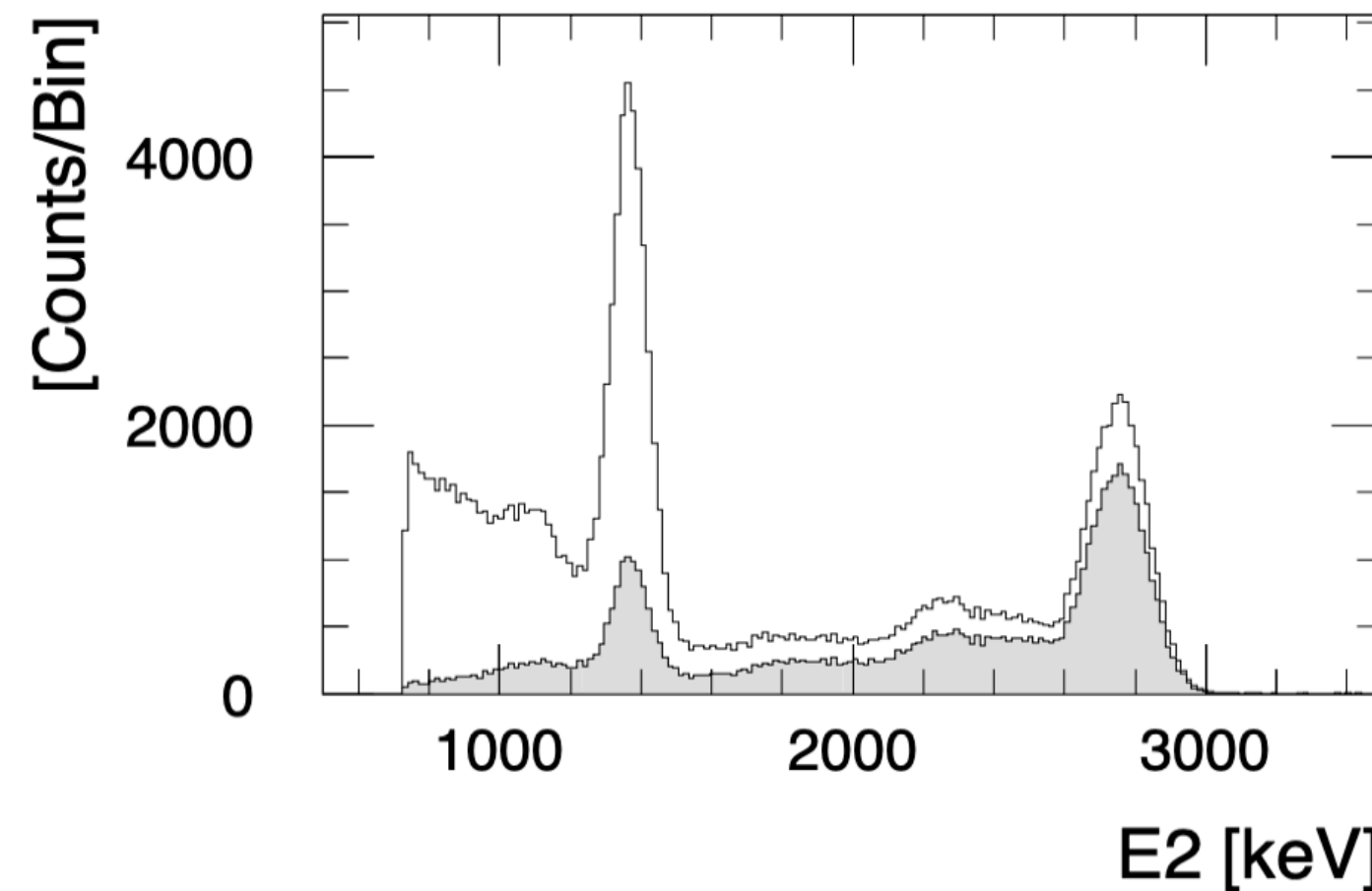
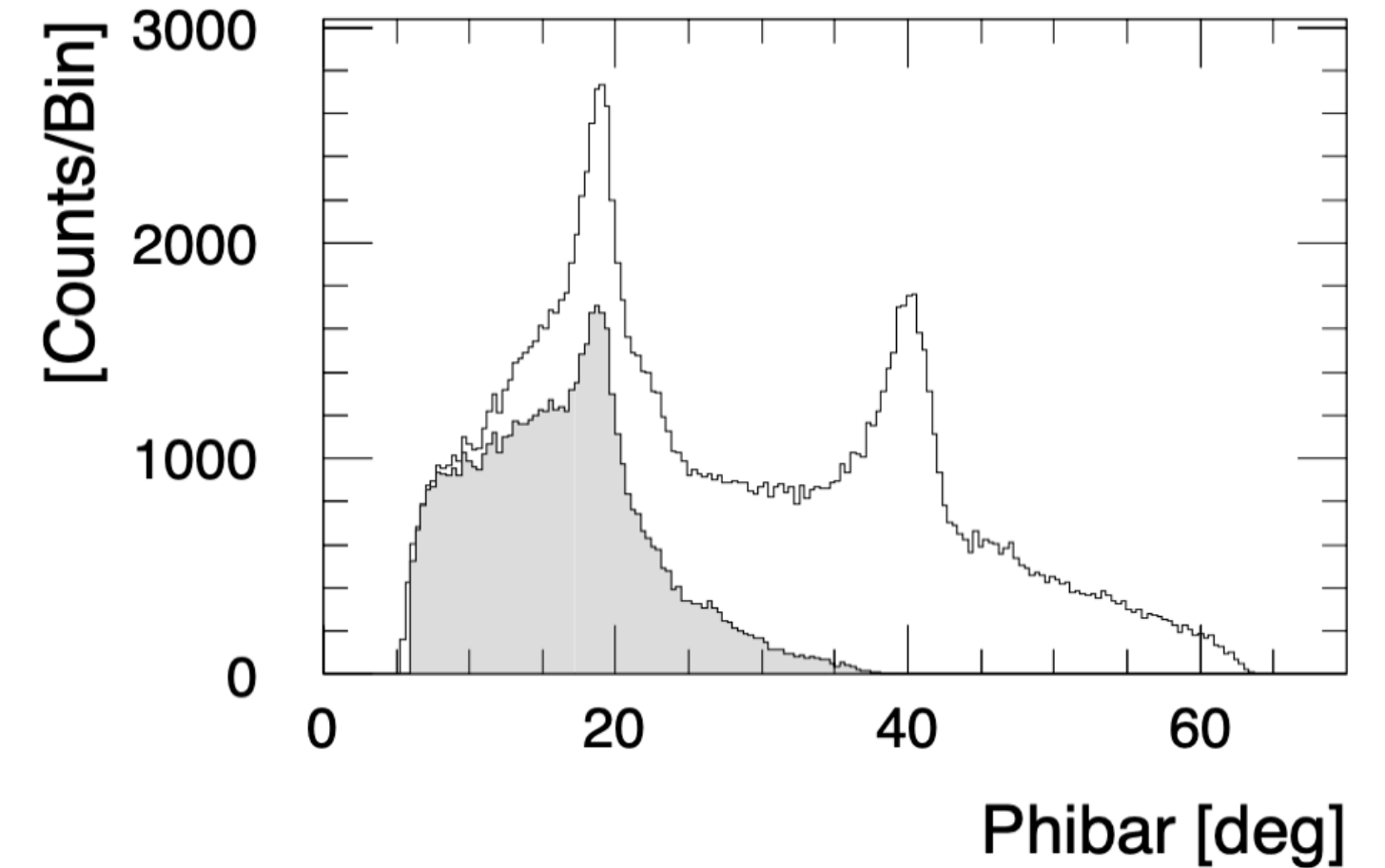
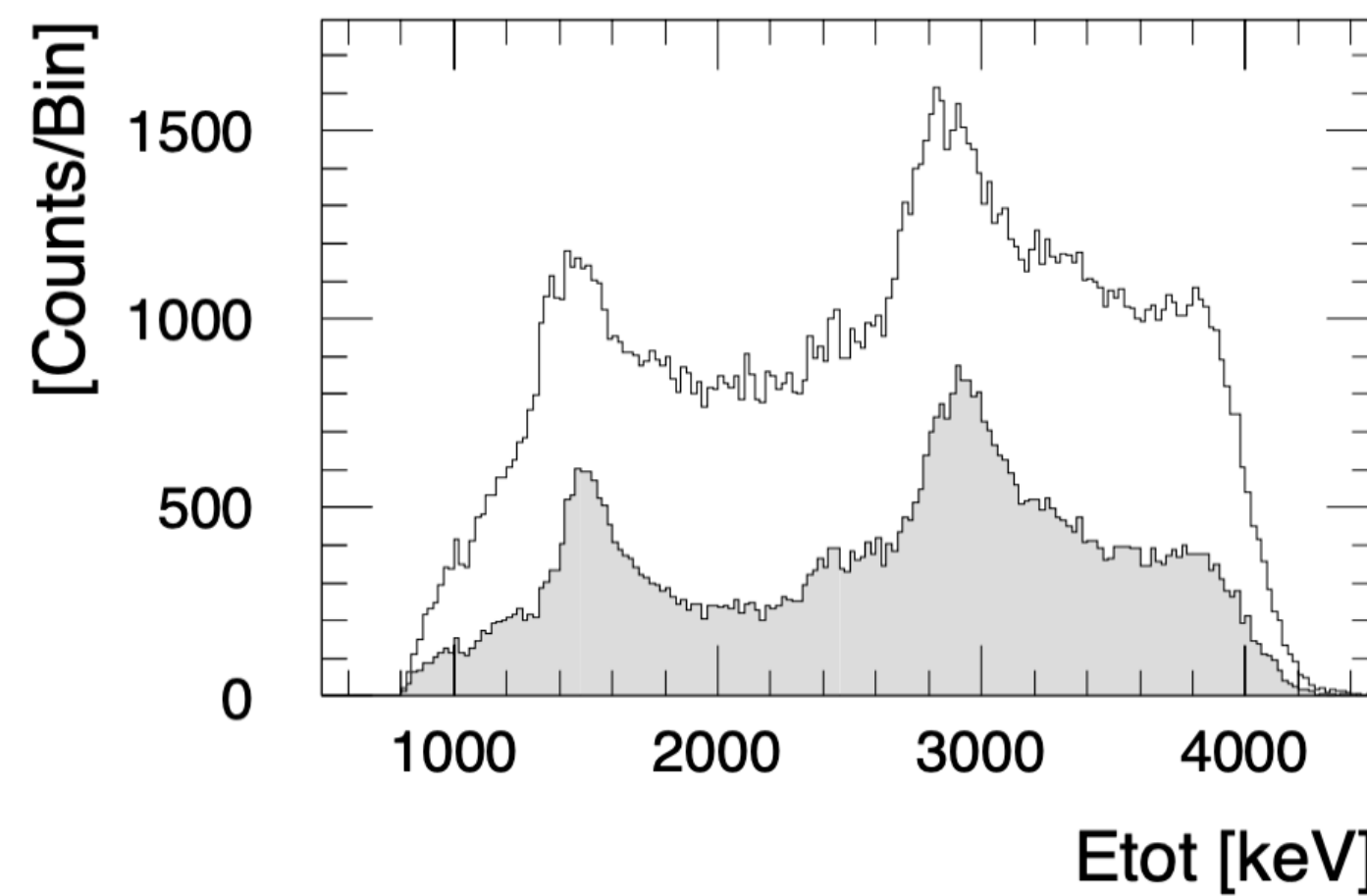
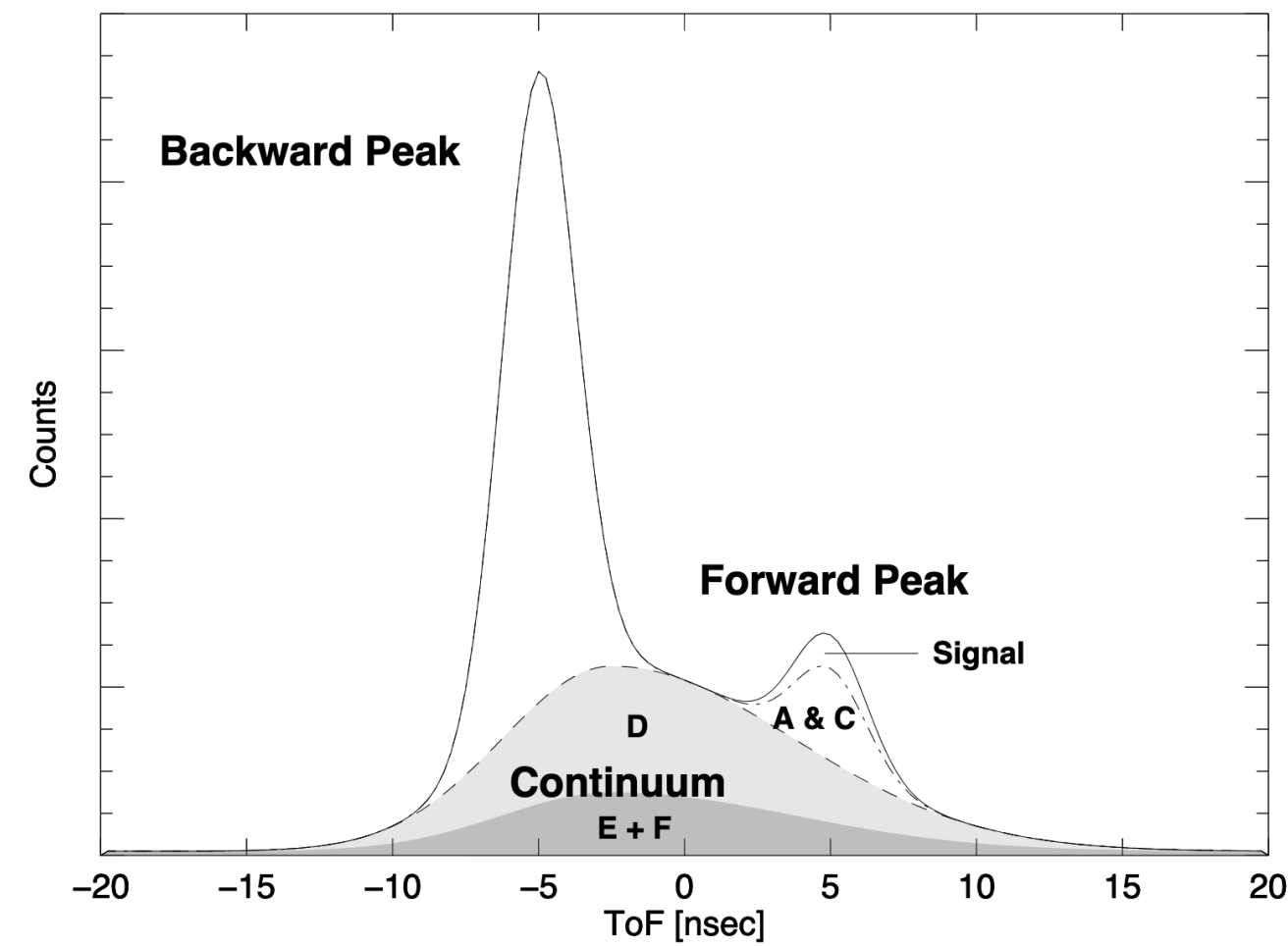
- 1) Admixture of ^{40}K (1.46 MeV), ^{22}Na (1.275 MeV) and ^{24}Na (1.37 MeV).
- 2) Associated with ^{26}Al in the galaxy, but also with a contribution from ^{28}Al activation.
- 3) Capture of ambient (thermalized) neutrons in H-rich D1 scintillator (2.223 MeV).
- 4) Associated with activation of ^{24}Na (2.75 MeV) and ^{208}Tl (2.6 MeV).
- 5) May be associated with activation of ^{24}Na (1.37, 2.75 MeV).

Weidenspointner et al. (2001), Astr. Ap., 368, 347.

COMPTEL Background

^{24}Na Simulations

The distribution of a given isotope in parameter space has been studied using simulations. This allowed for the identification and quantification of specific isotopes.



Weidenspointner et al. (2001), Astr. Ap., 368, 347.

COMPTEL Activation

Identified Isotopes

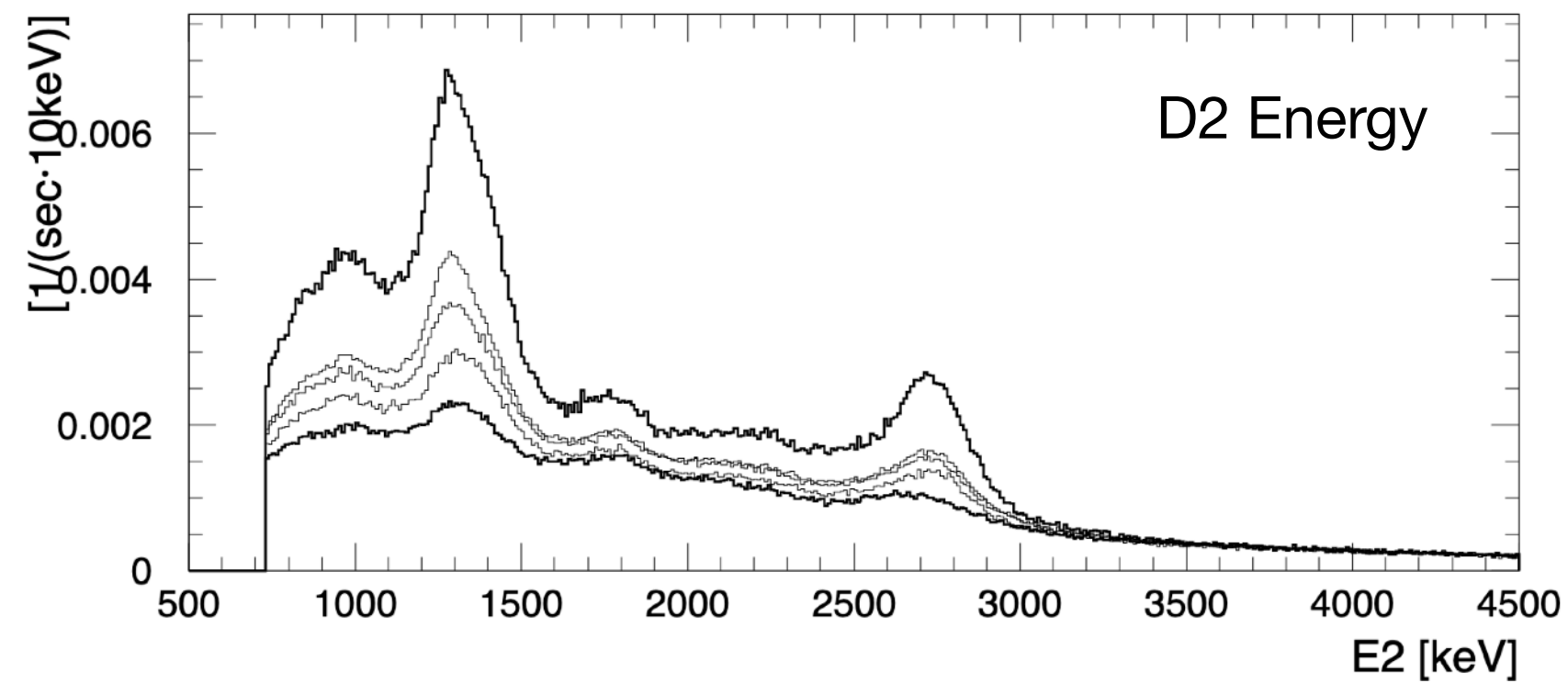
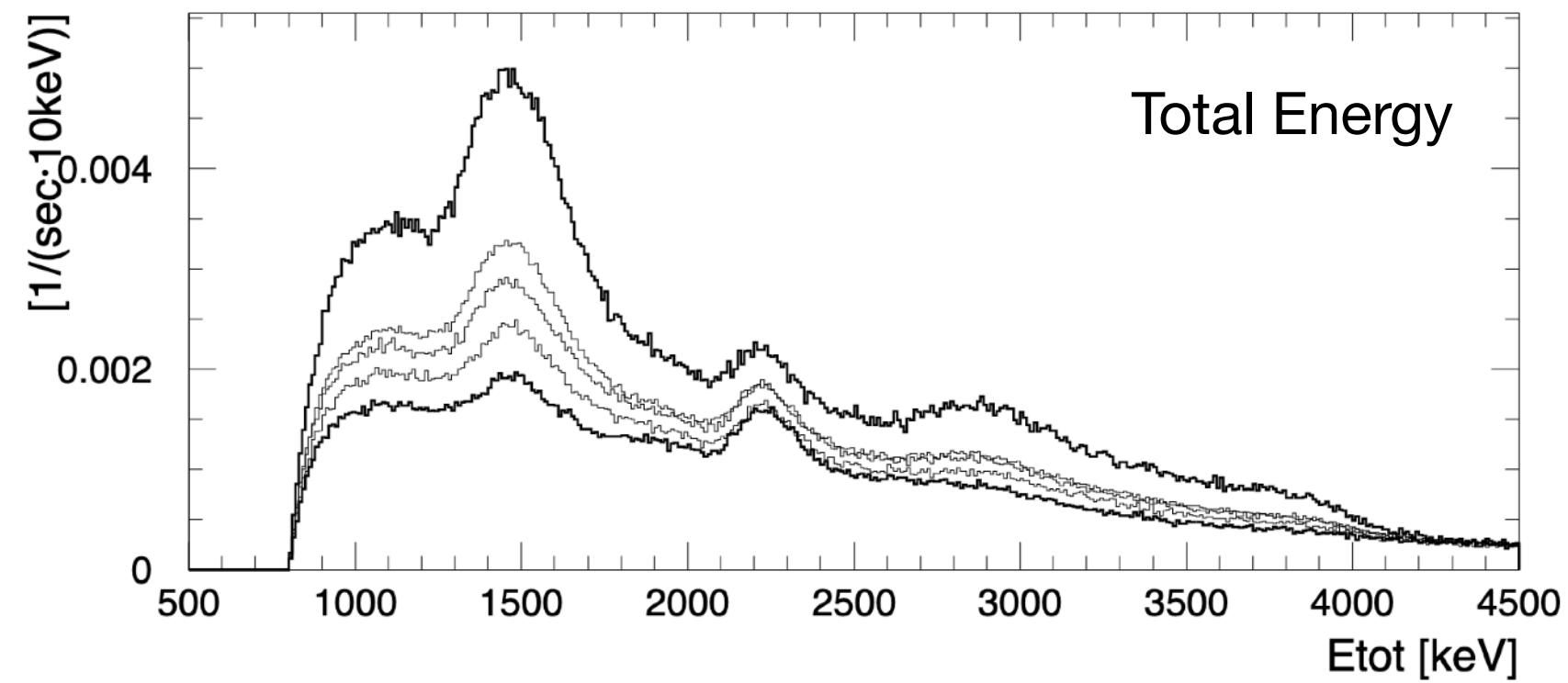
Isotope	Half-Life	Decay Modes and Photon Energies [MeV]	Main Production Channels
^2D	prompt	2.224	$^1\text{H}(\text{n}_{\text{ther}}, \gamma)$
^{22}Na	2.6 y	β^+ (91%): 0.511, 1.275 EC (9%): 1.275	$^{27}\text{Al}(\text{p}, 3\text{p}3\text{n}),$ $\text{Si}(\text{p}, 4\text{p}x\text{n})$
^{24}Na	14.96 h	β^- : 1.37, 2.75	$^{27}\text{Al}(\text{n}, \alpha),$ $^{27}\text{Al}(\text{p}, 3\text{p}\text{n})$
^{28}Al	2.2 min	β^- : 1.779	$^{27}\text{Al}(\text{n}_{\text{ther}}, \gamma)$
^{40}K	$1.28 \cdot 10^9$ y	EC (10.7%): 1.461	primordial
^{52}Mn	5.6 d	EC (64%): 0.744, 0.935, 1.434 β^+ (27%): 0.511, 0.744, 0.935, 1.434	$\text{Fe}(\text{p}, x), \text{Cr}(\text{p}, x),$ $\text{Ni}(\text{p}, x)$
^{57}Ni	35.6 h	β^+ (35%): 0.511, 1.377 EC (30%): 1.377	$\text{Ni}(\text{p}, x), \text{Cu}(\text{p}, x)$
^{208}Tl (^{232}Th)	$1.4 \cdot 10^{10}$ y	β^- (50%): 0.583, 2.614 β^- (25%): 0.511, 0.583, 2.614	primordial

Isotope	Efficiency (Imaging Sel.)	Material	Activity [$\text{g}^{-1} \text{s}^{-1}$]
^2D	$7 \cdot 10^{-4}$	D1 scintillator	$3.4 \cdot 10^{-3}$
^{22}Na	$8 \cdot 10^{-4}$	D1 Al structure	$7 \cdot 10^{-4}$
^{24}Na	$9 \cdot 10^{-4}$	D1 Al structure	$9 \cdot 10^{-4}$
^{28}Al	$2 \cdot 10^{-4}$	D1 Al structure	$2 \cdot 10^{-3}$
^{40}K	$2 \cdot 10^{-4}$	D1 PMT glass	0.2
^{52}Mn	$2 \cdot 10^{-3}$	Fe around D1 Cr around D1 Ni around D1 Cu around D1	$4 \cdot 10^{-4}$ $3 \cdot 10^{-4}$ $2 \cdot 10^{-4}$ $7 \cdot 10^{-5}$
^{57}Ni	$5 \cdot 10^{-4}$	Ni around D1 Cu around D1	$5 \cdot 10^{-4}$ $6 \cdot 10^{-5}$
^{208}Tl	$2 \cdot 10^{-3}$	D1 PMT glass	10^{-2}

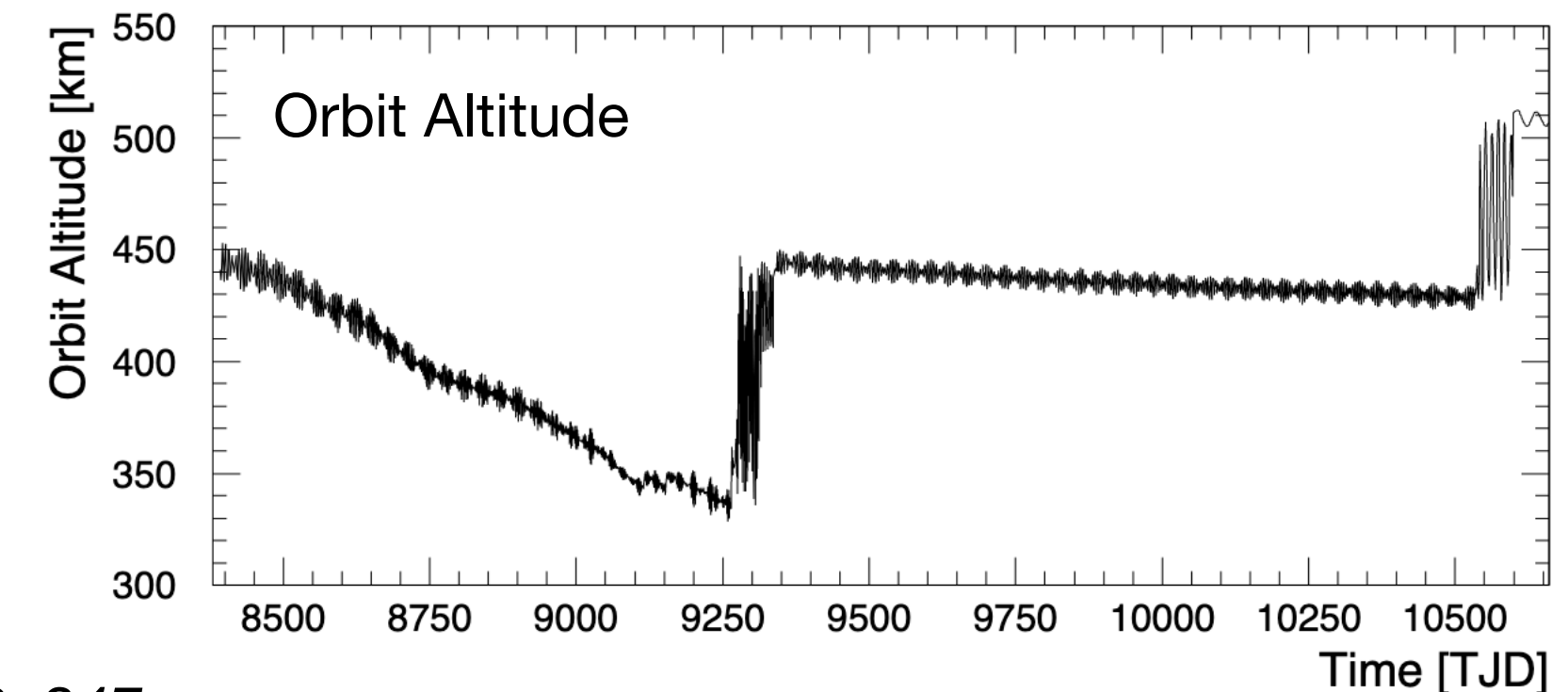
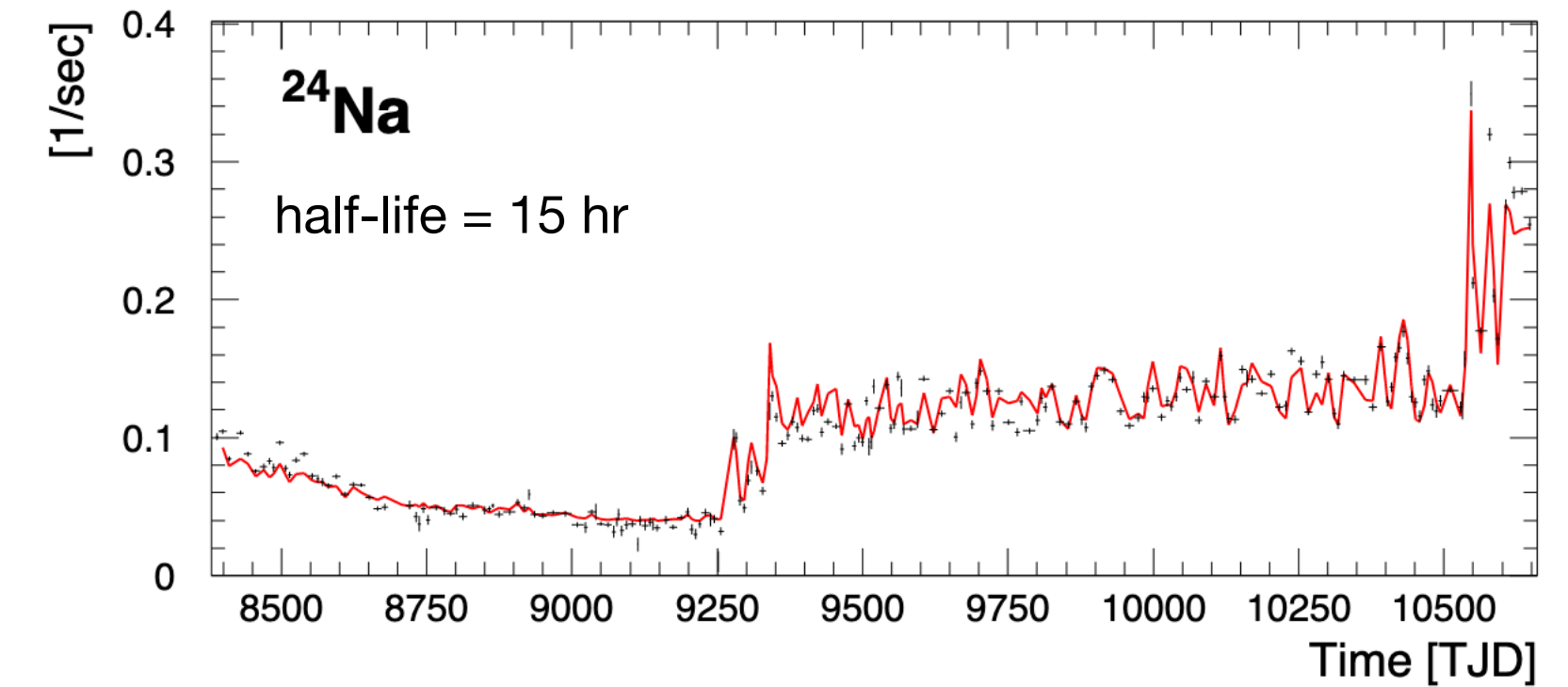
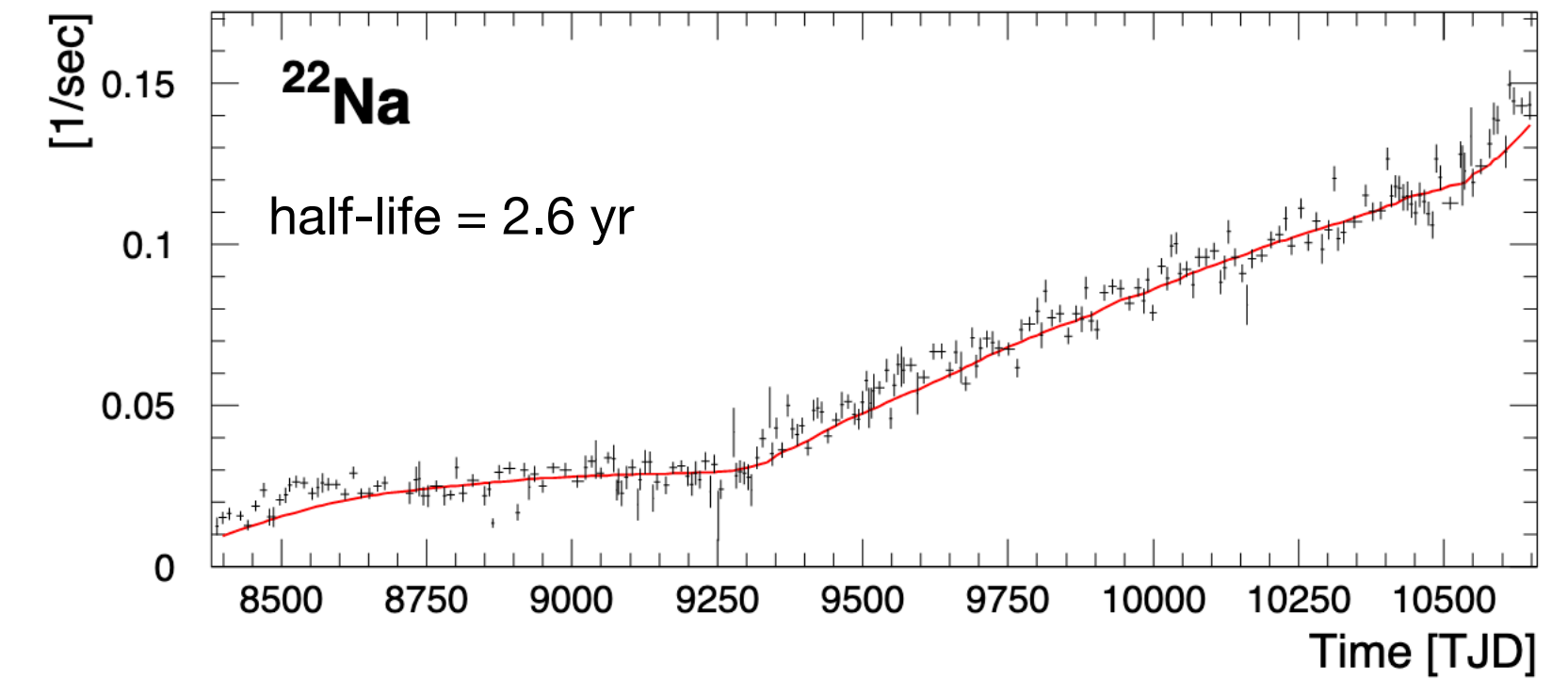
Weidenspointner et al. (2001), *Astr. Ap.*, 368, 347.

COMPTEL Background

Variation in Time



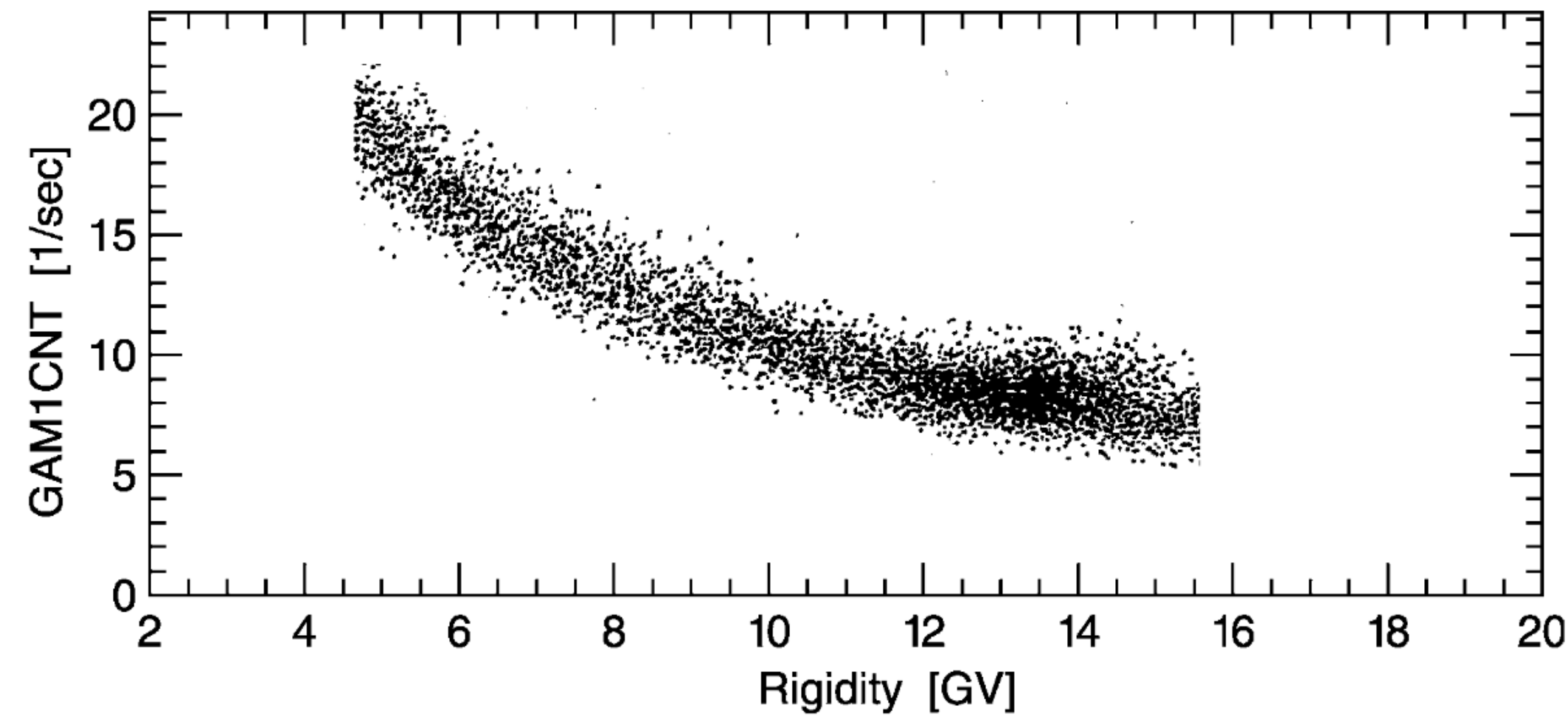
Activation components varied both in time and with changes in orbital altitude.



Weidenspointner et al. (2001), *Astr. Ap.*, 368, 347.

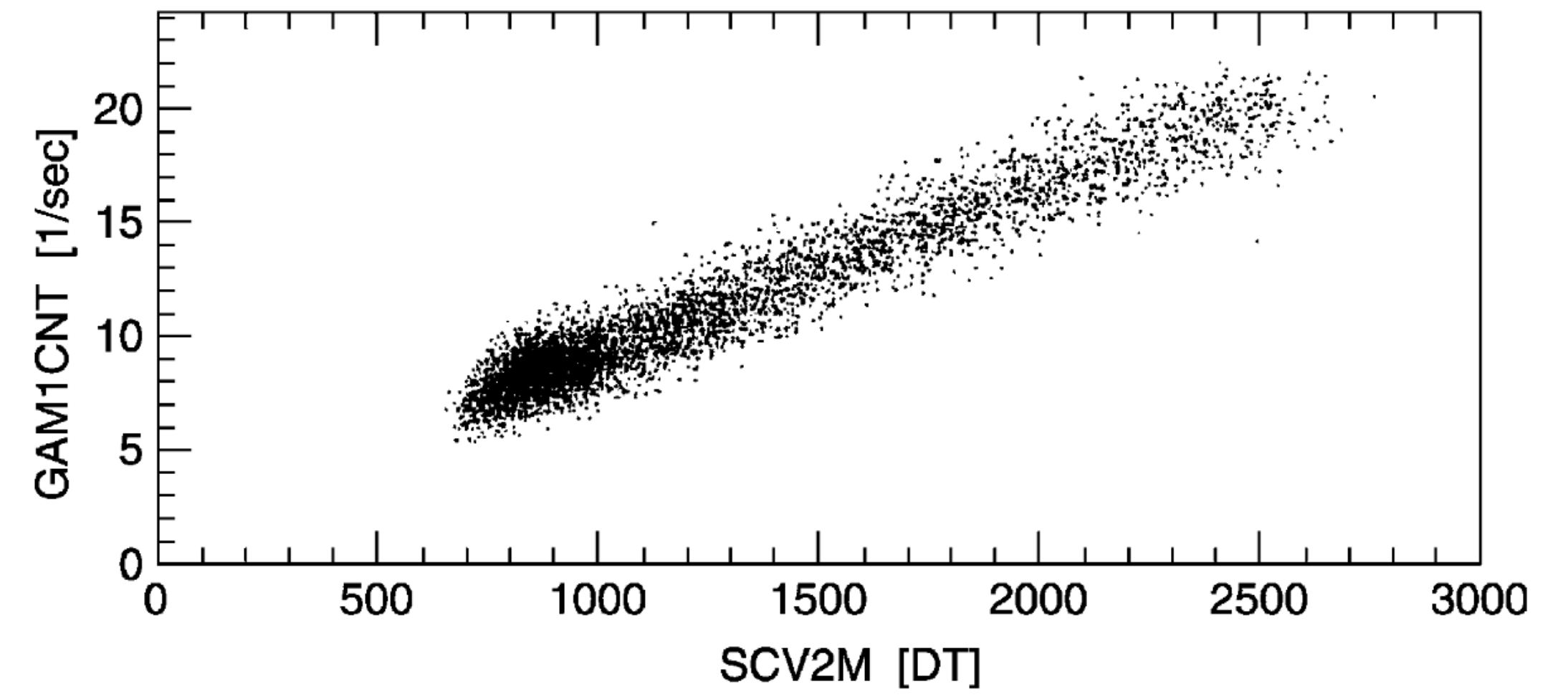
COMPTEL Background

Dependence on Local Particle Background



Gamma-ray Count Rate vs. Geomagnetic Rigidity

Extrapolation to large rigidity values provides an estimate of the background level induced by local particle flux.



Gamma-ray Count Rate vs. Veto (Particle) Rate

Extrapolation to zero veto rate shows that the residual background is a small fraction of the total background.

Most of the COMPTEL background was locally produced.

Schönfelder (2004), New Astr. Rev., 48, 193.

COMPTEL Results

Point Sources

The first (and only) COMPTEL source catalog listed 28 point sources, 4 extended sources, and 31 GRBs.

Incorporated data from the first 5 years of the 9 year mission.

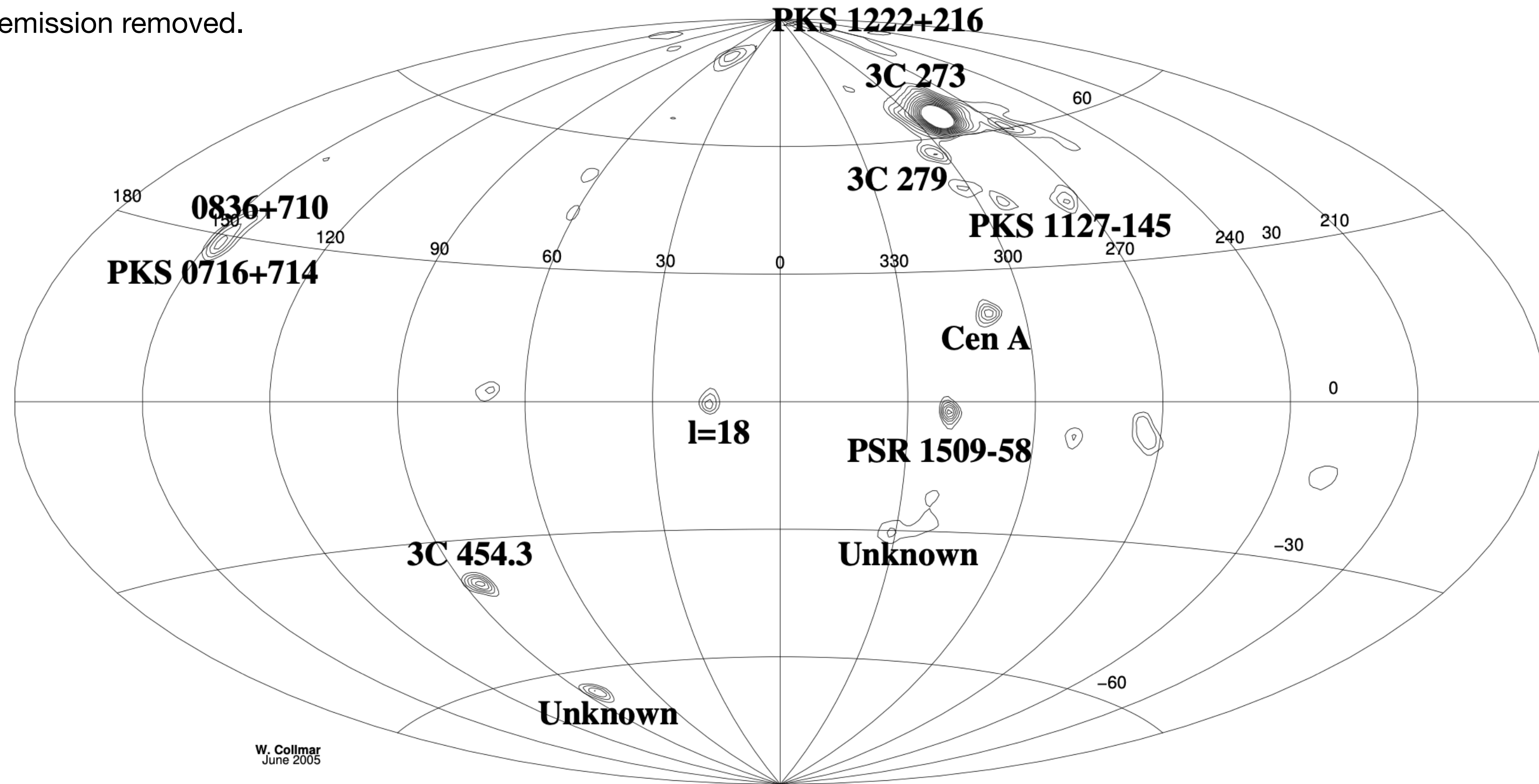
Schönfelder et al. (2003), Astr. Ap. Supp., 143, 145.

Type of Source	No. of Sources	Comments
Spin-Down Pulsars:	3	Crab, Vela, PSR B1509-58.
Stellar Black-Hole Candidates:	2	Cyg X-1, Nova Persei 1992 (GRO J0422+32).
Supernova Remnants: (Continuum Emission)	1	Crab nebula.
Active Galactic Nuclei:	10	CTA 102, 3C 454.3, PKS 0528+135, GRO J0516-609, PKS 0208-512, 3C 273, PKS 1222+216, 3C 279, Cen A, PKS 1622-297.
Unidentified Sources:		
• $ b < 10^\circ$	4	GRO J1823-12, GRO J2228+61 (2CG 106+1.5), GRO J0241+6119 (2CG 135+01), Carina/Vela region (extended).
• $ b > 10^\circ$	5	GRO J1753+57 (extended), GRO J1040+48, GRO J1214+06, HVC complexes M and A area (extended), HVC complex C (extended).
Gamma-Ray Line Sources:		
• 1.809 MeV (^{26}Al)	3	Cygnus region (extended), Vela region (extended, may include RX J0852-4621), Carina region.
• 1.157 MeV (^{44}Ti)	2	Cas A, RX J0852-4621 (GRO J0852-4642).
• 0847 and 1.238 MeV (^{56}Co)	1	SN 1991T.
• 2.223 MeV (n-capture)	1	GRO J0317-853.
Gamma-Ray Burst Sources: (within COMPTEL field-of-up to Phase IV/Cycle-5)	31	Location error radii vary from 0.34° to 2.79° (mean error radius: view 1.13°).

COMPTEL Results

3-10 MeV All-Sky Map

Crab and diffuse emission removed.



W. Collmar
June 2005

Collmar (2006), ASP Conf. Ser., 350, 120

COMPTEL Results

Active Galactic Nuclei

Original COMPTEL catalog
identified 10 AGN.

Later studies have identified
as many as 15 AGNs.

Among these are the “MeV
blazars” (first discovered by
COMPTEL) that are among
the most luminous blazars.

Source	Redshift	AGN Type	Significance
Cen A	0.0007	radio galaxy	high
Mkn 421	0.031	BL Lac object	low
3C 273	0.158	quasar	high
PKS 1222+216	0.435	quasar	medium
3C 279	0.538	quasar	high
PKS 1622-297	0.815	quasar	high
3C 454.3	0.859	quasar	high
PKS 0208-512	1.003	quasar	high
CTA 102	1.037	quasar	low
GRO J0516-609	1.09	quasar	medium
PKS 1127-145	1.187	quasar	medium
PKS 0528+134	2.06	quasar	high
PKS 0716+714	?	BL Lac object	low
0836+710	2.17	quasar	medium
PKS 1830-210	2.06	quasar	medium

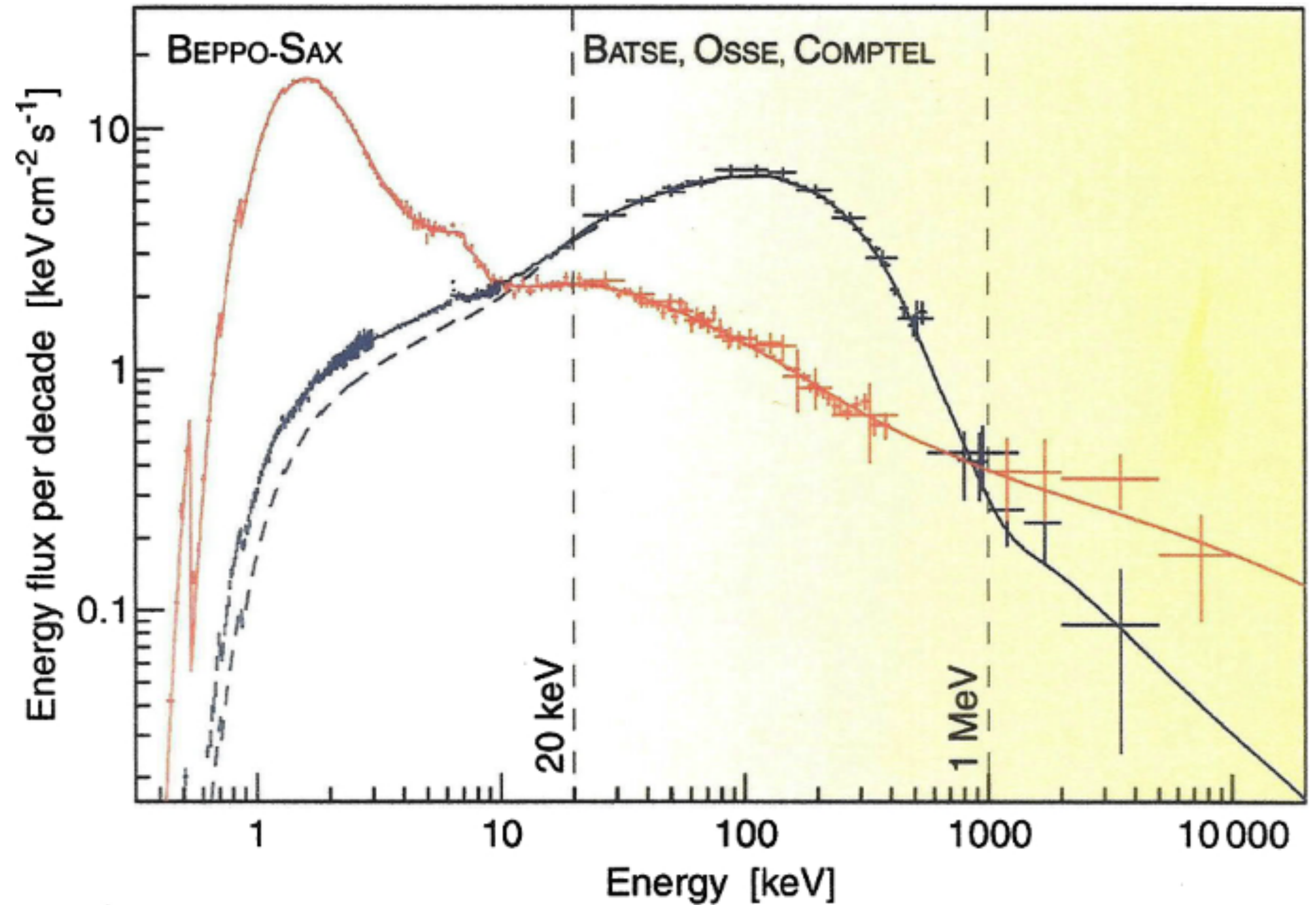
Collmar (2006), ASP Conf. Ser., 350, 120

COMPTEL Results

Cyg X-1

One of only two X-ray binaries detected by COMPTEL.

Observations showed a non-thermal component which varied with the state of the hard X-ray emission.



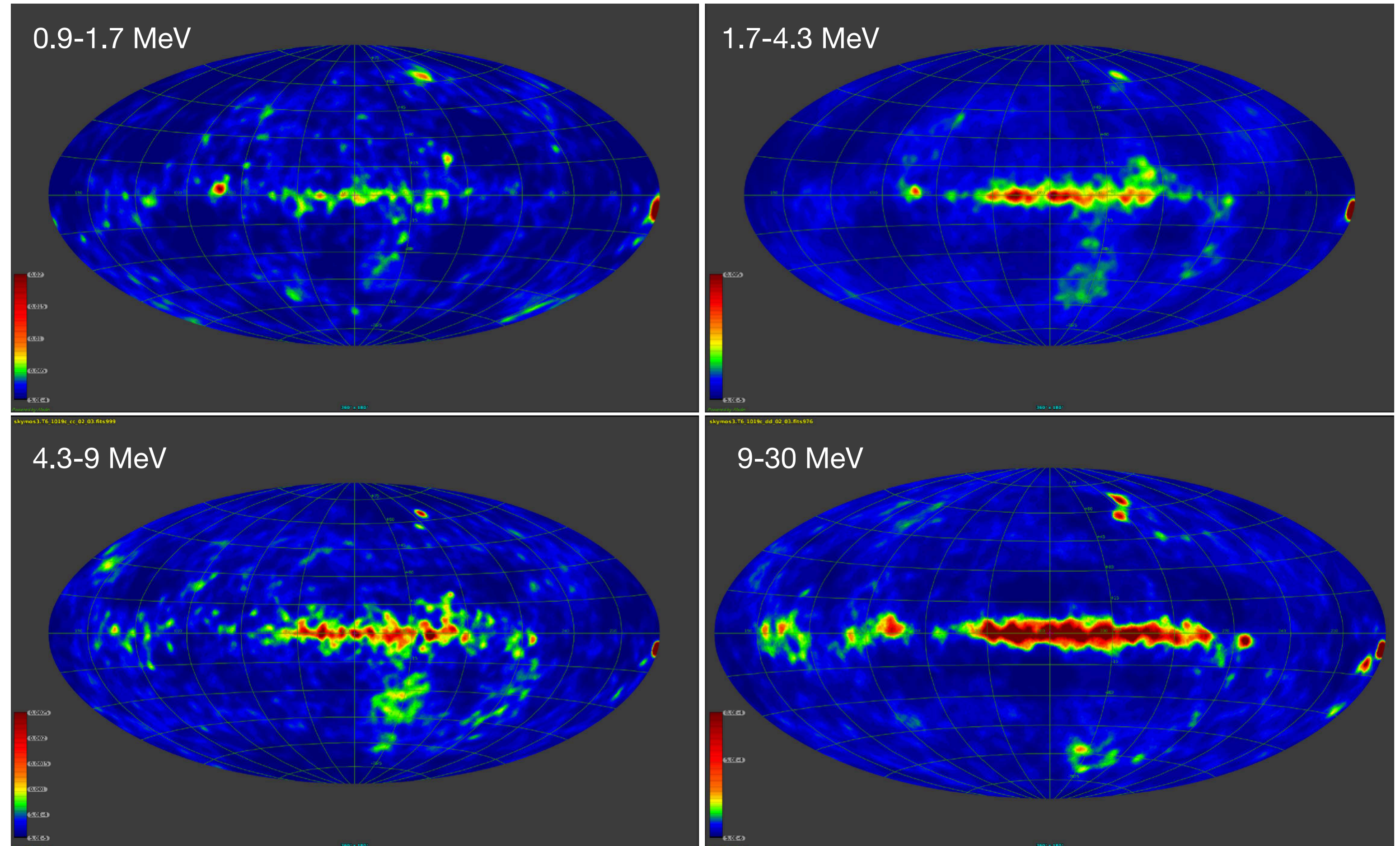
McConnell et al. (2002), Ap. J., 572, 984

COMPTEL Results

Galactic Diffuse Emission

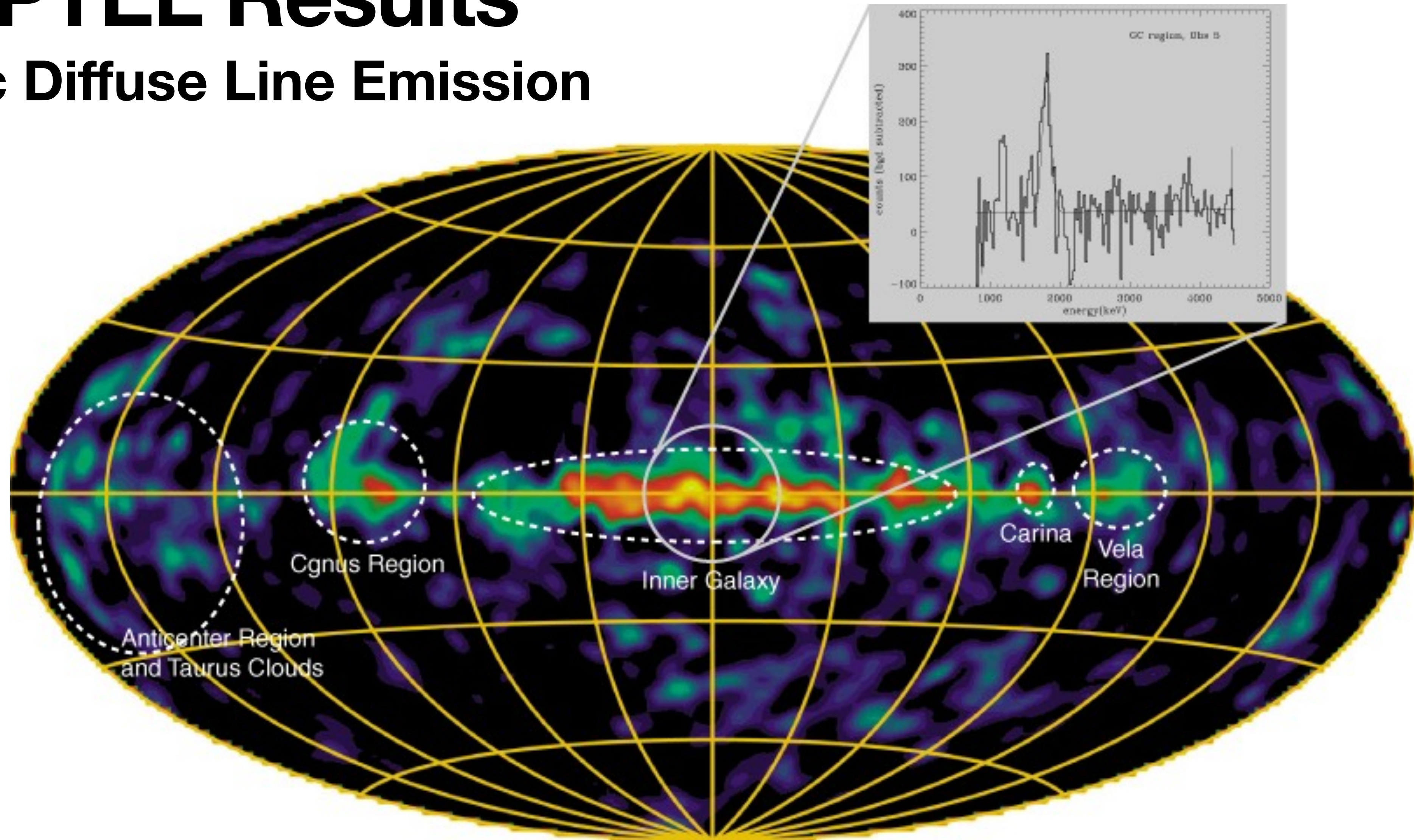
Recent studies have incorporated improved analysis, based in part on advancements in computational capabilities (more memory, faster processors).

Strong & Collmar (2019), Men. S.A.It., 90, 297.



COMPTEL Results

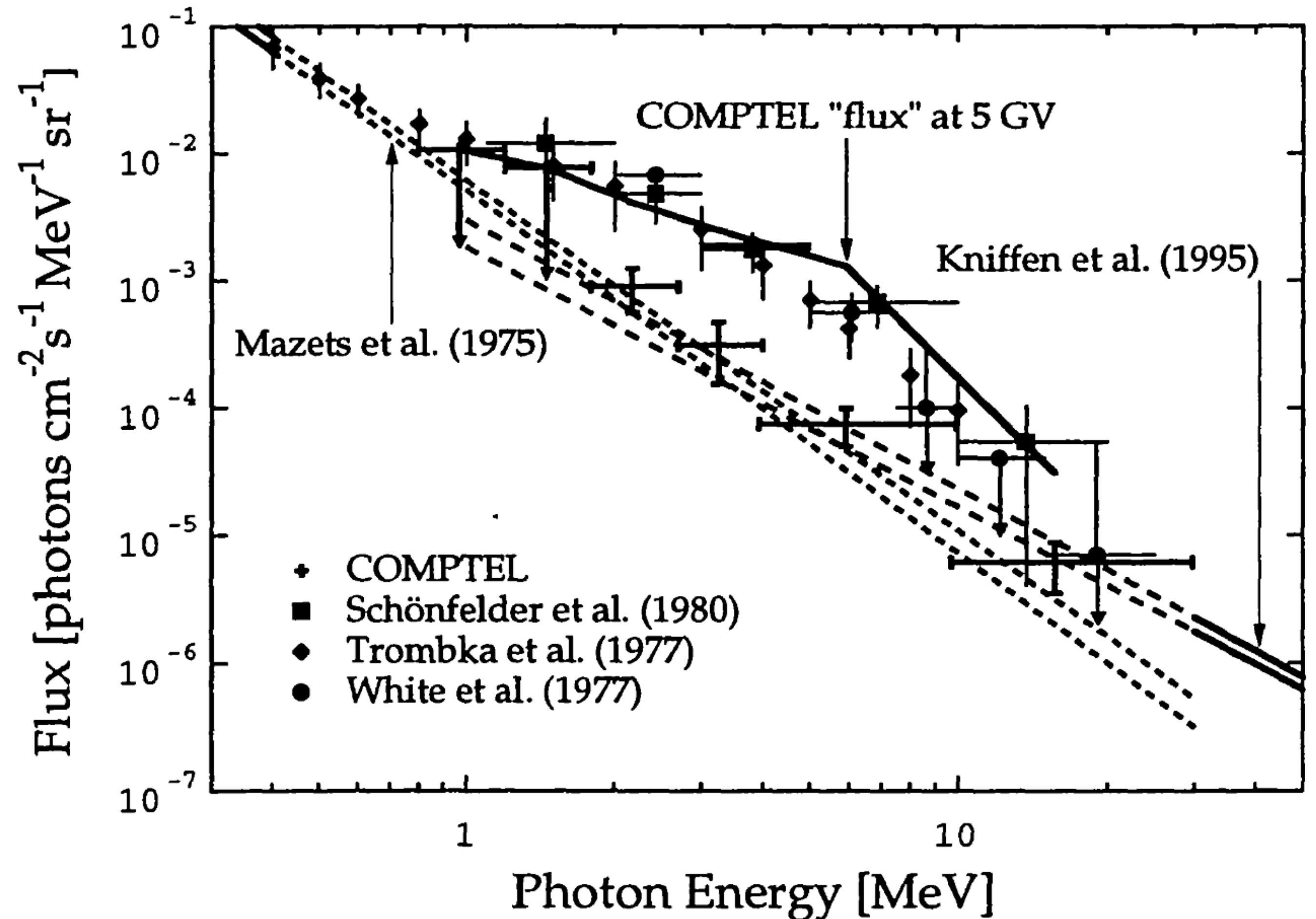
Galactic Diffuse Line Emission



COMPTEL Results

Cosmic Diffuse Emission

COMPTEL dispelled the existence of the “MeV bump” in the cosmic diffuse spectrum and showed that it could be attributed to instrumental background.



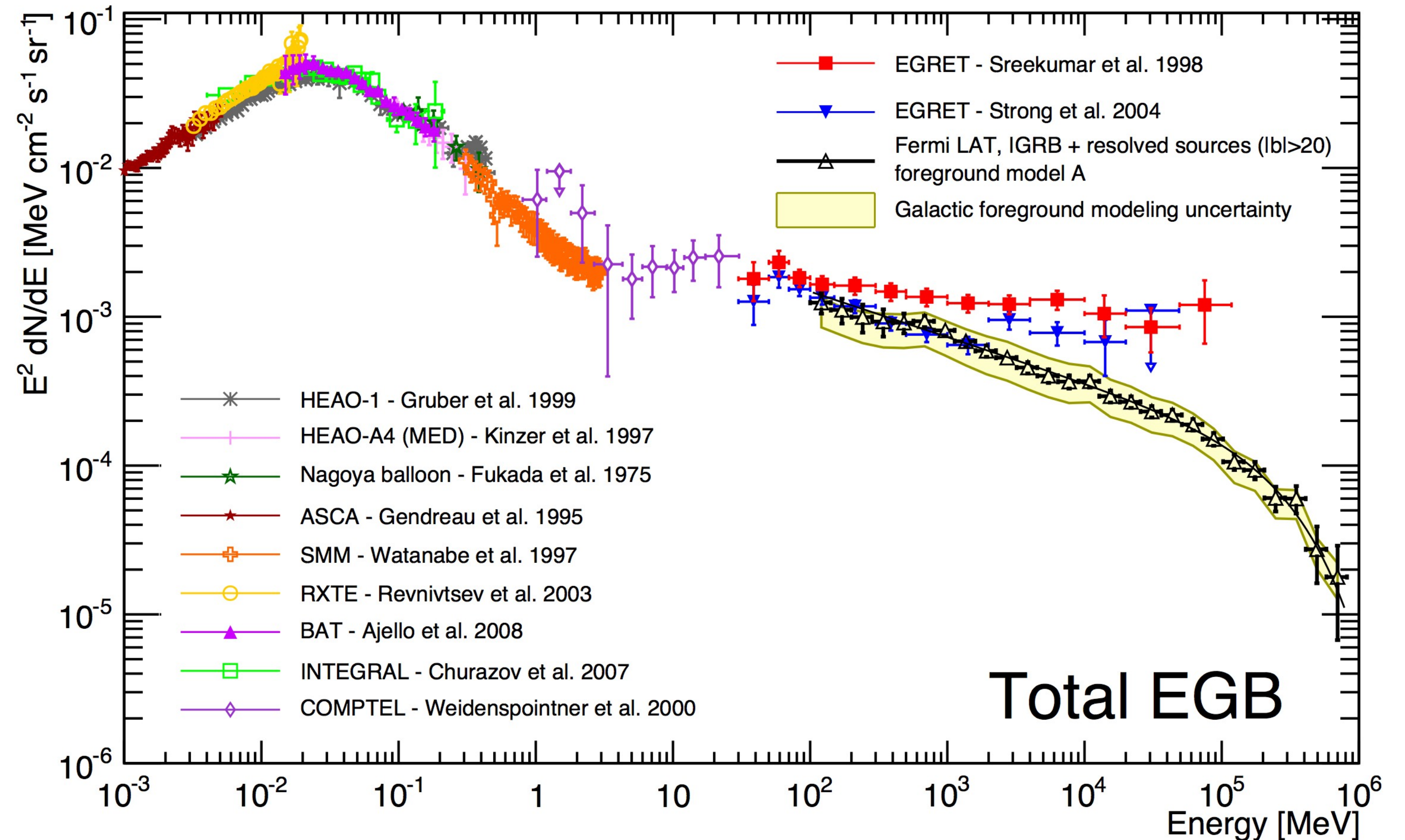
Kappadath et al. (1996), Astron. Astr. Supp., 120, 619.

COMPTEL Results

Cosmic Diffuse Spectrum

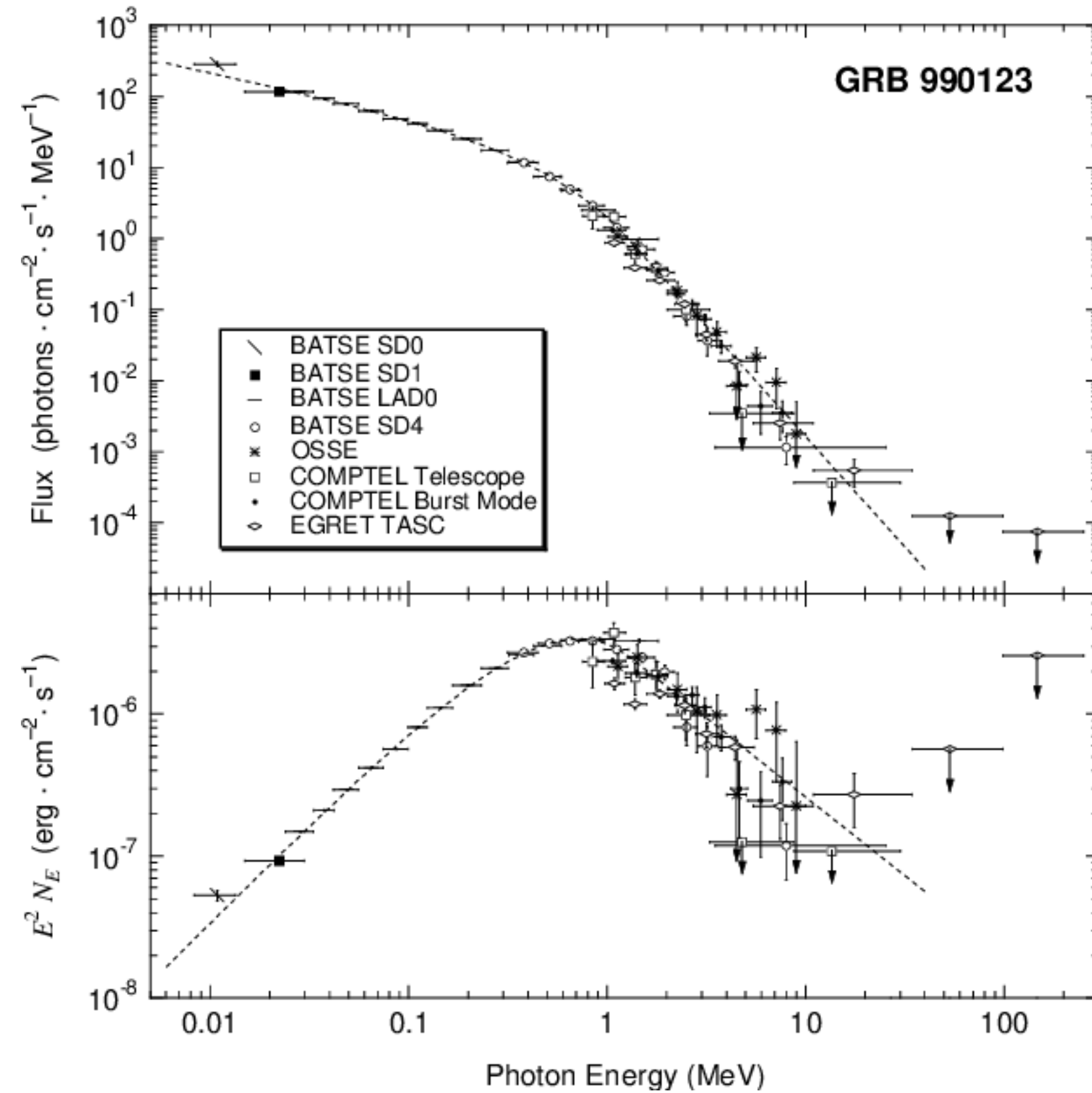
The COMPTEL results provide a smooth connection between low-energy and high-energy measurements.

Studies suggest that the emission can be explained by unresolved AGN and/or See.

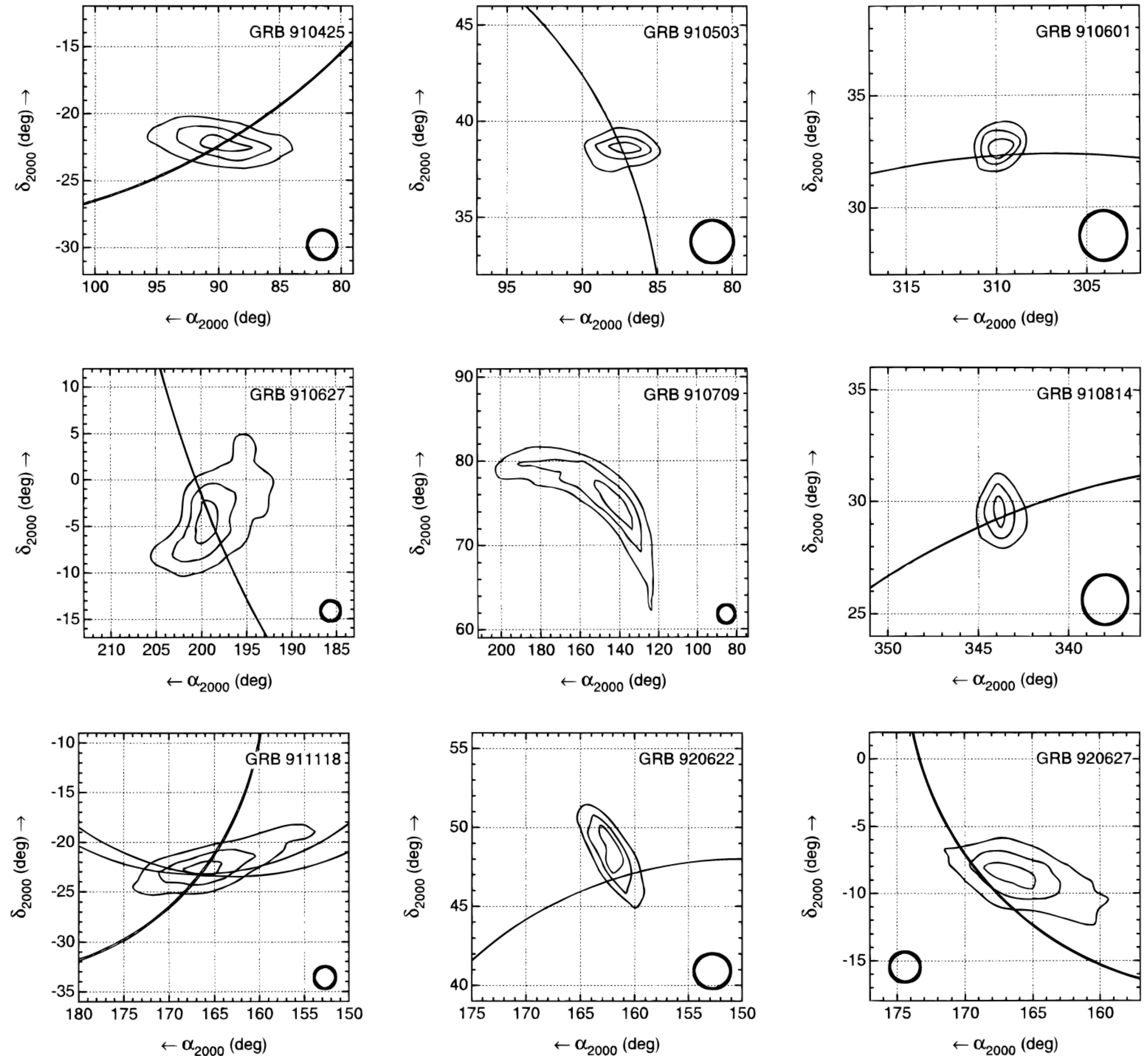


COMPTEL Results

Gamma Ray Bursts



Briggs et al. (1999), Ap. J., 524, 82



Kippen et al. (1998), Ap. J., 492, 246

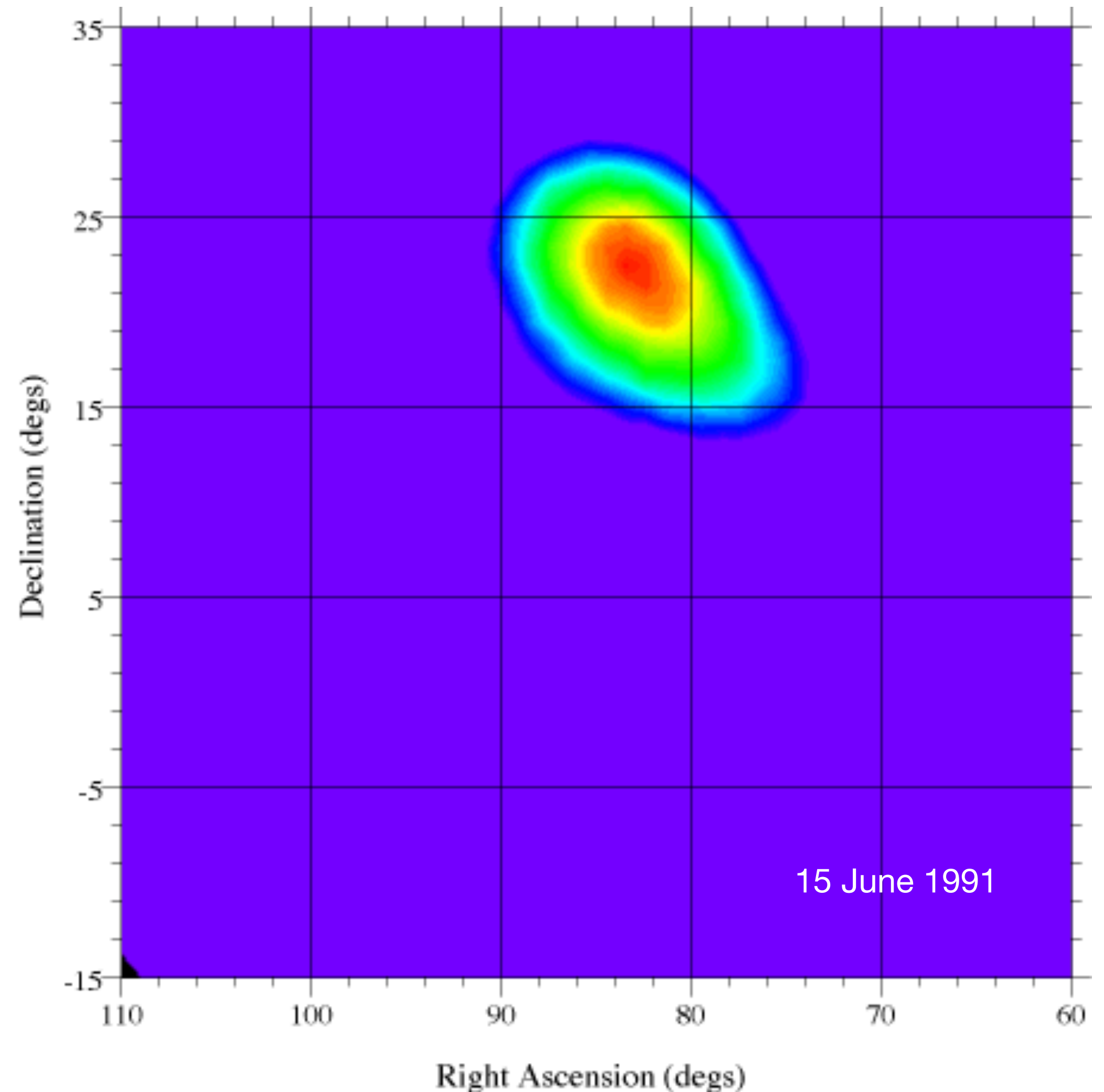
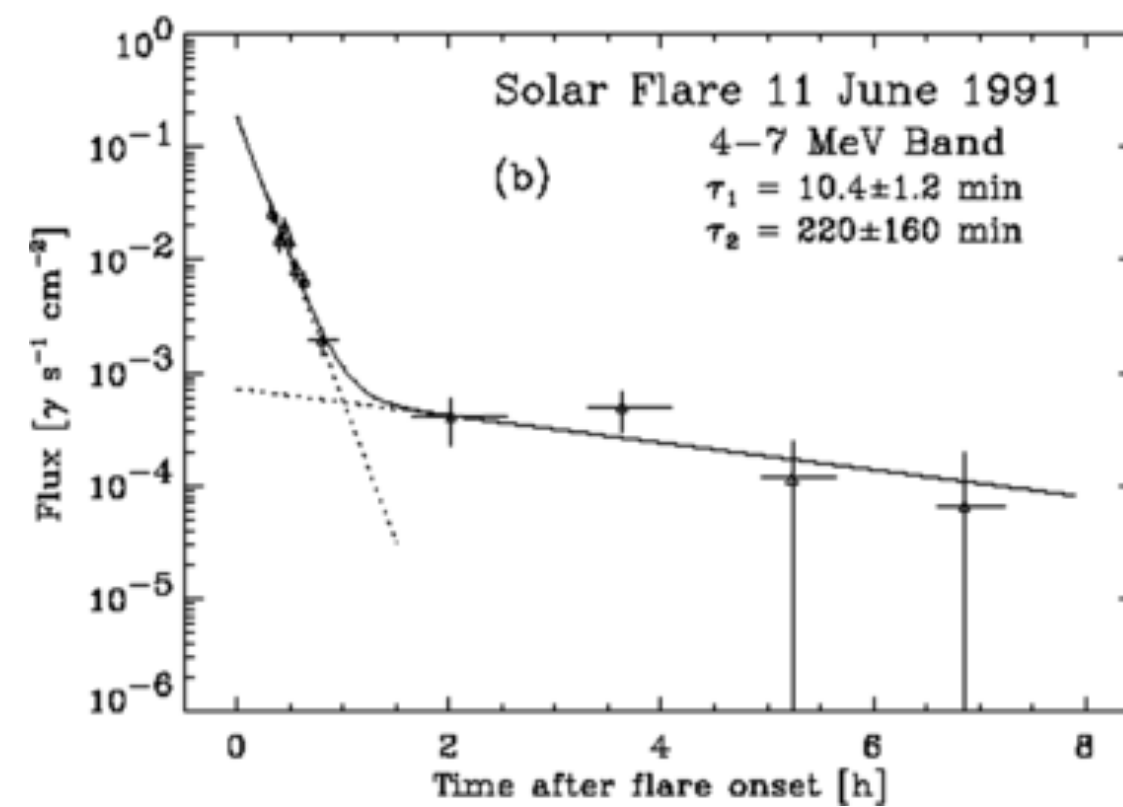
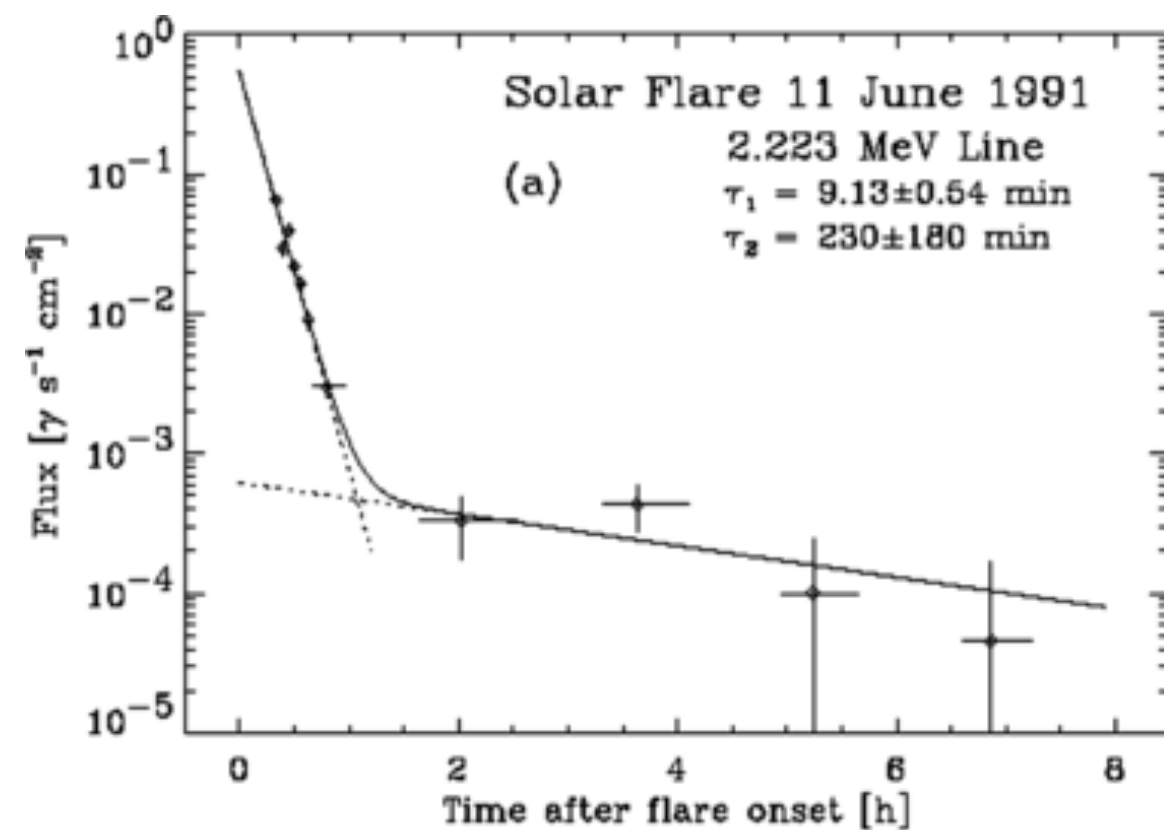
COMPTEL Results

Solar Flares

In the same way that COMPTEL could image photons through Compton scattering, it could also image neutrons through n-p scattering in the D1 scintillator.

Both PSD and ToF could be used to isolate neutron events from photon events.

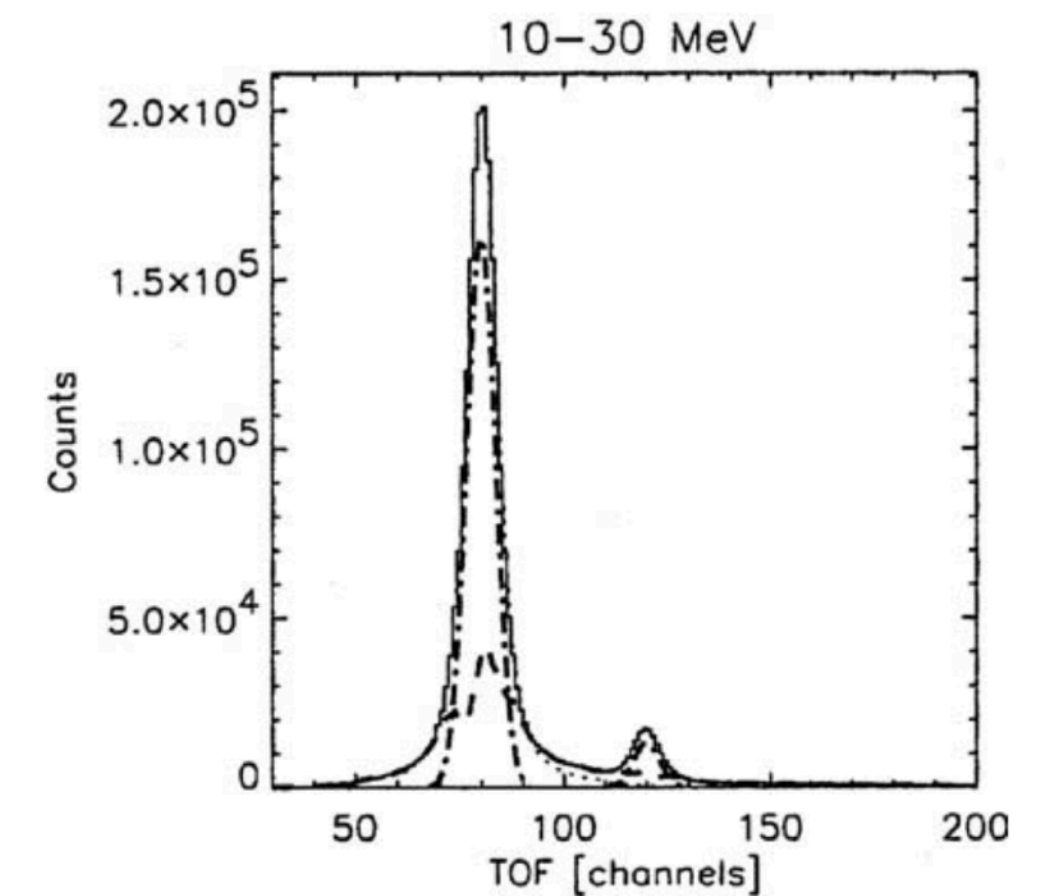
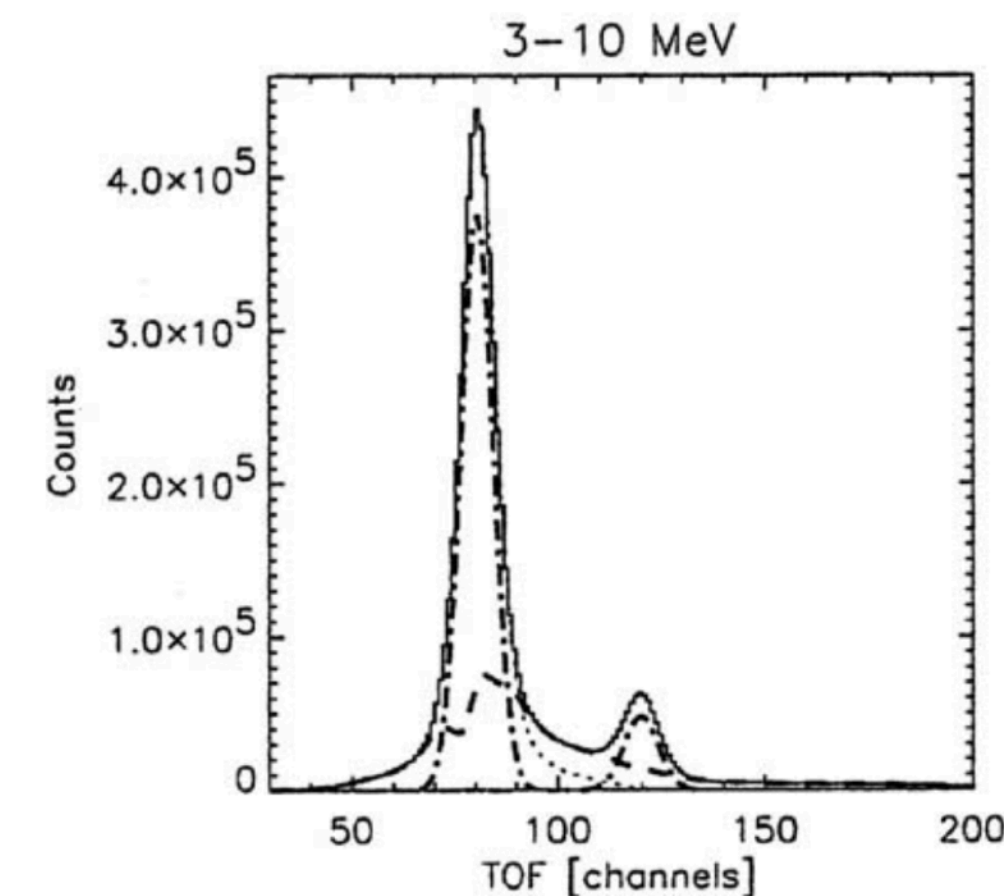
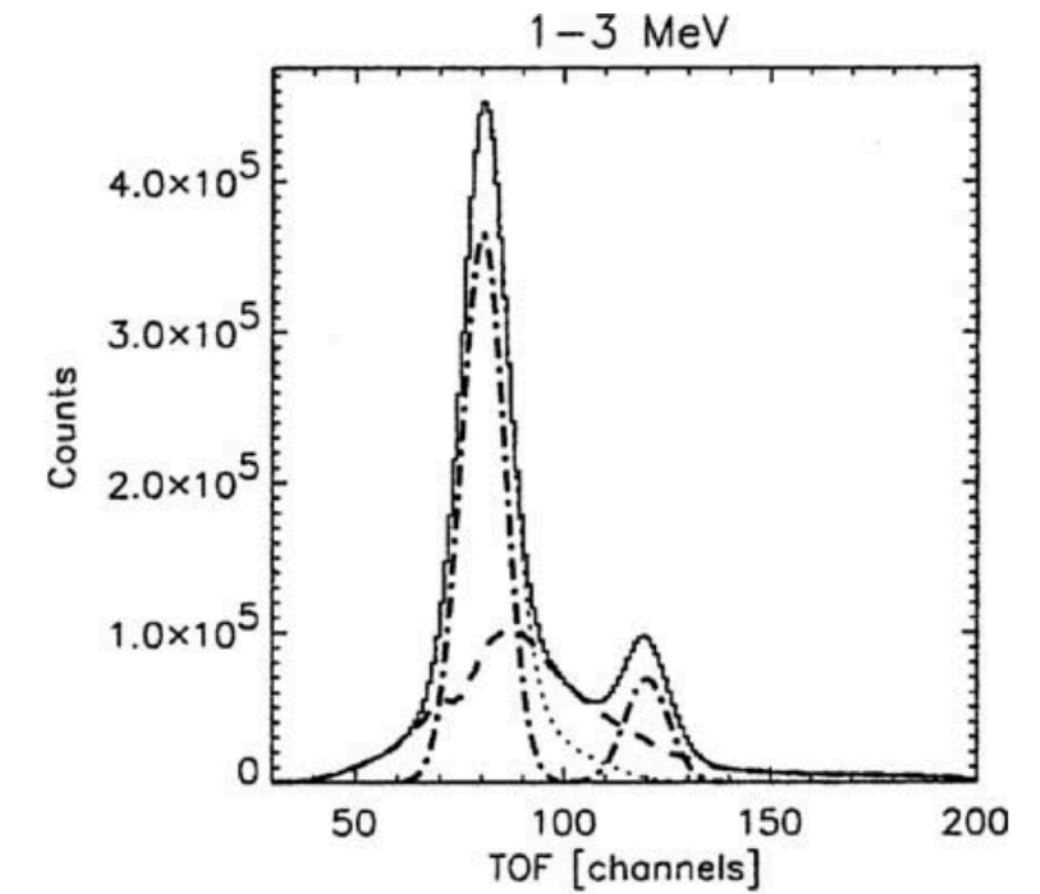
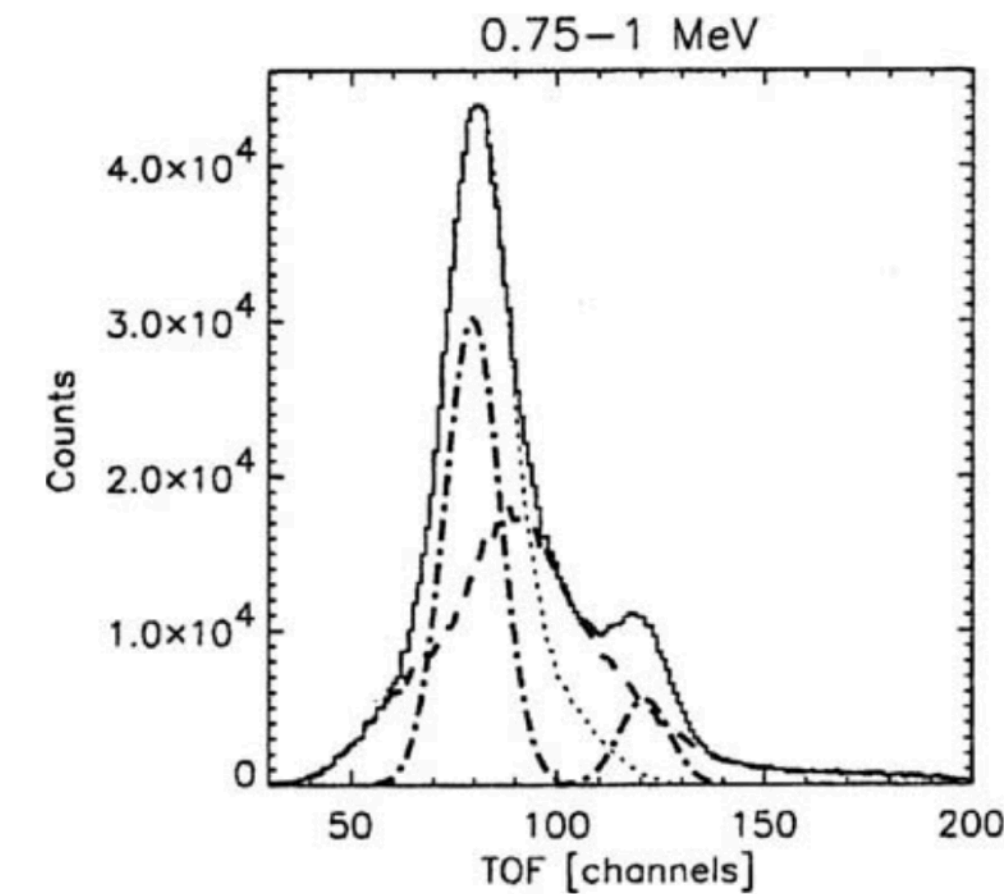
High S/N ratio permitted observations of extended emission in the MeV range.



The COMPTEL Legacy

Importance of Time-of-Flight

- The most effective background rejection tool.
- Up-scattered events were about 10x more abundant than down-scattered events.
- Different background event types exhibited different signatures in ToF.

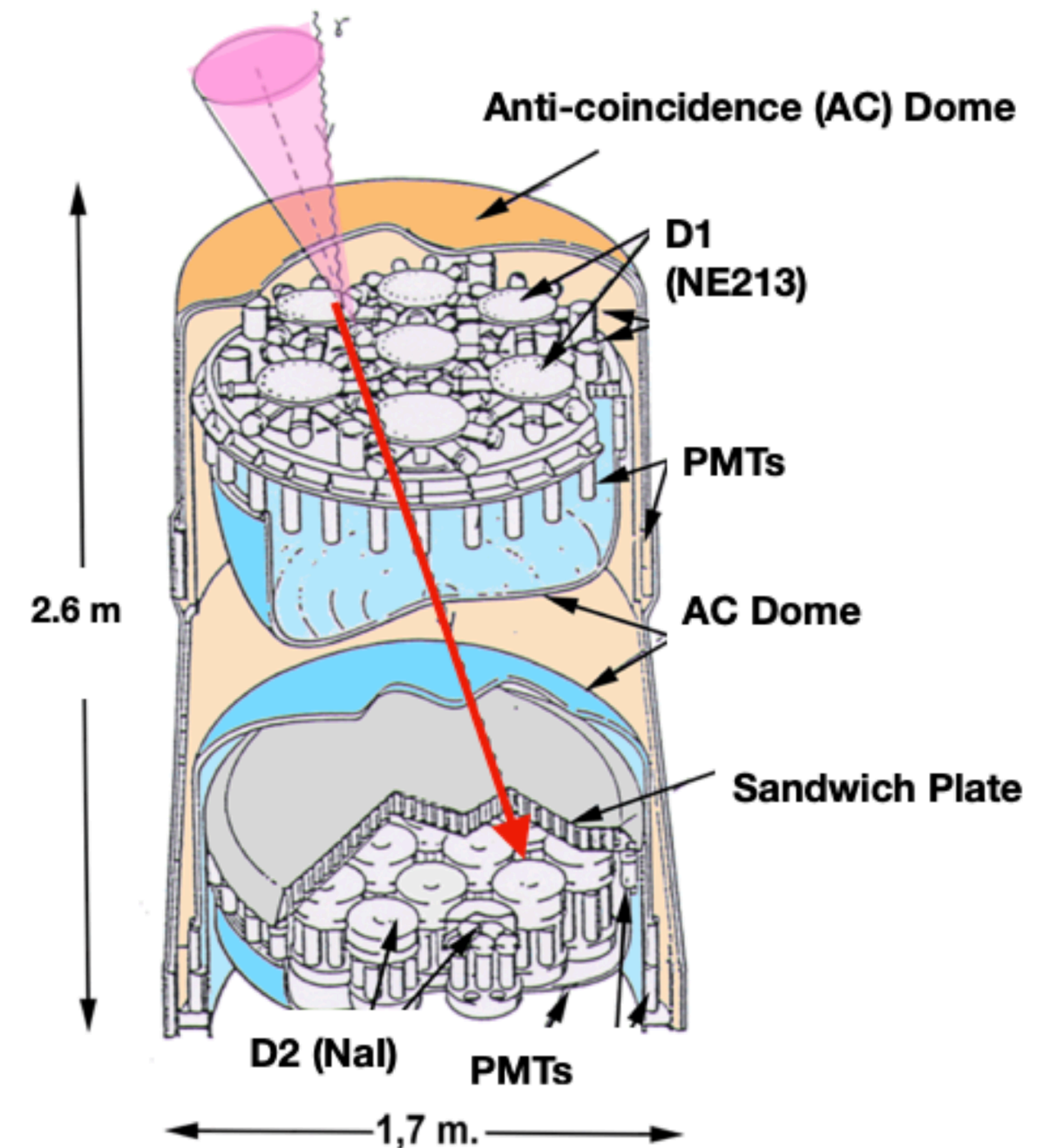


Schönfelder (2004), New Astr. Rev., 48, 193.

The COMPTEL Legacy

Lessons Learned

- Improved angular resolution, which depends on spatial resolution and energy resolution.
- Use of ToF or some comparable parameter.
- Restricting the photon arrival direction to something less than an event circle (“event arc”).
- Minimize use of passive material around the instrument.
- Maximize use of event selections on $\bar{\varphi}$ and scatter direction.
- Careful choice of orbit parameters. Low inclination and low altitude are preferred.
- Sufficiently narrow coincidence window between D1 and D2.

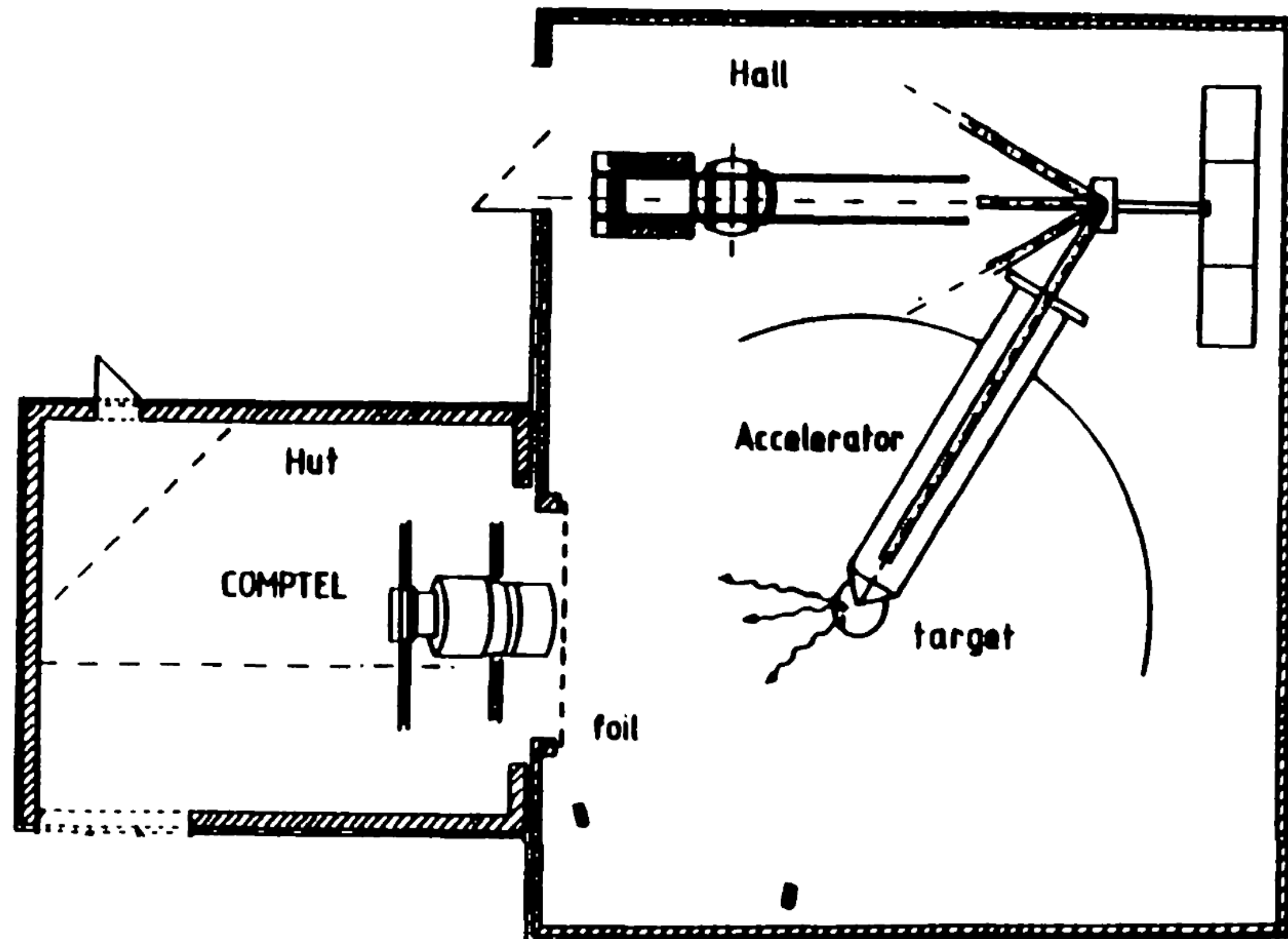


Schönfelder (2004), *New Astr. Rev.*, 48, 193.

Backup Slides

Calibration at Neuherberg

Gesellschaft für Strahlen- und Umweltforschung (GSF)



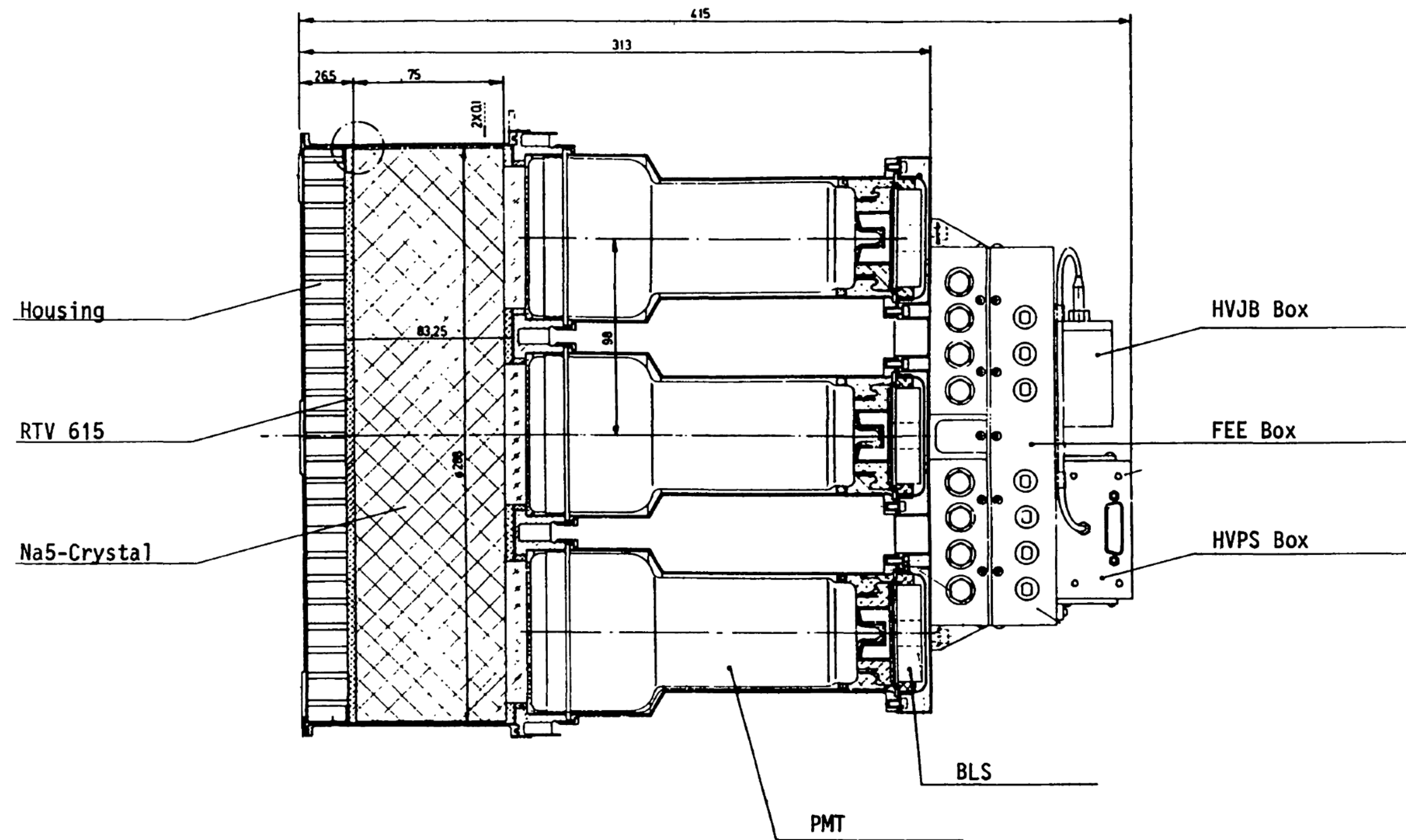
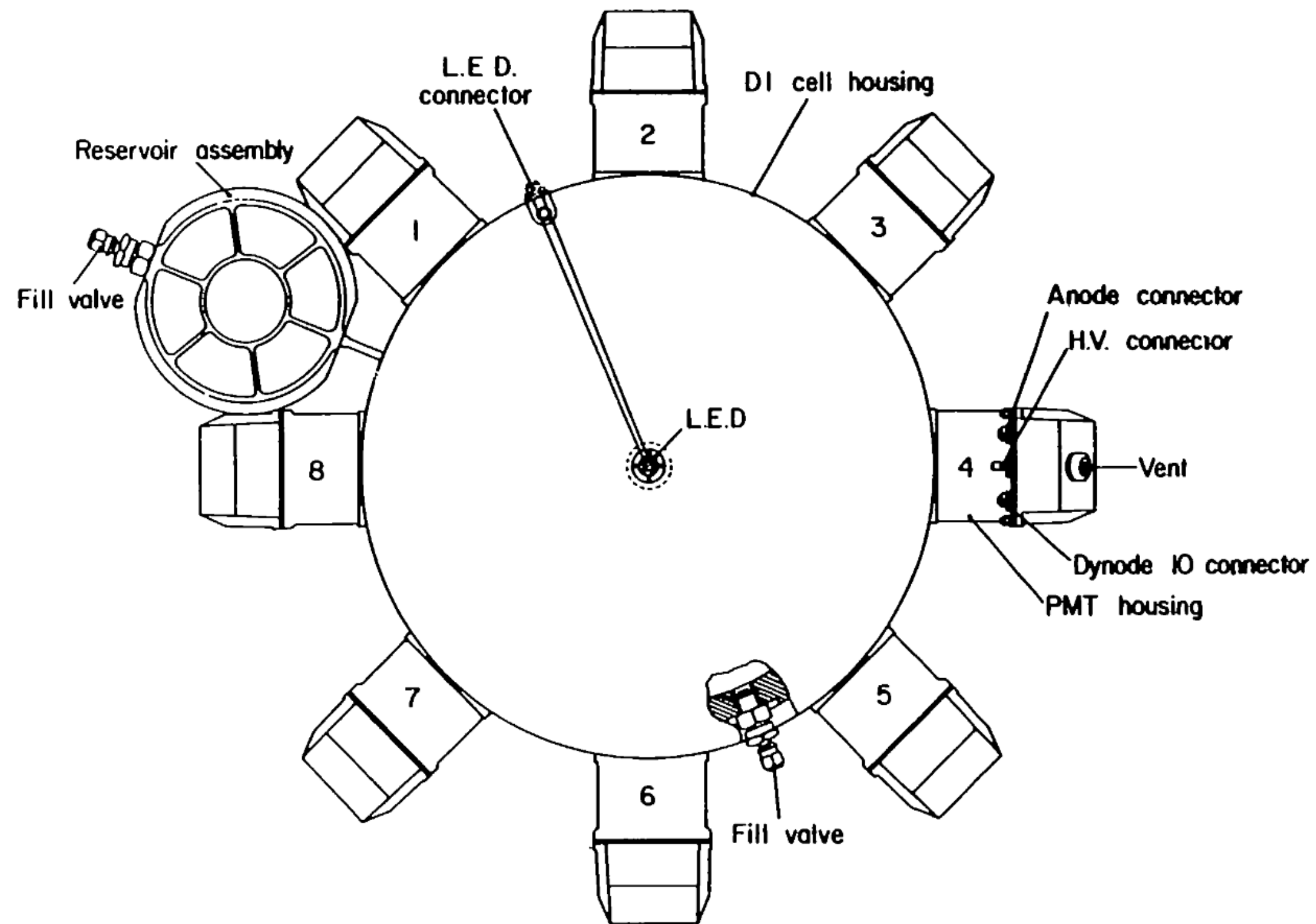
GAMMA-RAY SOURCES USED FOR CALIBRATION

Source	Photon Energy (MeV)
^{137}Cs	0.662
^{54}Mn	0.835
^{22}Na	0.511, 1.275
^{88}Y	0.898, 1.836
^{24}Na	1.369, 2.754
$^{241}\text{Am}/^9\text{Be}$	4.430
$^{19}\text{F}(p, \alpha\gamma)^{16}\text{O}$	6.13
$^{11}\text{B}(p, \gamma)^{12}\text{C}$	12.14, 16.57, 4.43
$^3\text{H}(p, \gamma)^4\text{He}$	20.52

Schönfelder et al. (1993), *Ap. J. Supp.*, 86, 657.

COMPTEL Detectors

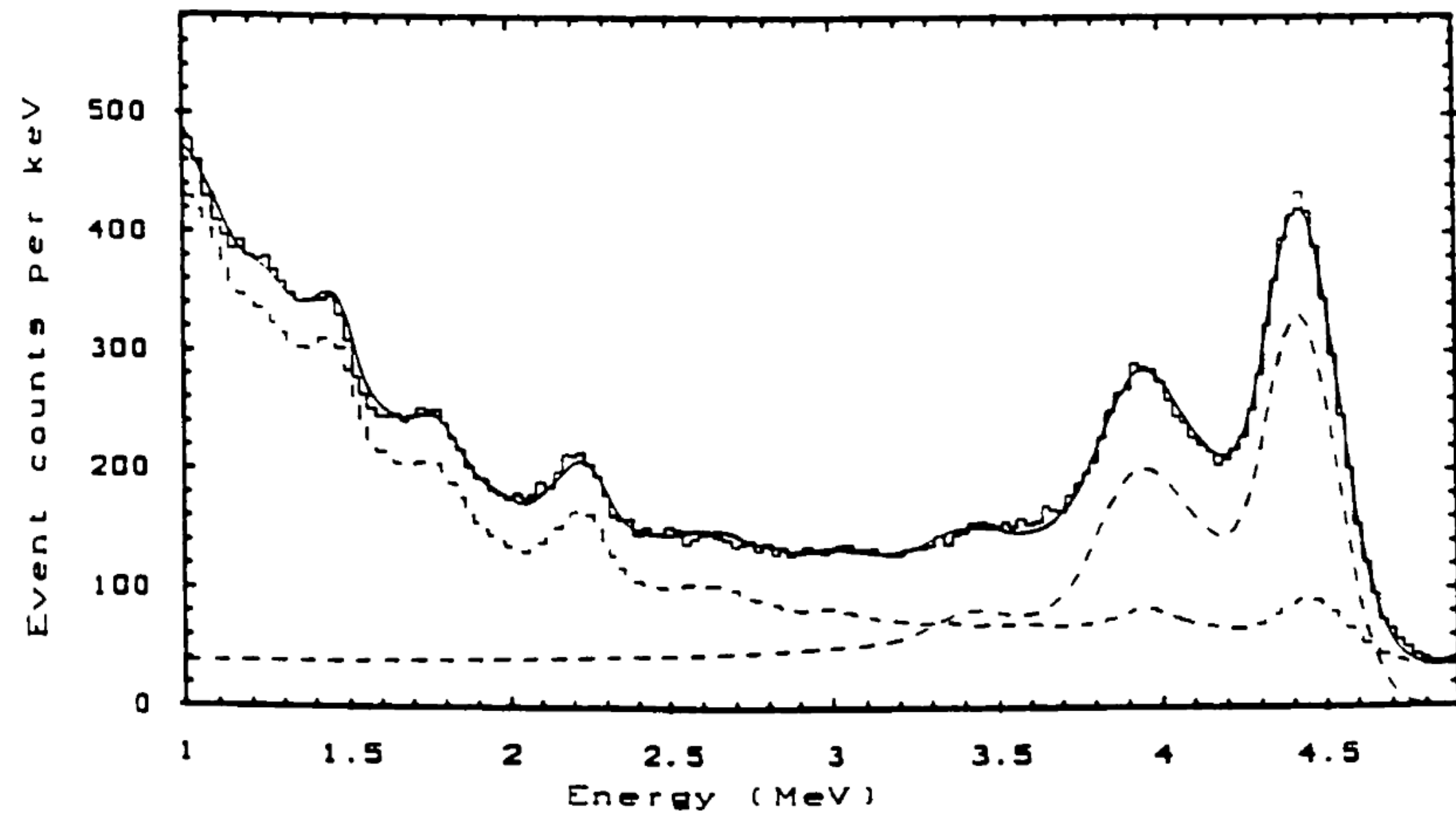
D1 and D2 Modules



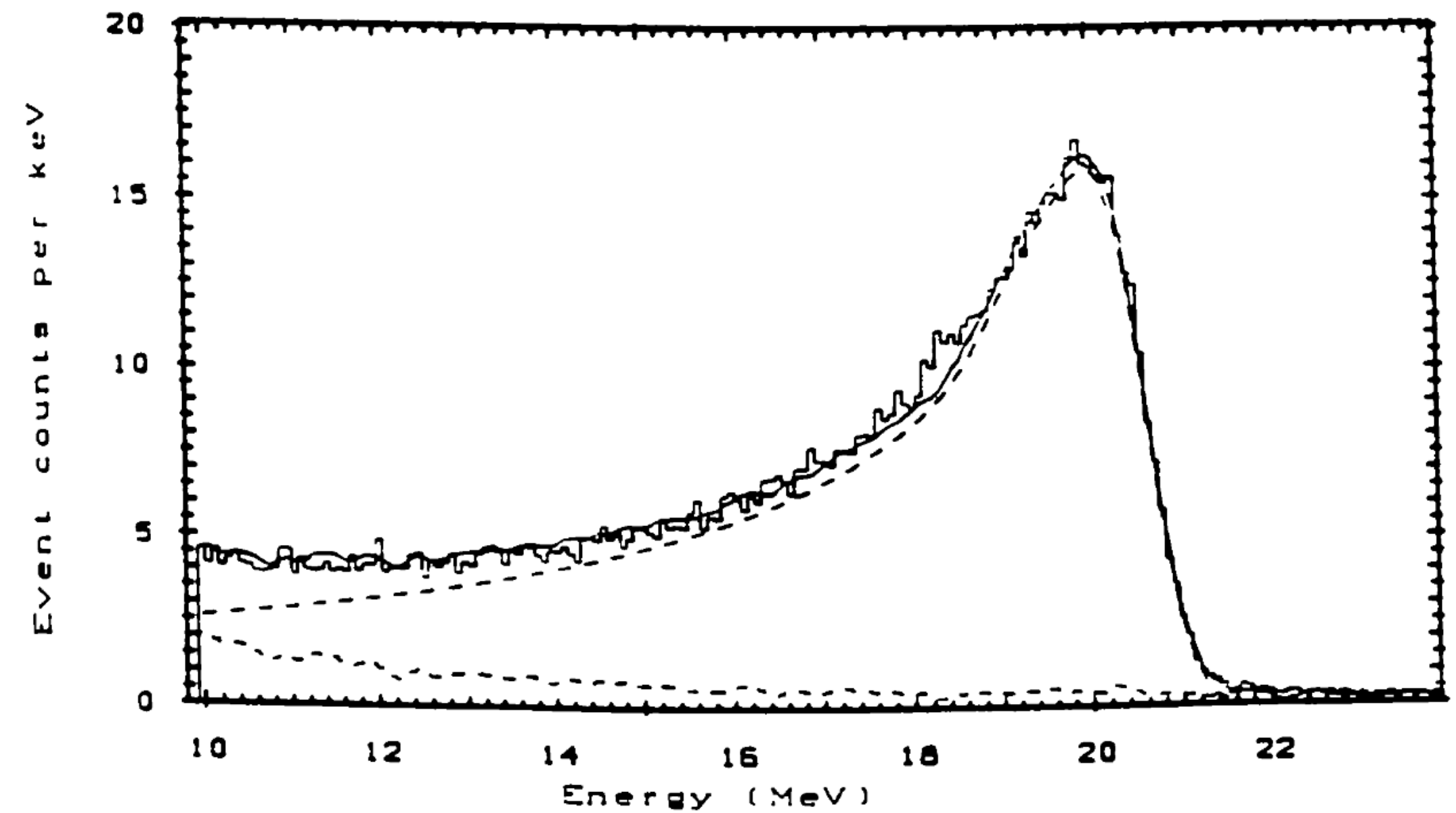
Schönfelder et al. (1993), *Ap. J. Supp.*, 86, 657.

D2 Spectra

Pre-Flight Calibration Data



AmBe source - 4.438 MeV γ -rays

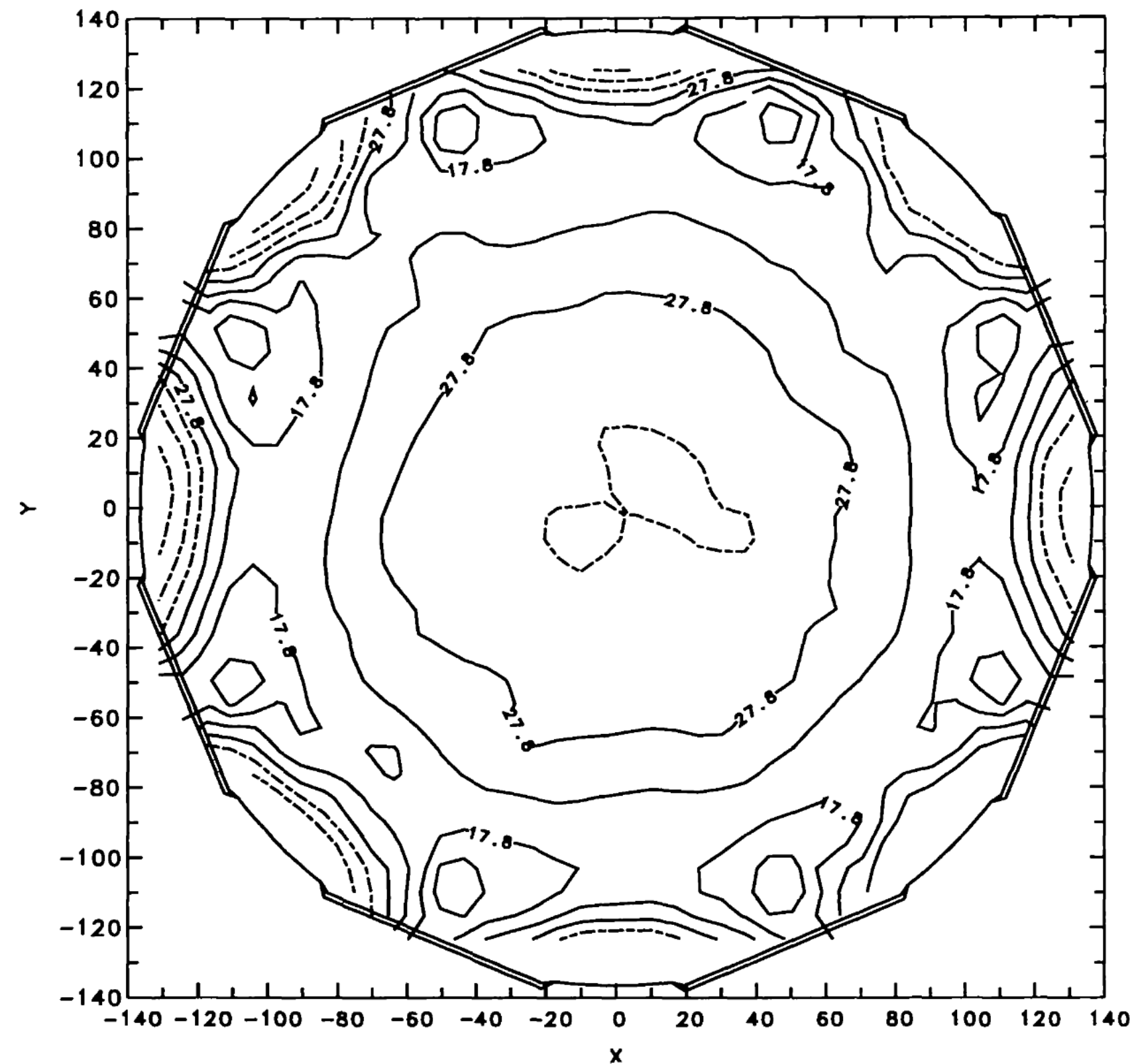


Protons on Tritium - 20.52 MeV γ -rays
 ${}^3\text{H}(p, \gamma){}^4\text{He}$

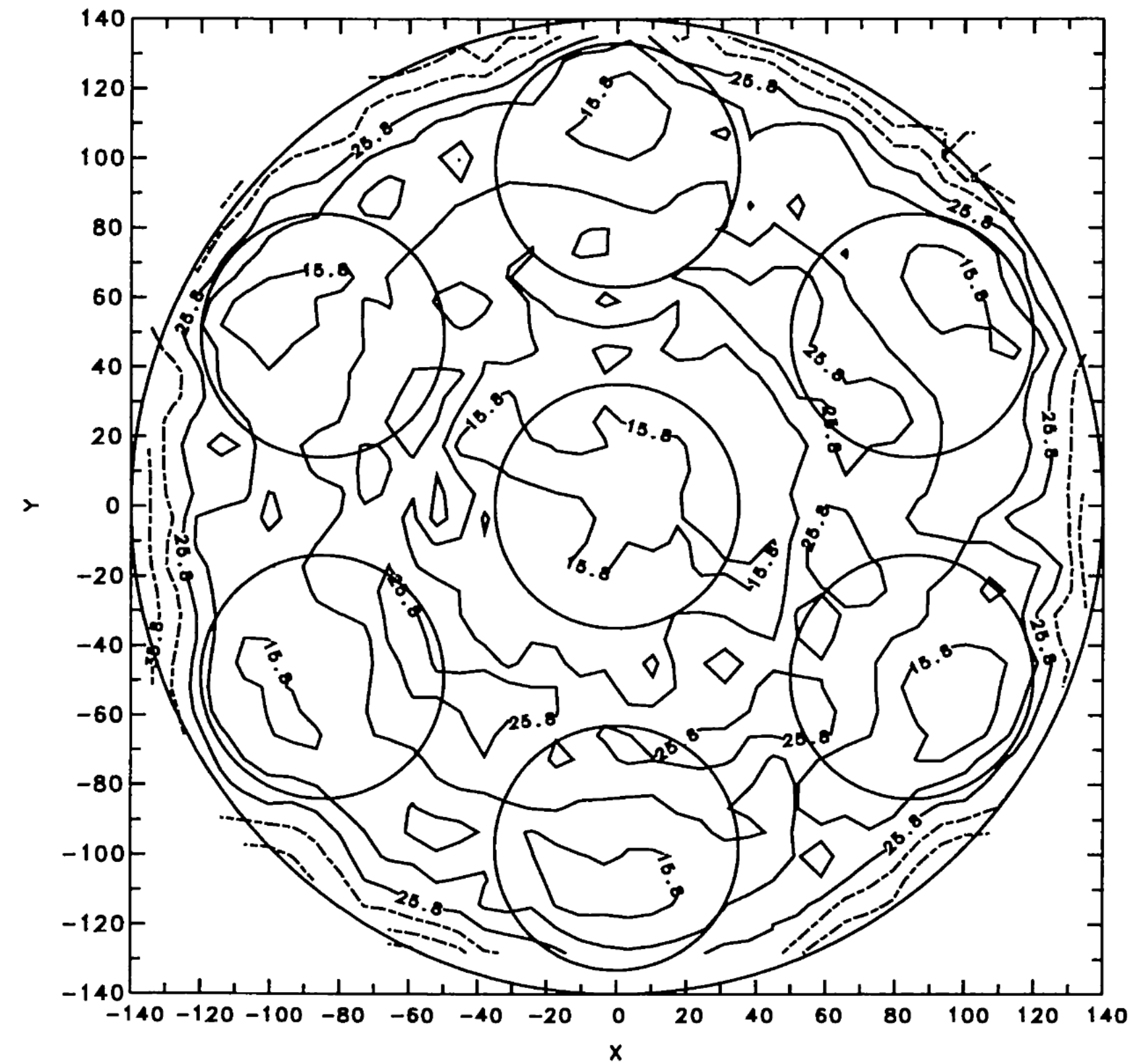
Schönfelder et al. (1993), Ap. J. Supp., 86, 657.

D1 / D2 Event Localization

Neural Net Location Algorithm



D1 1σ Localization Map
0.6 cm to 6.1 cm (avg = 2.3 cm)



D2 1σ Localization Map
0.5 cm to 2.5 cm (avg = 1.5 cm)

Schönfelder et al. (1993), Ap. J. Supp., 86, 657.

In-Flight Operating Modes

Most of the time was spent in Normal Mode.

Event rate in Normal Mode < 20 Hz.

STANDARD COMPTON IN-FLIGHT MODES

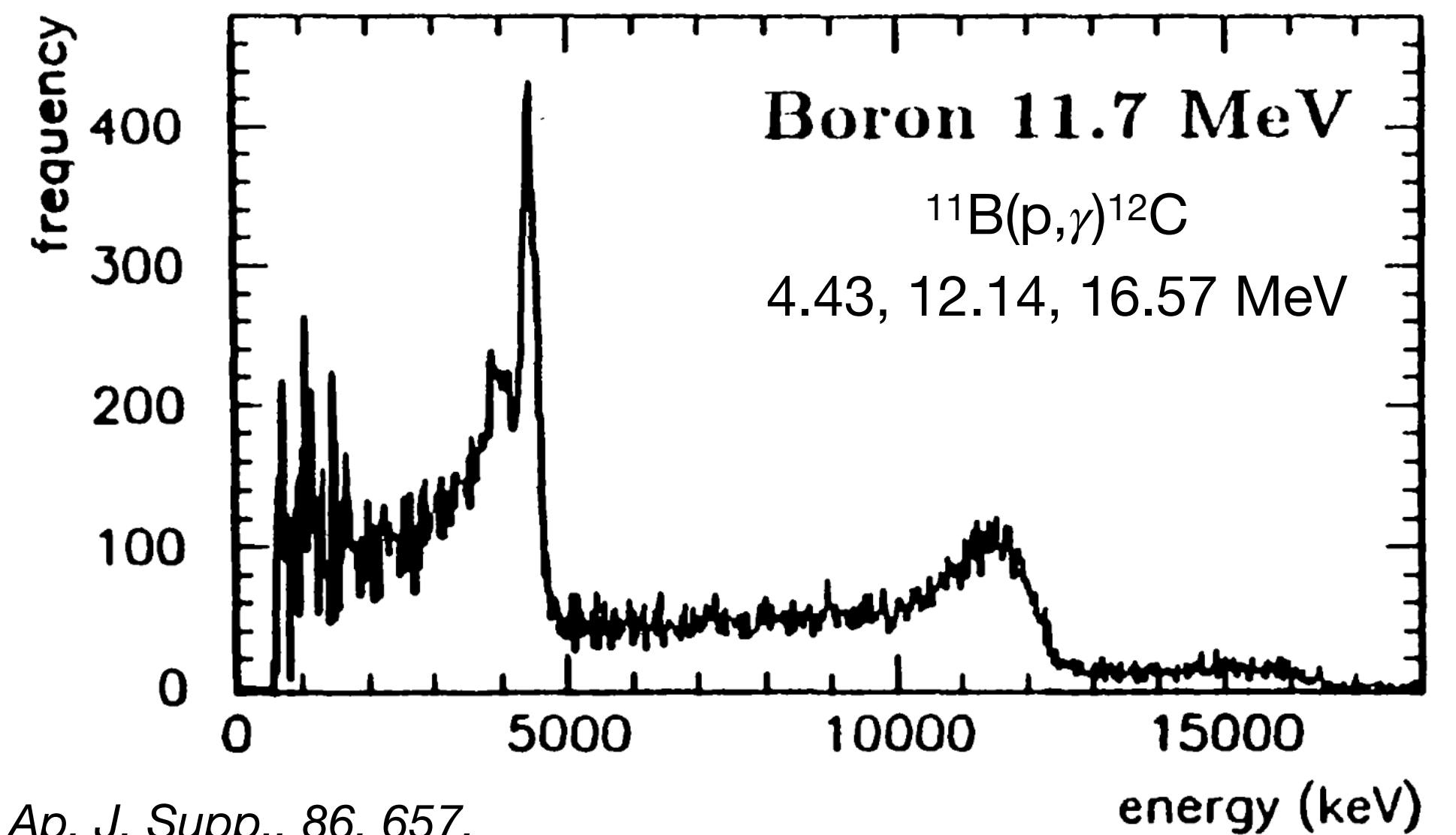
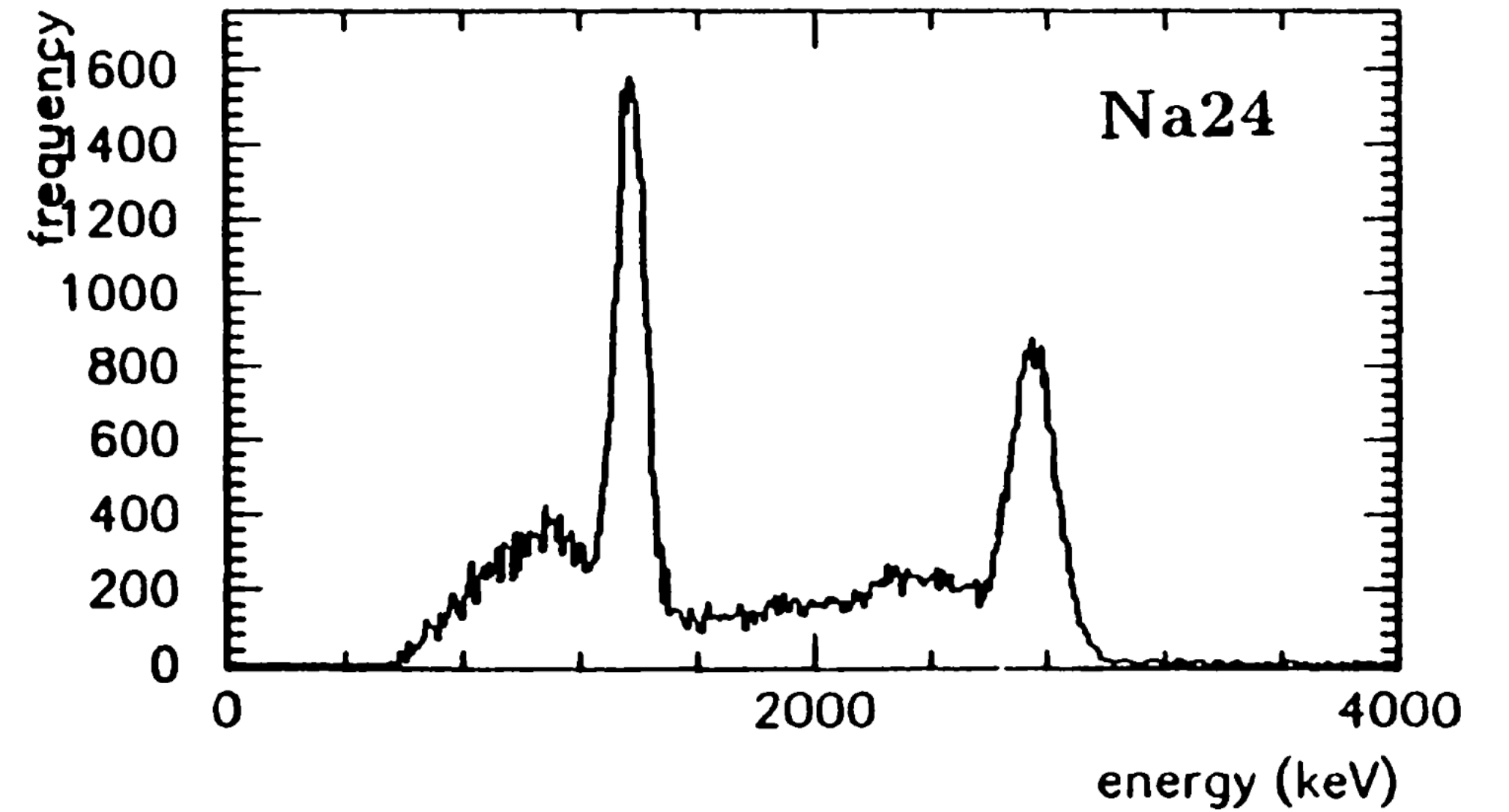
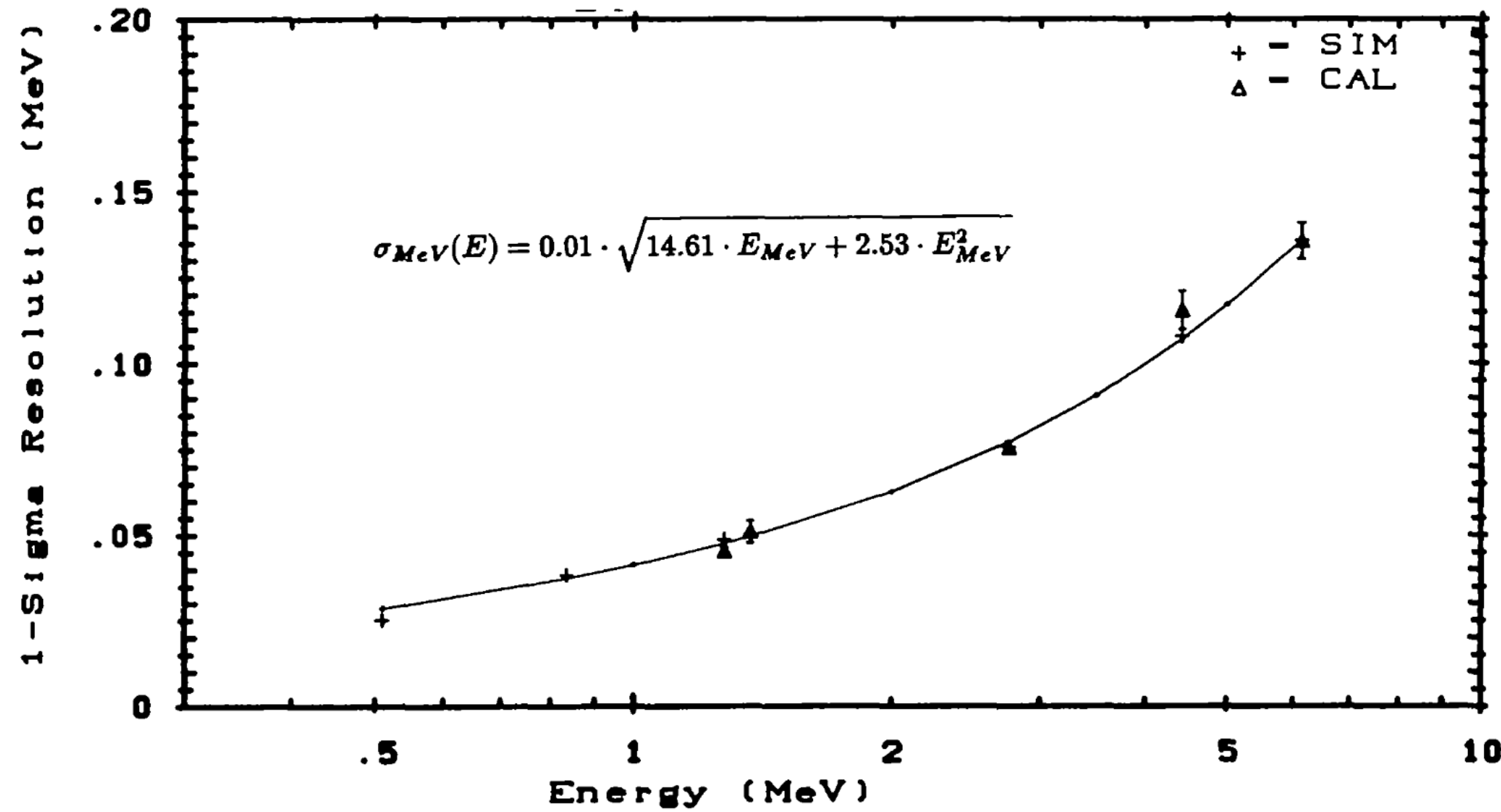
Mode	Description	Purpose
Normal operation mode	Nominal configuration	Astrophysical data
Solar neutron mode	Neutron event selection (0 ns < TOF < 40 ns)	Astrophysical data
Earth albedo mode	View Earth	Atmospheric data (gamma rays and neutrons)
SAA mode	HVPS off during SAA passage	FEE and BSA calibration
Proton/charged-particle event mode	Vetos ignored	Veto calibration
D ₁ single-event mode	D ₂ ignored	D ₁ calibration
D ₂ single-event mode	D ₁ ignored	D ₂ calibration
LED mode	High rate	Calibrate cell gains
Safe mode	Low voltage only	Safety

Schönfelder et al. (1993), Ap. J. Supp., 86, 657.

COMPTEL Response

Total Energy Resolution

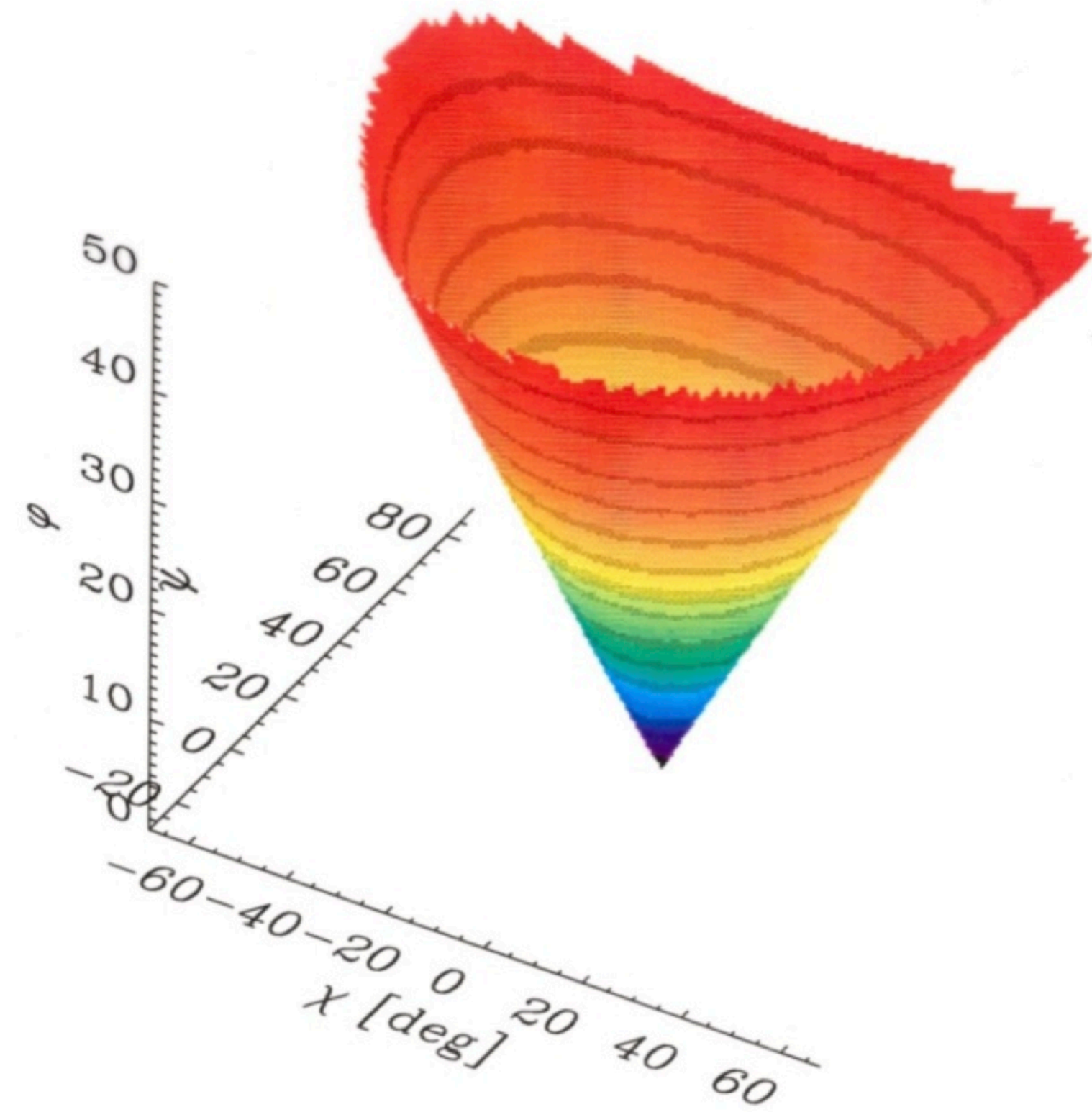
Pre-flight calibration data



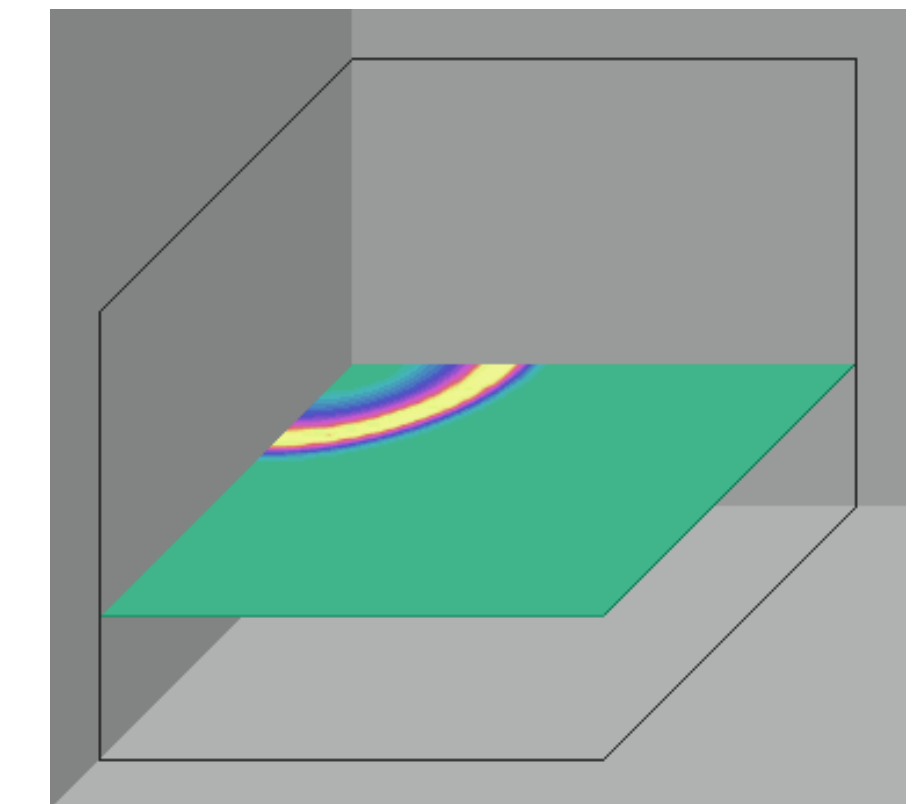
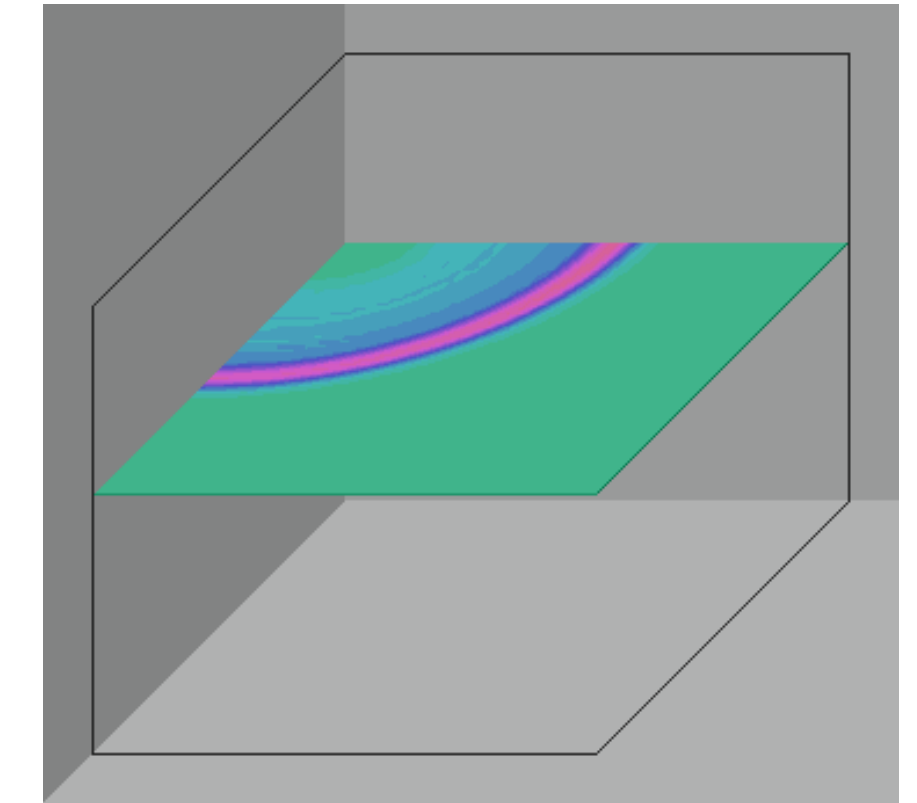
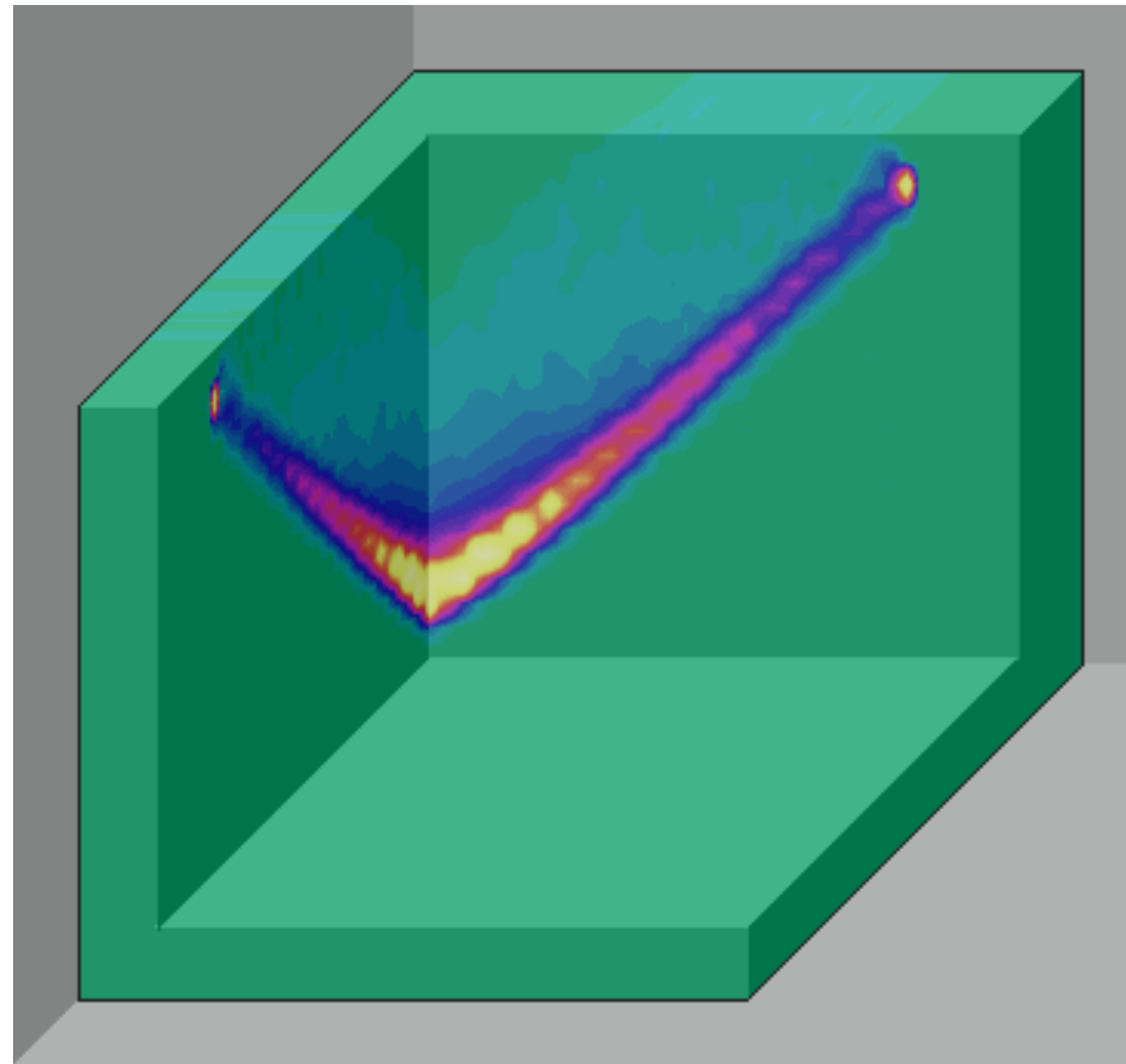
Schönfelder et al. (1993), *Ap. J. Supp.*, 86, 657.

COMPTEL Response

Point Spread Function



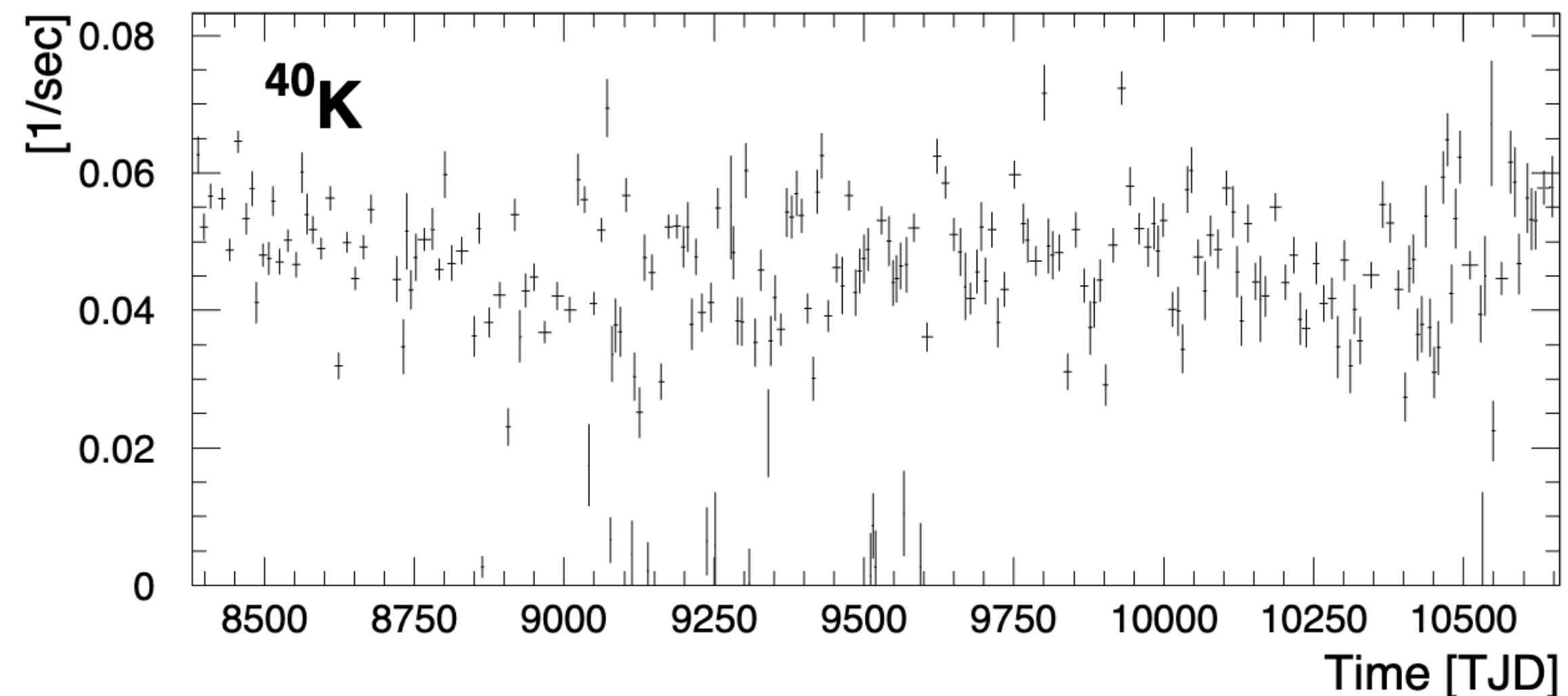
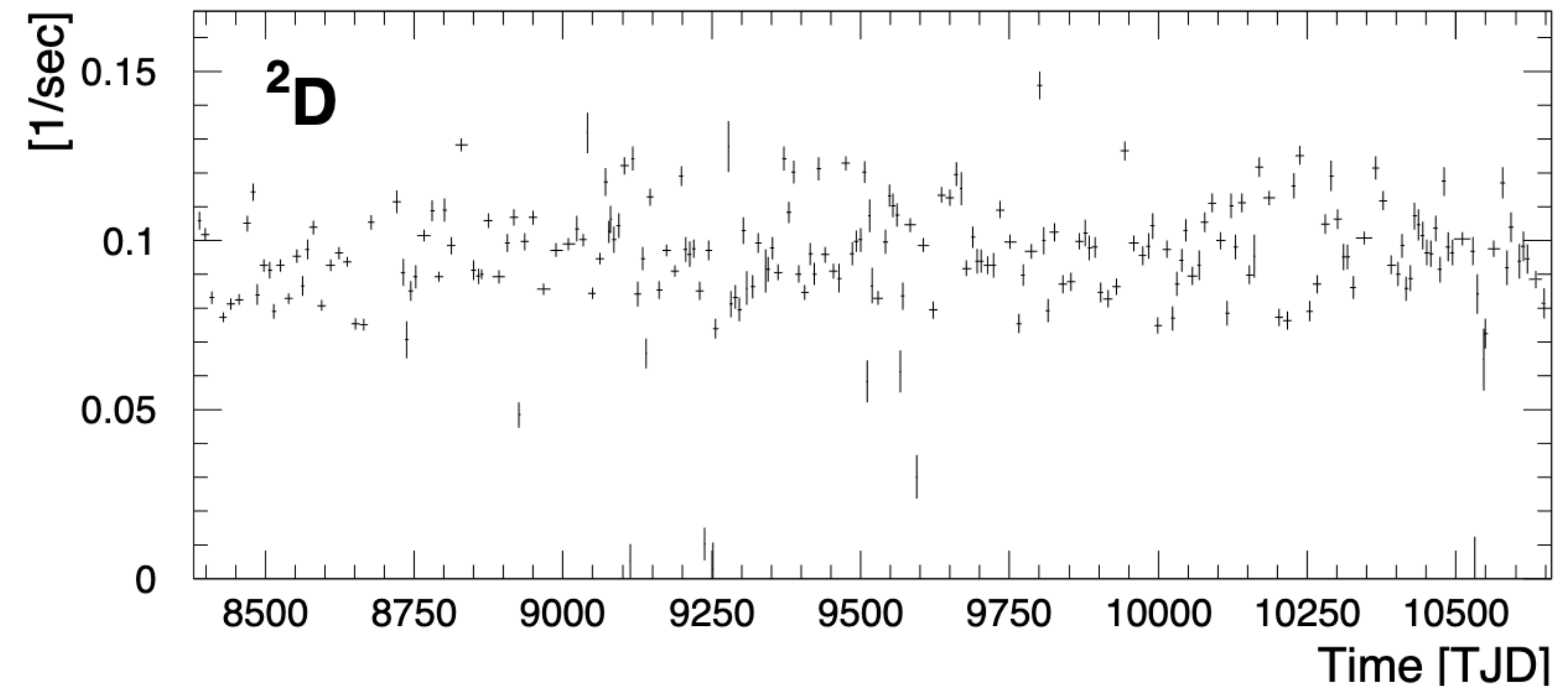
Event Distribution in $(\chi, \psi, \bar{\varphi})$ Space



COMPTEL Background

Variation in Time

Other background components (especially ^{40}K with its 1.3 billion year half-life) were much more constant in time.



Weidenspointner et al. (2001), Astr. Ap., 368, 347.

Recently Accepted Paper

COMPTEL Data can now be Analyzed with GammaLib

COMPTEL data analysis using GammaLib and ctools

J. Knödlseher¹, W. Collmar², M. Jarry¹, and M. McConnell^{3,4}

¹ Institut de Recherche en Astrophysique et Planétologie, Université de Toulouse, CNRS, CNES, 9 avenue Colonel Roche, 31028 Toulouse, Cedex 4, France

² Max-Planck-Institut für extraterrestrische Physik, Postfach 1603, 85740 Garching, Germany

³ University of New Hampshire, Space Science Center, Durham, NH 03824, U.S.A.

⁴ Southwest Research Institute, Dept. of Earth, Oceans, and Space, Durham, NH. 03824, U.S.A.

Received April, 2022; Accepted ???

ABSTRACT

More than 20 years after the end of NASA's Compton Gamma-Ray Observatory mission, the data collected by its COMPTEL telescope provide still the most comprehensive and deepest view of our Universe in MeV gamma rays. While most of the COMPTEL data are archived at NASA's High Energy Astrophysics Science Archive Research Center (HEASARC), the absence of any publicly available software for their analysis prevents confronting them to the scientific advances made in the field of gamma-ray astronomy at higher energies. To make this unique treasure again accessible for science we developed an open source software that enables a comprehensive and modern analysis of the archived COMPTEL telescope data. Our software is based on a dedicated plugin to the GammaLib library, a community-developed toolbox for the analysis of astronomical gamma-ray data. We implemented high-level scripts for building science analysis workflows in ctools, a community-developed gamma-ray astronomy science analysis software framework. We describe the implementation of our software and provide the underlying algorithms. Using data from the HEASARC archive, we demonstrate that our software reproduces derived data products that were obtained in the past using the proprietary COMPTEL software. We furthermore demonstrate that our software reproduces COMPTEL science results published in the literature. This brings back COMPTEL telescope data into life, allowing for their confrontation with recent advances in gamma-ray astronomy, and gives the community a **means** to unveil its still hidden treasures.

Key words. methods: data analysis – gamma rays: general – stars: neutron – binaries: general – **nucleosynthesis**

Accepted for publication in
Astronomy & Astrophysics